Immune signature in pemphigus and its potential for therapeutic JAK inhibition

Dissertation

der Mathematisch-Naturwissenschaftlichen Fakultät

der Eberhard Karls Universität Tübingen

zur Erlangung des Grades eines

Doktors der Naturwissenschaften

(Dr. rer. nat.)

vorgelegt von

Julia Holstein, M.Sc.

aus Kontorka (Kasachstan)

Tübingen

2021

Gedruckt mit Genehmigung der Mathematisch-Naturwissenschaftlichen Fakultät der Eberhard Karls Universität Tübingen.

Tag der mündlichen Qualifikation:	04.10.2021
Dekan:	Prof. Dr. Thilo Stehle
1. Berichterstatter:	Prof. Dr. Kamran Ghoreschi
2. Berichterstatter:	Prof. Dr. Robert Feil
3. Berichterstatter:	Prof. Dr. Gerhard Krönke

SUMMARY

Pemphigus vulgaris and pemphigus foliaceus are rare bullous autoimmune diseases of the skin and mucous membranes mediated by autoreactive antibodies directed against the desmosomal cadherins desmoglein (Dsg)1 and Dsg3. Binding of these antibodies leads to acantholysis, the loss of cell-cell adhesion between keratinocytes and thus manifests in blisters and erosions of the skin and mucosa in patients suffering from pemphigus. Previous data indicate that T helper type 2 (Th2) cells and related cytokines play a major role in disease initiation and manifestation, yet the contribution of other T cell subsets remains unclear and evidence is emerging for the involvement of Th17 cell subsets and associated cytokines in pemphigus pathogenesis. To address this issue, the cytokine signature in lesional skin of pemphigus patients was determined by whole transcriptome sequencing and quantitative real-time PCR (qPCR). Further, the distribution of Th and follicular T helper (Tfh) cells in peripheral blood from pemphigus patients with different disease activity stages was analyzed by flow cytometry. Transcriptome analysis identified a broad spectrum of cytokines and chemokines, including interleukins (IL), as well as other immune mediators differentially expressed in lesional pemphigus skin compared to healthy skin samples. Most importantly, an IL-17A-dominated immune signature and an upregulation of the IL-17A signaling pathway were revealed in the skin of pemphigus patients. The dominance of IL-17A and associated cytokines was further validated by qPCR. Moreover, flow cytometry analyses demonstrated elevated levels of IL-17A-producing Th17, Th17.1, Tfh17 and Tfh17.1 cells in the blood of patients with active pemphigus disease. Of note, levels of Th17, Tfh17 and Tfh17.1 cell subsets positively correlated with the levels of circulating Dsg3-reactive memory B cells in active patients. Follow-up experiments by the collaborating partners in Marburg identified Tfh17 cells as the primary inducers of Dsg-specific antibody production by B cells. These findings demonstrate that Tfh17 cells are substantially implicated in pemphigus pathogenesis and offer novel therapeutic approaches, for instance with small molecules targeting cytokine signal transduction of cells involved in disease initiation and manifestation.

In the next step, such small compounds aiming to block Janus kinase (JAK)/signal transducer and activator of transcription (STAT)-mediated signal transduction were investigated for their ability to interfere with various signaling cascades initiated by cytokines in $CD4^+$ Th cells. In

particular, compounds targeting JAK3 were assessed and compared with the clinically established pan-JAK inhibitor Tofacitinib. In this setting, four of the five inhibitors tested were able to selectively block JAK3-mediated signal transduction without affecting other JAKs. Furthermore, the compounds abrogated the signaling cascade activated by IL-21, a cytokine crucial for Tfh cell differentiation and autoantibody formation. Immunohistochemical staining revealed STAT1 and STAT3 activation in epidermal keratinocytes of perilesional pemphigus skin. Blockade of JAK1 as well as JAK3 in primary human epidermal cells resulted in a protective effect towards cell sheet fragmentation of keratinocyte monolayers in dispase-based dissociation assays. Taken together, these findings indicate a potentially beneficial effect of JAK inhibition in patients suffering from pemphigus and provide the basis for further investigations regarding the therapeutic application of JAK inhibitors in clinical practice.

ZUSAMMENFASSUNG

Pemphigus vulgaris und Pemphigus foliaceus sind seltene blasenbildende Autoimmunerkrankungen der Haut und der Schleimhäute, die durch die Bildung autoreaktiver Antikörper gegen die desmosomalen Cadherine Desmoglein (Dsg)1 und Dsg3 hervorgerufen werden. Die Bindung solcher Antikörper an Desmosomen führt zur Akantholyse, dem Verlust von Zell-Zell-Verbindungen zwischen Keratinozyten, was sich bei Patienten mit Pemphigus durch die Bildung von Blasen und Erosionen der Haut und Schleimhaut äußert. Vorausgegangene Studien deuten darauf hin, dass Typ2-T-Helferzellen (Th2) und zugehörige Zytokine eine wichtige Rolle bei der Krankheitsentstehung und -manifestation spielen. Das Mitwirken anderer T-Zellpopulationen ist jedoch unklar und es gibt zunehmend Hinweise auf eine Beteiligung von Th17-Zellen und assoziierten Zytokinen an der Pathogenese von Pemphigus-Erkrankungen. Um diese Fragestellung zu untersuchen, wurde die Zytokinsignatur in läsionaler Haut von Pemphigus-Patienten mittels Transkriptom-Sequenzierung und quantitativer Echtzeit-PCR (qPCR) bestimmt. Weiterhin wurde die Verteilung von Th- und follikulären T-Helferzellen (Tfh) im peripheren Blut von Patienten mit Pemphigus in unterschiedlichen Aktivitätsstadien mittels Durchflusszytometrie analysiert. Die Transkriptomanalyse zeigte ein breites Spektrum von Zytokinen und Chemokinen, einschließlich Interleukinen (IL), sowie andere Immunmediatoren, die in läsionaler Haut von Patienten mit Pemphigus im Vergleich zu gesunden Hautproben unterschiedlich exprimiert wurden. Am bedeutendsten war, dass eine IL-17A-dominierte Immunsignatur und eine Überregulation des IL-17A-Signalwegs in der Haut von Pemphigus-Patienten festgestellt wurde. Die Dominanz von IL-17A und assoziierten Zytokinen wurde durch den Einsatz der qPCR validiert. Darüber hinaus zeigten durchflusszytometrische Analysen erhöhte Mengen von IL-17A-produzierenden Th17-, Th17.1-, Tfh17- und Tfh17.1-Zellen im Blut von Patienten mit aktiver Pemphigus-Erkrankung. Bemerkenswerterweise korrelierten die Anteile der Th17-, Tfh17- und Tfh17.1-Zelluntergruppen positiv mit der Menge der zirkulierenden Dsg3-reaktiven Gedächtnis-B-Zellen bei der aktiven Patientengruppe. Nachfolgende Experimente der Kooperationspartner in Marburg identifizierten Tfh17-Zellen als die primären Auslöser der Dsg-spezifischen Antikörperproduktion durch B-Zellen. Diese Erkenntnisse zeigen, dass Tfh17-Zellen maßgeblich an der Entstehung der Pemphigus-Erkrankung mitwirken und erlauben neue therapeutische Ansätze, zum Beispiel mit niedermolekularen Substanzen, die gezielt die

Zytokin-Signaltransduktion von jenen Zellen beeinflussen, die an der Krankheitsentwicklung und -manifestation beteiligt sind.

Im nächsten Schritt wurden solche niedermolekularen Verbindungen, die zur Inhibition der Januskinase (JAK)/Signal-Transduktor und Aktivator der Transkription (STAT)-vermittelten Signaltransduktion dienen, hinsichtlich ihrer Eignung untersucht, in verschiedene Signalkaskaden einzugreifen, die durch Zytokine in $CD4^+$ Th-Zellen aktiviert werden. Insbesondere wurden gegen JAK3 gerichtete Verbindungen untersucht und mit dem klinisch etablierten pan-JAK-Inhibitor Tofacitinib verglichen. Im Rahmen dieser Untersuchungen konnten vier der fünf getesteten Inhibitoren selektiv die JAK3-vermittelte Signaltransduktion blockieren, ohne die Funktion anderer JAKs zu beeinträchtigen. Darüber hinaus unterbrachen die verwendeten Substanzen die IL-21-Signalkaskade, welche eine entscheidende Rolle bei der Tfh-Zelldifferenzierung und der Bildung von Autoantikörpern spielt. Immunhistochemische Färbungen zeigten zudem eine Aktivierung von STAT1 und STAT3 in epidermalen Keratinozyten der periläsionalen Haut von Patienten mit Pemphigus. Die Inhibition von JAK1 sowie JAK3 in primären humanen epidermalen Zellen schützte Keratinozyten-Monolayer vor der Akantholyse im dispasebasierten Dissoziationstest. Zusammengefasst deuten diese Ergebnisse auf eine potenziell vorteilhafte Wirkung einer JAK-Inhibition bei Patienten mit Pemphigus hin und bilden die Grundlage für weitere Untersuchungen zur therapeutischen Anwendung von JAK-Inhibitoren im klinischen Alltag.

TABLE OF CONTENTS

FIGURES

TABLES

ABBREVIATIONS

ADAMTS9-AS2	A disintegrin and metalloproteinase with thrombospondin motifs 9 antisense RNA 2
APC	Antigen-presenting cell
BCL6	B cell lymphoma 6
BCR	B cell receptor
CADM2	Cell adhesion molecule 2
CCR6	CC chemokine receptor type 6
CD	Cluster of differentiation
cDNA	Complementary deoxyribonucleic acid
CPDA	Citrate-phosphate-dextrose-adenine
C_q	Quantification cycle
CXCL	CXC chemokine ligand
CXCR	CXC chemokine receptor
DAB	3,3-Diaminobenzidine
DEG	Differentially expressed gene
DIF	Direct immunofluorescence
Dsc	Desmocollin
Dsg	Desmoglein
ELISA	Enzyme-linked immunosorbent assay
FACS	Fluorescence-activated cell sorting
GC	Germinal center
GM-CSF	Granulocyte macrophage colony-stimulating factor
GO	Gene ontology
H&E	Hematoxylin and eosin
HLA	Human leukocyte antigen
IFN	Interferon
Ig	Immunoglobulin
IHC	Immunohistochemistry
IIF	Indirect immunofluorescence
IL	Interleukin

JAK	Janus kinase
KEGG	Kyoto Encyclopedia of Genes and Genomes
MHC	Major histocompatibility complex
MMP	Matrix metalloproteinase
NHEK	Normal human epithelial keratinocytes
PBMC	Peripheral blood mononuclear cell
PF	Pemphigus foliaceus
PF-049	PF-04965842
PV	Pemphigus vulgaris
qPCR	Quantitative real-time polymerase chain reaction
RNA	Ribonucleic acid
RT	Room temperature
SCID	Severe combined immunodeficiency
Skepi-L	Skepinone-L
STAT	Signal transducer and activator of transcription
Tc	Cytotoxic T cell
TCR	T cell receptor
Tfh	Follicular T helper cell
Tfr	Follicular regulatory T cell
TGF-β	Transforming growth factor beta
Th	T helper cell
Tofa	Tofacitinib
Treg	Regulatory T cell
TYK2	Tyrosine kinase 2
γc	Common γ chain

1. INTRODUCTION

1.1. Adaptive immune system

The immune system defends the organism against infections and is typically divided into the innate and the adaptive immune response. The innate or non-specific immunity serves as the first defense mechanism. However, innate responses do not specifically recognize certain pathogens and do not provide targeted protection against re-infection. In contrast to the innate immune response, adaptive or specific immunity is based on the clonal selection of lymphocytes, a subgroup of white blood cells with uniform appearance but distinct functions. Lymphocytes possess a variety of highly specific receptors, this allows the immune system to recognize any foreign antigen [1]. The main players in adaptive immunity are B and T lymphocytes. They originate in the bone marrow from a common lymphoid precursor cell and maturation takes place in the bone marrow for B cells and in the thymus for T cells. From here, they enter the blood circulation as mature naïve lymphocytes and circulate to secondary lymphoid tissues. During maturation, a single lymphocyte precursor cell results in a large number of lymphocytes, each with its own specific antigen receptor. Potentially autoreactive immature lymphocytes carrying receptors for the individual's own proteins (autoantigens) are usually eliminated before complete maturation, thus ensuring tolerance to autoantigens. Once a foreign antigen binds to a specific receptor of a mature naïve lymphocyte, the cell is activated and starts to proliferate. This results in lymphocytic clones with receptors capable of binding the same antigen [2]. These cells differentiate into effector cells that combat the pathogen. At the same time, differentiated memory cells are generated, which enable a faster and more effective reaction in case of re-infection [3].

B and T lymphocytes vary in the structures of their expressed antigen receptors and their surface molecules. The so-called cluster of differentiation (CD) molecules enable the identification and characterization of distinct immunological cell types based on their surface proteins and typically act as co-receptors, supporting antigen-recognition [4]. Circulating B cells express the antigen-specific B cell receptor (BCR) and the co-receptors CD19 and CD20, which can facilitate their activation [5, 6]. The BCR is produced by the same genes that encode antibodies, a group of proteins also known as immunoglobulins (Ig). After binding of an antigen to the BCR, the B cell proliferates and differentiates into a plasma cell, which produces

antigen-specific antibodies. Depending on the antigen, B cell activation takes place with or without the help of T lymphocytes [3, 7]. The T cell receptor (TCR) differs from the BCR in structure and binding properties. It forms a functional receptor complex with CD3, which is required for signaling upon antigen binding and this complex is assisted by different co-receptors [8]. The first contact of a T cell with its specific antigen results in the formation of one of several types of T effector lymphocytes with different activities. Cytotoxic T cells (Tc) express CD8 and can induce cell death when cells present the antigen on their surface upon infection with viruses or other intracellular pathogens. T helper cells (Th) express CD4 and produce mediators called cytokines, which activate the functions of other cells, such as antibody production by B cells or phagocytosis of pathogens by macrophages. Regulatory Th cells (Treg) also express CD25 and suppress the proliferation and activity of other effector lymphocytes. By this Tregs help dampening immune responses [3, 7].

While the BCR and antibodies can recognize almost any type of chemical structure, T cell receptors typically only bind protein antigens. Furthermore, the TCR recognizes a peptide epitope only if the peptide is bound to a certain glycoprotein and presented on the cell surface of another cell. These glycoproteins are called major histocompatibility complex (MHC) molecules or human leukocyte antigen (HLA) molecules and there are two types expressed on antigen-presenting cells (APCs): MHC class I and MHC class II. The MHC class I molecule is expressed on every nucleated cell and presents peptides originating from the cell itself (endogenous pathway) to Tc cells, which subsequently kill the presenting cell by induction of apoptosis. MHC class II is expressed on so-called professional APCs like B cells, macrophages or dendritic cells. Professional APCs internalize antigens, process them into peptide fragments and present the fragments bound to MHCII on their surface (exogenous pathway) to Th and Treg cells [7, 9].

1.2. T helper cells and associated cytokines

Antigen recognition of T cells leads to the transduction of TCR signals, which enable the activation of these cells. In order to gain effector function and to generate T lymphocytes with different phenotypes, additional cytokine and costimulatory signals are required. The interaction of these signals finally governs the differentiation into a specialized effector type

with a lineage-specific cytokine-profile and distinct functions. There are several subtypes of differentiated $CD4^+$ T cells playing crucial roles in maintaining beneficial immune responses. On the other hand, Th cells are also implicated in pathogenesis of inflammatory autoimmune diseases [10]. An increasing number of Th cell subsets has been described in recent years. Figure 1 illustrates an overview of the most relevant $CD4^+$ T cell subgroups. The early reported subsets were the type 1 (Th1) and type 2 (Th2) cells, primarily producing the cytokines interferon (IFN)-γ and interleukin (IL)-4, respectively [11].

Th1 lymphocytes are particularly important for host defense against intracellular pathogens like viruses by initiating cell-mediated responses and inflammation. Following contact between an APC and a naïve T cell, the APC secretes IL-12, which activates signal transducer and activator of transcription (STAT)4, leading to differentiation of the IFN-γ expressing Th1 phenotype [12, 13]. In turn, the expression of IFN-γ further stimulates APCs to produce IL-12 and also promotes Th1 cell differentiation by activation of the transcription factor STAT1 and the T-box transcription factor TBX21, resulting in a positive feedback loop to strengthen the immune response [14, 15]. Th1 cells may also play a role in the development of organ-specific autoimmune diseases like type 1 diabetes [16, 17].

For mediating immune responses against extracellular toxins, allergens or parasites, Th2 cells are crucial to provide humoral immunity. These cells secrete primarily IL-4, but also IL-5 and IL-13 and can stimulate B cells to produce antibodies. IL-4 is the major driver of type 2 Th cell differentiation and activates STAT6 leading to upregulation of GATA3 expression, the master transcriptional factor of Th2 differentiation. Due to IL-4 release by Th2 cells a positive feedback loop is triggered and enhances the immune response [18-20]. However, Th2 cells seem to be implicated in the development of allergic inflammatory diseases like asthma [21].

In addition to the well-known Th1 and Th2 cell subsets, Th17 cells were discovered in 2005 [22-24]. They play an essential role in orchestrating responses against extracellular pathogens like bacteria and fungi by recruiting other immune cells to produce inflammatory cytokines, chemokines and antimicrobial peptides. On the other hand, they have been found to be responsible for various forms of inflammatory autoimmune disorders like psoriasis or multiple sclerosis [25, 26]. During development, IL-6-mediated STAT3 activation together with

transforming growth factor (TGF)-β induces upregulation of ROR transcription factors and thus initiates Th17 differentiation and secretion predominantly of the inflammatory cytokine IL-17 [27-29]. However, IL-21 and IL-23 may similarly be involved in STAT3 activation and Th17 development and maintenance [23, 30, 31]. Due to the cells' capability of also producing TGF-β, this cytokine may serve in a positive feedback mechanism in Th17 differentiation [32].

TGF-β is not only involved in Th17 differentiation, but also in the development of Treg cells. Together with the activation of STAT5 by IL-2, the Treg associated transcription factor FOXP3 is upregulated and the production of TGF-β by Tregs is induced, resulting in a positive feedback loop [33-35]. Treg cells are essential for maintaining self-tolerance and controlling differentiation, proliferation and function of T effector cells in order to prevent immune and autoimmune reactions [36].

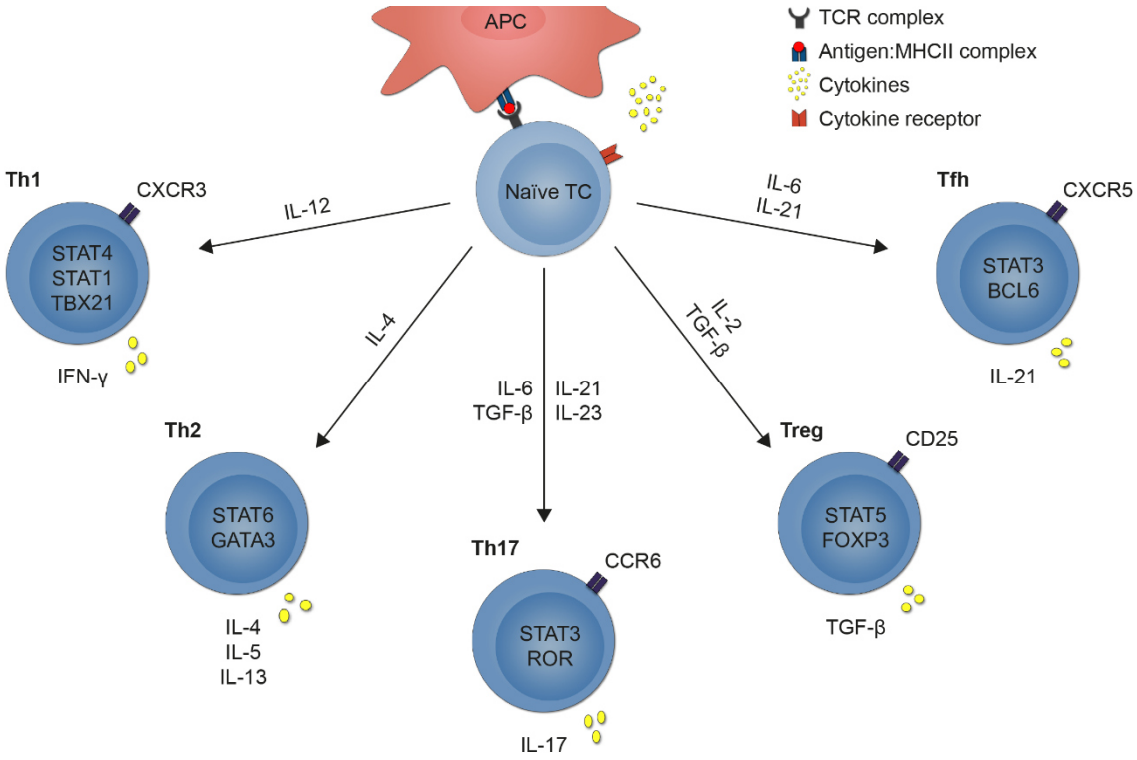

Figure 1: T helper cell subsets, associated cytokines and transcription factors involved in differentiation. The antigen-specific TCR/CD3 complex on the surface of naïve $CD4^+$ cells recognizes the antigen peptide:MHCII complex presented on antigen-presenting cells (APC). In addition, APCs secrete cytokines, which signal through cytokine receptors on the T cells (TC) and polarize them towards an effector phenotype carrying specific surface receptors, secreting defined cytokines and having particular functions.

Studies on human and mouse immune cells revealed that the cellular source of IL-17 is heterogeneous and is not only defined by classical Th17 cells, but also by Th17 cells with a transient phenotype that additionally produces IFN-γ [37, 38]. These so-called Th17.1 cells are considered to play a special pathogenic role in the setting of certain organ-specific autoimmune diseases like multiple sclerosis as shown by experimental models and human data [37, 39, 40]. The expression of surface markers enables to distinguish between Th17 and Th17.1 cell subsets. While classical Th17 cells typically express the CC chemokine receptor type 6 (CCR6) and Th1 cells bear the CXC chemokine receptor (CXCR)3, Th17.1 cells express both CCR6 and CXCR3 on their surface [41, 42].

In recent years, more specialized T cell subsets emerged and helped to understand that not all T cells are equivalently involved in inducing autoantibody production through B cells [43]. The most critical T cells for initiating autoreactive B cell responses and generating long-term serological memory are the T follicular helper (Tfh) cells [44]. By interactions with B cells, they form germinal centers (GC), sites of B cell proliferation, differentiation and memory generation, and thereby promote autoantibody production [45, 46]. These cells express CXCR5 on their surface and seem to play a pivotal role in autoimmune disorders. During development, the presence of IL-6 and IL-21 is required and induces activation of STAT3 and B-cell lymphoma 6 (BCL6). Tfh cells produce high levels of IL-21 resulting in a positive feedback mechanism towards Tfh differentiation [45, 47].

1.3. JAK/STAT signaling pathway

Cytokine-triggered signal transduction of many cytokines critically involved in T cell differentiation and in the pathogenesis of inflammatory skin diseases is mediated by Janus kinase (JAK)/signal transducer and activator of transcription (STAT) signaling, providing this pathway a major role in inflammation and autoimmunity. There are four JAKs (JAK1, JAK2, JAK3 and tyrosine kinase 2 (TYK2)), which associate with the cytoplasmic regions of specific type I and type II cytokine receptors. Binding of the corresponding cytokine leads to dimerization of the receptor and to activation of JAKs through phosphorylation. This in turn results in dimerization and phosphorylation of STAT molecules (STAT1, STAT2, STAT3, STAT4, STAT5a/b or STAT6), which translocate into the nucleus and modulate the expression of many

genes involved in differentiation, proliferation and survival (Figure 2) [48]. Table 1 depicts an overview of some important JAK/STAT pathway components for cytokine signaling.

Table 1: JAK/STAT pathway component activation [49, 50]

Cytokine receptor family	Cytokine	Associated JAKs	STAT phosphorylation
Common γ chain	IL-2	JAK1, JAK3	STAT5, STAT1, STAT3
	IL-4	JAK1, JAK3	STAT6, STAT5
	IL-21	JAK1, JAK3	STAT3, STAT1, STAT5
Glycoprotein 130	IL-6	JAK1, JAK2, TYK2	STAT3
IL-12 receptor β1	IL-12	JAK2, TYK2	STAT4
	IL-23	JAK2, TYK2	STAT3
Type I interferon	IFN-α	JAK1, TYK2	STAT1, STAT2
Type II interferon	IFN-γ	JAK1, JAK2	STAT1

JAK1, JAK2 and TYK2 are ubiquitously expressed in mammals, while JAK3 is predominantly expressed in hematopoietic and lymphoid tissue where it plays a crucial role in lymphocyte development and homeostasis [51, 52]. JAK3 exclusively associates with receptors bearing the common γ chain (γc), a receptor unit typically used by IL-2, IL-4, IL-7, IL-9, IL-15 and IL-21. Consequently, loss of function mutations of JAK3 might lead to the severe combined immunodeficiency (SCID) syndrome in humans. Patients suffering from SCID lack natural killer (NK) cells, T cells and functional B cells, resulting in exposure to various infections with bacteria, viruses or fungi [53, 54].

Inhibition of components within the JAK/STAT signaling pathway may affect many cellular functions, making them popular targets for the development of new drugs. JAK inhibitors (JAKi), for instance, intervene in cytokine signal transduction at the JAK level by blocking their activation and consequently diminishing downstream STAT activity (Figure 2). At present, a variety of JAK inhibitors are under investigation in different stages of preclinical development and clinical trials. The first JAKi developed for the treatment of autoimmune diseases, Tofacitinib (Tofa), was initially claimed to selectively block JAK3 signaling [55]. Further studies also revealed the inhibition of JAK1 and to a lesser extent JAK2 signal transduction [56].

Tofacitinib was developed for the treatment of rheumatoid arthritis and was approved in the USA in 2012 and in the EU in 2017 [57]. Like Tofacitinib, other first generation JAK inhibitors block multiple JAKs, resulting in broad cytokine inhibition that may have adverse off-target activity and side effects. Besides infections and malignancies, potential side effects include anemia and leukopenia due to the vital role of JAK2 in hematopoiesis [58, 59]. Especially for the long-term treatment required by inflammatory and autoimmune diseases, more selective agents targeting just one individual JAK are under investigation and may reduce side effects caused by simultaneous JAK inhibition.

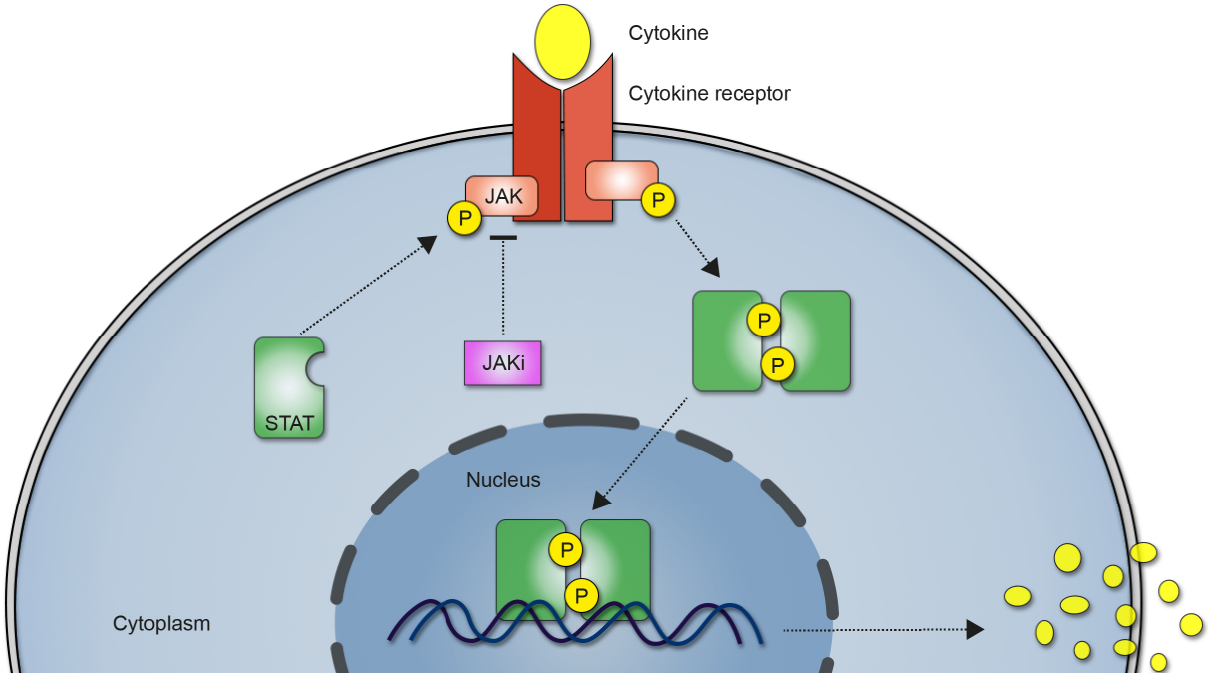

Figure 2: JAK/STAT signaling pathway. Upon cytokine binding to the specific receptors expressed on the cell surface, the associated Janus kinase (JAK) proteins get activated by phosphorylation and subsequently activate signal transducer and activator of transcription (STAT) molecules, which form dimers and enter the nucleus to regulate the transcription of various genes like cytokines and other proteins. JAK phosphorylation may be inhibited by different compounds like JAK inhibitors (JAKi) resulting in blocked signal transduction.

1.4. Structure of the skin

With its surface area of 1.5 to 2 m^2 the skin is the largest organ of the human body and has many important functions. Among other functions, it serves as a mechanical barrier with protective functions to the outside and is part of the innate immune system. The structure of the skin is divided into epidermis, dermis and subcutis. The epidermis forms the outermost

epithelial layer of the skin. It consists of keratinocytes in different stages of differentiation, which are connected by cell-cell contacts like desmosomes, adherens junctions or gap junctions. Epidermal keratinocytes undergo a differentiation process from proliferating basal cells in the *stratum basale* towards the surface of the epidermis through the *stratum spinosum* to the *stratum granulosum*, where they lose their nuclei and their cytoplasm appears granular. Finally, when the cells have lost their nuclei and cytoplasmic organelles, they become corneocytes in the *stratum corneum*, the outermost part of the epidermis (Figure 4). Corneocytes are frequently replaced by desquamation and renewal from the lower epidermal layers, which makes them an essential part of the skin barrier function. The dermis lies between the epidermis and the subcutaneous adipose tissue. The structure connecting the epidermis to the dermis is called dermal-epidermal junction and is formed by protein structures that anchor the cytoskeleton of the basal keratinocytes to the fibril elements of the papillary dermis. Epidermal basal cells are attached to the basement membrane by hemidesmosomes and transmembrane anchoring filaments. The basement membrane consists of lamina lucida and lamina densa which is attached to the papillary dermis by anchoring fibrils made of type VII collagen [60, 61].

1.5. Desmosome

Desmosomes are intercellular adhesive structures that link neighboring cells to each other and improve the cohesion of the tissue by connecting the intermediate filament of one cell to the intermediate filament of other cells. They are typically found in tissue exposed to intense mechanical stress such as stratisfied squamous epithelia of the skin and mucosa as well as some non-epithelial tissues like the myocardium [62-64]. Desmosomes connect neighboring cells through discoid junctions with a length of 0.2 - 0.3 µm and a circular or oval shape. The intercellular space between the cells measures about 24 nm and in each adjacent cell are two electron-dense plaques, the outer dense plaque (ODP) and the inner dense plaque (IDP) [62, 65]. The IDP is less dense than the ODP and it is attached to bundles of keratin intermediate filament [66]. Figure 3 shows the molecular model of the desmosome. It consists of at least three protein families: the desmosomal cadherins desmoglein (Dsg) and desmocollin (Dsc) form the intercellular region and mediate adhesion by binding to each other, whereas the plaques are built of armadillo and plakin family proteins. The intracellular ends of desmogleins

and desmocollins interact with plakoglobin. These interactions are stabilized by plakophilin. Plakoglobin binds to desmoplakin, which finally is attached to the intermediate filament cytoskeleton in the IDP [67, 68].

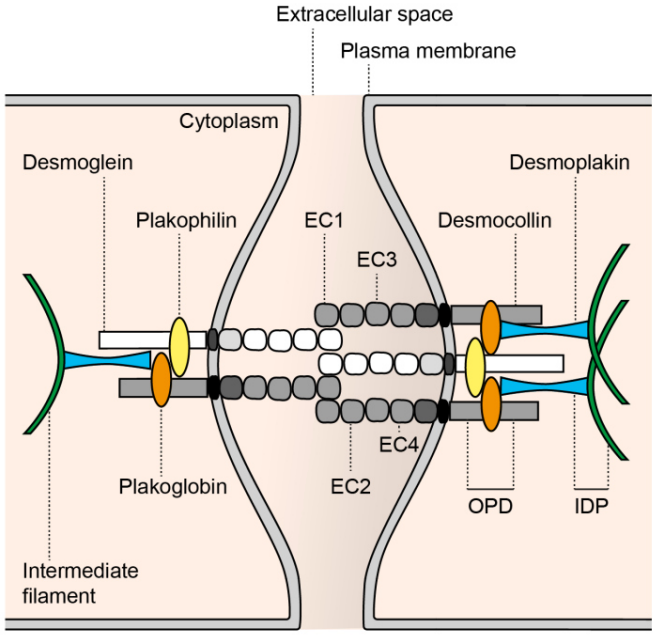

Figure 3: Desmosome schematic diagram. The desmosome consists of desmoglein and desmocollin that can bind through homophilic and heterophilic interaction of the extracellular (EC) domain to partner molecules on the same cell (*cis*) as well as on the neighboring cell (*trans*). In the outer dense plaque (ODP), the cytoplasmic domains of desmoglein and desmocollin are attached to plakoglobin and plakophilin. These adaptor molecules are linked to the intermediate filament cytoskeleton in the inner dense plaque (IDP) via desmoplakin.

Like classical cadherins, desmosomal cadherins are calcium-dependent glycoproteins possessing a transmembrane domain, which mediate the cell-cell contact in different tissues. Four desmogleins (Dsg1, Dsg2, Dsg3 and Dsg4) and three desmocollins (Dsc1, Dsc2 and Dsc3) are distinguished [69]. Their structure consists of four highly conserved extracellular (EC) domains (EC1, EC2, EC3 and EC4), an extracellular anchor, a single transmembrane domain followed by an intracellular anchor and variable intracellular domains [70]. Extracellular calcium promotes adhesion by bringing the extracellular domains into a rigid and functional conformation [71]. In contrast to classical cadherins, where homophilic interactions are most likely to occur, the interaction of the extracellular domains of desmosomal cadherins can be homophilic or heterophilic [70, 72]. The expression of desmosomal proteins is tissue- and

differentiation-specific. Dsg2 and Dsc2 are expressed in all desmosome-possessing tissues and are the only members of desmosomal cadherins found in simple epithelia and in the myocardium. In contrast, Dsg4 is present in hair follicle and highly differentiated keratinocytes, whereas Dsg1, Dsg3, Dsc 1 and Dsc3 are only found in stratified squamous epithelia like skin and oral mucosa [73-75]. The composition of desmosomal cadherins varies within the epidermal layers of the skin, depending on keratinocyte differentiation and stratification (Figure 4). Dsg1, Dsg4 and Dsc1 are mainly found in the superficial layers, whereby Dsg4 is only present in the *stratum granulosum*, Dsc1 is also found in the spinous layer and Dsg1 is expressed throughout the epidermis in decreasing concentrations. The expression of Dsg3, Dsc2 and Dsc3 is increasingly found in the deep epidermis, whereas Dsg2 is only present in the basal layer [76].

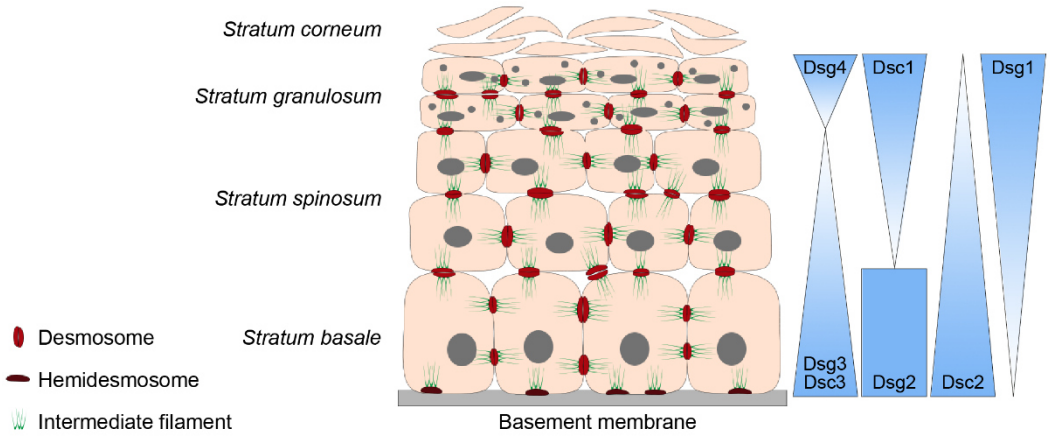

Figure 4: Expression patterns of desmosomal proteins throughout the epidermis. Keratin intermediate filaments are linked to desmosomes and to hemidesmosomes at sites of cell-cell contact and the basement membrane, respectively. On the right, the expression levels of desmosomal cadherins in the specific layers of the epidermis are shown. Desmoglein (Dsg)1, Dsg4 and desmocollin (Dsc)1 expression levels are strongest in the superficial layers, whereas expression of Dsg3, Dsc2 and Dsc3 is most prominent in the deeper epidermis. Dsg2 is only expressed in the *stratum basale*.

1.6. Autoimmune bullous diseases

Autoimmune disorders are based on a defective tolerance to autoantigens, which results in the production of autoantibodies and subsequently in inflammation and tissue damage. The exact cause of autoimmune diseases is unknown, but it is assumed that they underlie a failure of regulatory mechanisms and are triggered by a combination of genetic predisposition and

environmental factors [77]. There are different types of autoimmune disorders, one group of them are the blistering autoimmune dermatoses. These forms of dermatoses are life-threatening diseases of the skin or mucous membranes, which usually have chronic relapsing course. Circulating autoantibodies directed against anchor proteins of the dermal-epidermal junction or against intercellular anchoring proteins of the epithelial cells lead to loss of adhesion and thus subsequently results in blister formation and extensive erosions. Depending on the localization of the gap formation, intra- or subepidermal blistering autoimmune dermatoses are distinguished. If autoantibodies against hemidesmosome anchoring proteins or collagen VII are present, subepidermal blistering occurs and is referred to as pemphigoid disorders. This group includes bullous pemphigoid, linear IgA dermatosis or epidermolysis bullosa acquisita [78]. Disruption of the keratinocyte adhesion and intraepidermal blistering causes diseases of the pemphigus group. The most important target antigens of pemphigus disorders are Dsg1 and Dsg3. The presence of autoantibodies against these antigens causes acantholysis, the loss of cell-cell adhesion between keratinocytes and thus subsequently results in blister formation and extensive erosions. The two main subtypes of pemphigus diseases are pemphigus vulgaris (PV), characterized by oral and skin erosions, and pemphigus foliaceus (PF), which is exclusively defined by skin lesions [79].

1.7. Pemphigus: Epidemiology and genetic factors

The prevalence of pemphigus varies geographically and between ethnic groups [80]. Although PF, as endemic PF, is the prevalent type in some Latin American and African countries including Brazil and Tunisia, PV is the more common form of pemphigus in most of the world [81, 82]. At diagnosis, most patients are between 40 and 60 years old, whereby pemphigus may appear at all ages [80]. Most studies report a predominance in females, though more male patients are found in some Asian nations like Saudi Arabia and Kuwait [83, 84]. The annual incidence of PV within Europe varies from 0.5 cases per million in Germany to 8 cases per million in Greece [85, 86]. In Asia, the incidence varies from 1.6 cases per million in Saudi Arabia (pemphigus erythematosus and PV) to 7.2 cases per million in Israel (all pemphigus diseases) [83]. Among the Jewish people in Israel, the prevalence was three times higher than among the Arab population [87]. In the United States of America, the incidence among people with a Jewish background was eight times higher than among people with other ethnic

backgrounds [88]. The ethnic preference and geographical distribution of pemphigus occurrence indicate a genetic predisposition, and the existence of an endemic form of PF suggests that environmental factors may also trigger pemphigus disorders. Most patients have no family history of pemphigus. However, there are studies indicating a genetic predisposition in association with the HLA type. A meta-analysis revealed a statistically significant relation of *HLA-DRB1*04, HLA-DRB1*08* and *HLA-DRB1*14* with PV susceptibility [89]. *HLA-DRB1*04:02* is frequently found in Jewish populations [90]. The largest genome-wide association study of pemphigus has recently been conducted in the Chinese population, where *HLA-DQB1*05:03* has been identified as the most associated allele in both PV and PF [91]. These findings indicate that specific MHC class II alleles are crucial for the recognition of autoantigens by T cells in pemphigus patients, resulting in the production of autoantibodies mediated by T cell-B cell interactions.

1.8. Pathogenesis of pemphigus diseases

Pemphigus diseases are mainly mediated by autoantibodies of the isotype IgG, which are directed against Dsg1 and Dsg3. Binding of these autoantibodies leads to acantholysis and intraepidermal blistering in mucous membranes and in the skin [79, 92]. The autoantibody profile and the blistering site differ among the two pemphigus subtypes. While PF patients show only antibodies against Dsg1 and patients with mucosal-dominant PV have only anti-Dsg3 antibodies, those suffering from PV of the mucocutaneous-type have both anti-Dsg1 and anti-Dsg3 autoantibodies. Blister formation in the skin of PV patients takes place in the deeper epidermis above the basal layer (suprabasal skin blistering), while PF blisters develop in the upper layers in the *stratum granulosum* (superficial skin blistering). Patients with mucosal-dominant type PV usually show no blister formation in the skin, but only mucosal involvement. The location of blister development is explained by the desmoglein compensation hypothesis corresponding to the distribution pattern of desmosomal cadherins (Figure 5). In PF, where only anti-Dsg1 antibodies are present, Dsg3 functionally compensates for the autoantibody-induced loss of Dsg1 binding in the deeper epidermis and blistering occurs only in the superficial layers. In mucosal-dominant-type PV, Dsg1 compensates for Dsg3 throughout the epidermis so there is no blister formation in the skin. In mucocutaneous PV, the function of both Dsg1 and Dsg3 is impaired and blisters develop in the deep epidermis. Mucous

membranes express Dsg1 and Dsg3 in the entire squamous epithelium layer, though the expression of Dsg3 is much higher. Antibodies directed against Dsg1 have no impact on cell adhesion due to compensation through Dsg3. On the contrary, in the presence of anti-Dsg3 antibodies, the low expression of Dsg1 is not sufficient to compensate for the loss of Dsg3 and suprabasal blistering occurs [76, 93, 94].

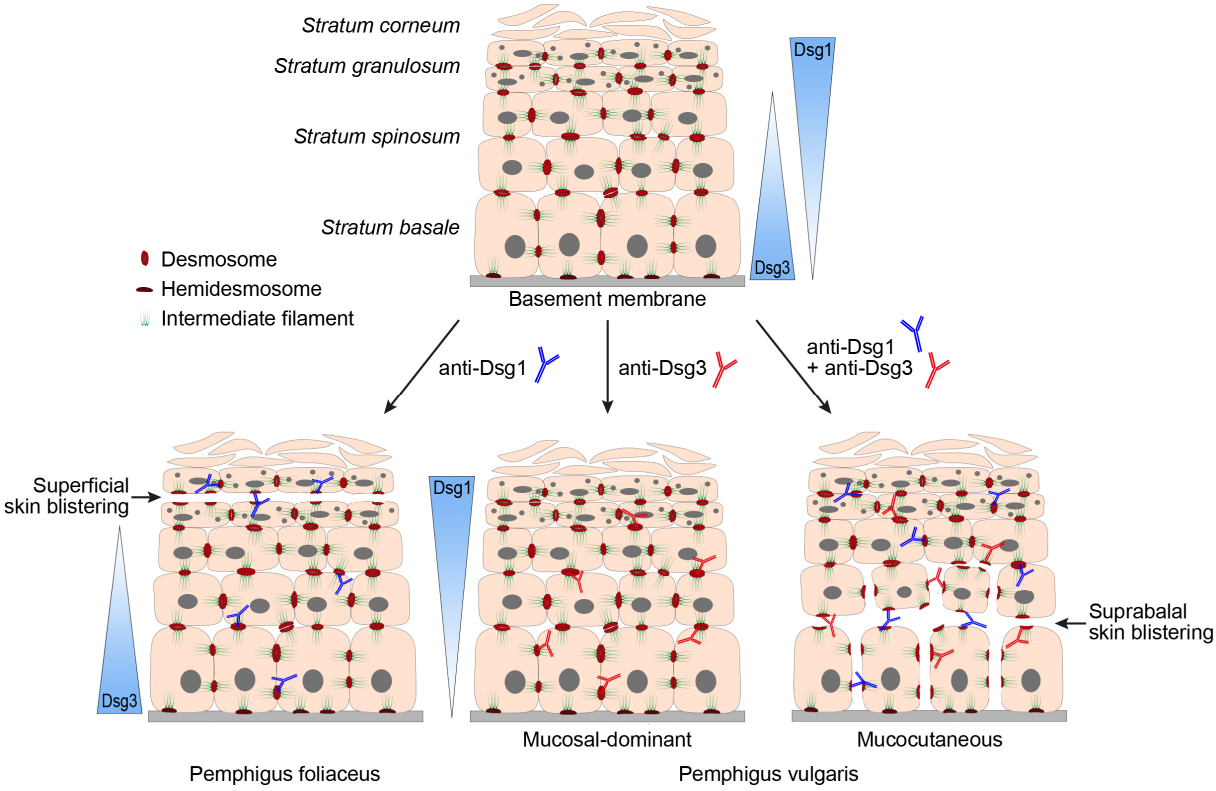

Figure 5: The desmoglein compensation theory explains the location of blister formation based on the antibody profile in pemphigus foliaceus and pemphigus vulgaris. According to this model, Dsg3 compensates for the impaired Dsg1 binding in pemphigus foliaceus, when only anti-Dsg1 antibodies are present, and blistering occurs in the superficial layers of the epidermis. No blisters are developed in the skin of mucosal-dominant pemphigus vulgaris (PV) patients because Dsg1, which is present throughout the epidermis, compensates for the blocked Dsg3-mediated adhesion. Only if both anti-Dsg1 and anti-Dsg3 antibodies are present in PV, suprabasal gap formation occurs due to autoantibody-induced loss of adhesion.

Two major mechanisms of autoantibody-mediated acantholysis have been identified: direct interference of desmosomal cohesion by autoantibody binding (steric hindrance) and triggering of intracellular signaling pathways in keratinocytes through binding of autoantibodies, which indirectly affects desmosomal adhesion. The theory of direct

autoantibody interference is supported by the observation that pathogenic monoclonal antibodies cause blistering in mice. AK23, a monoclonal antibody derived from a PV mouse model and directed against a binding motif on EC 1 of Dsg3, which is important for adhesive *trans*-interaction with Dsg3 on opposing cells, has been shown to be pathogenic *in vivo*, whereas antibodies directed against other parts of the extracellular Dsg3 domain were ineffective to induce blistering [95, 96]. It was also demonstrated that both IgG from PV patients' sera and AK23 directly inhibited the homophilic Dsg3 binding in a cell-free system [97]. In addition, monoclonal pathogenic autoantibodies from pemphigus patients were reported to disrupt the EC1-EC2 *cis*-adhesion of Dsg3 molecules [98]. Intracellular signals following autoantibody binding also promote keratinocyte dissociation. Immunofluorescent staining and electron microscopic observations showed that autoantibody binding leads to clustering or internalization of Dsg from the cell surface, resulting in depletion of Dsg1 and Dsg3 [99-101]. It has been shown that several signaling pathways are activated, leading to loss of keratinocyte cohesion. Among them are the p38 mitogen-activated protein kinase (MAPK), the protein kinase C (PKC)/phospholipase C (PLC) and the epidermal growth factor receptor (EGFR) pathways [102-105]. Inhibition of p38 MAPK blocked autoantibody-mediated Dsg3 clustering and internalization together with loss of adhesion *in vitro* and prevented PV IgG induced blistering in mice [106, 107]. Combination of several non-pathogenic monoclonal anti-Dsg3 antibodies binding to different parts of Dsg3 induced blisters *in vivo*, suggesting a synergistic pathogenic effect as found in patients [108]. Both steric hindrance and signaling pathway alterations seem to operate in pemphigus disease [106].

The generation of pathogenic autoantibodies requires B cell activation by autoreactive $CD4^+$ Th cells. Adoptive transfer of one Dsg3-reactive T cell clone together with naïve B cells isolated from immunized $Dsg3^{-/-}$ mice led to autoantibody production and development of a PV phenotype in $Rag2^{-/-}$ mice, whereas transfer of B cells only showed no such effect [109]. Furthermore, Dsg3-reactive Th2 cells were able to stimulate unprimed B cells to secrete Dsg3-specific antibodies *in vivo* [110]. In blood of PV patients with active disease, the frequencies of autoreactive Th2 cells were elevated compared to patients in remittent disease stage or healthy controls and Th2 levels correlated with anti-Dsg3 IgG titers [111]. In addition, Dsg3-specific T cells were found in PV patients and secreted Th2 associated cytokines upon stimulation *in vitro* [112]. Moreover, autoreactive Th1 cells could be identified in PV patients

as well as in healthy individuals, while Dsg3-reactive Th2 cells were exclusively found in PV patients [113].

In accordance with this, sera from patients with PV and PF showed increased concentrations of Th2 cytokines such as IL-4 and IL-10 and suppressed Th1 cytokines like IL-2 and IFN-γ [114]. Taken together, autoreactive Th2 cells seem to play a crucial role in the regulation of pathogenic autoantibody production. However, elevated levels of IL-6 and TNF were found in PV patients' blood and another study reported increased IFN-γ concentrations compared to healthy individuals [115-117]. In lesional skin of PV patients, both type 1 and type 2 related cytokines could be detected [118]. Of note, Dsg3-specific IL-21^{+} T cells and the Tfh associated cytokines IL-21 and IL-27 as well as the Th17 cell associated cytokines IL-17A and IL-23 were also elevated in PV blood [116, 117, 119]. Additionally, IL-17, IL-21 and IL-23 were detected in lesional skin of PV patients by immunofluorescent staining and flow cytometry [120, 121]. Moreover, some groups reported an increase of Th17 cells and suppressed Treg cells in peripheral blood of pemphigus patients [122, 123]. These findings suggest that a more complex Th cell response may be critical for the development of pemphigus diseases.

1.9. Clinical appearance and diagnosis of pemphigus

Due to the predominant expression of Dsg3 in mucous tissues, mucosal-dominant PV initially manifests with painful erosive lesions of the oral mucosa in most cases. Buccal mucosa, gingiva, tongue and palate are particularly affected. Other mucous membranes may also be involved like esophageal, nasal, conjunctival, anal or genital mucosa. Over 50 % of the PV patients develop the mucocutaneous PV type with flaccid blisters and erosions of the skin, mostly in areas exposed to mechanical stress and seborrheic areas, whereas the entire skin can be affected. There is also the less frequent cutaneous type of PV without mucosal involvement, where blisters develop in the deeper epidermis and anti-Dsg1 antibodies are predominant. Without treatment, the lesions hardly heal and are highly painful. Viral or bacterial superinfections are relatively common in cutaneous and mucous lesions. In PF, only the skin is affected, there is no mucosal involvement. Lesional skin presents erythematous with scaly and crusted erosions, and seborrheic areas of the skin are mainly affected, including the face and the upper trunk. Due to their superficial localization and fragility, blisters are

rarely seen in patients with PF. In active disease stage, PV and PF are both positive for Nikolsky sign, gentle rubbing of unaffected skin causes exfoliation of the superficial layers and subsequent blistering [92, 124, 125]. Fingernail involvement was also reported in both PV and PF [126, 127].

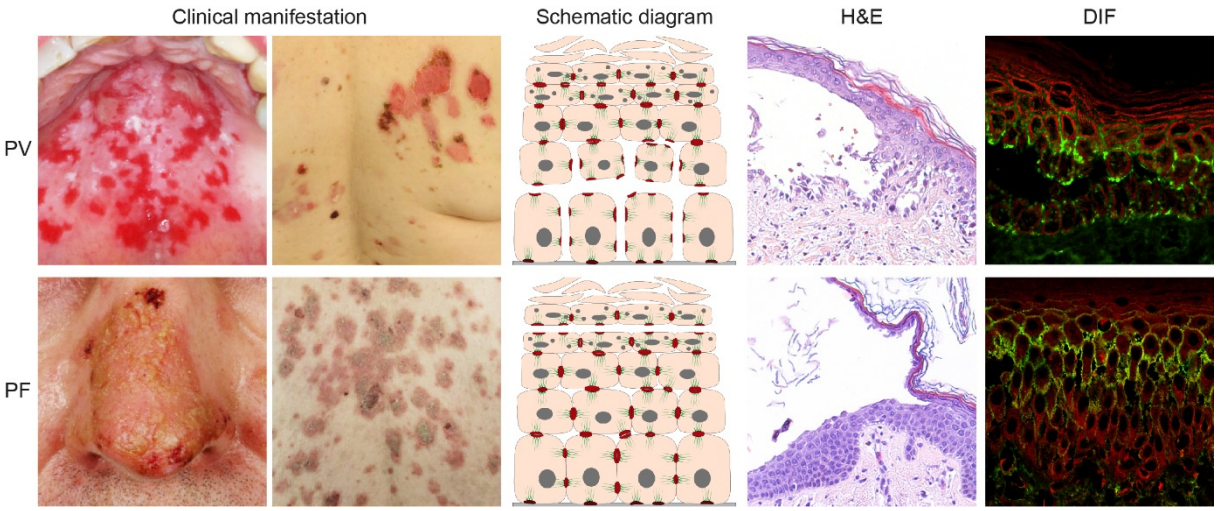

Figure 6: Synopsis of clinical and pathological characteristics of pemphigus diseases. Clinically pemphigus presents with lesions and blisters of the skin and mucosa (in case of pemphigus vulgaris, PV) or the skin alone (in case of pemphigus foliaceus, PF). Clinical images of patients' skin were provided by Solimani et al. [128]. Blistering occurs in PV in the deeper epidermis with basal keratinocytes acquiring a tombstone-like appearance as shown in the schematic diagram and as seen in hematoxylin and eosin staining (H&E, magnification 100x). In PF, blisters develop in the upper layers of the epidermis without acantholytic cells. Direct immunofluorescence (DIF) staining reveals deposition of IgG autoantibodies (green) at the surface of keratinocytes in the lower (for PV) or upper (for PF) layers of the epidermis, respectively (Evans blue counterstaining in red, magnification 400x).

Diagnosis of pemphigus disease is based on the combination of clinical presentation, histopathology of lesional skin, direct immunofluorescence (DIF) microscopy of perilesional skin, and detection of autoantibodies in patients' sera by indirect immunofluorescence (IIF) microscopy and enzyme-linked immunosorbent assay (ELISA). Figure 6 gives an overview of the clinical and pathological characteristics of PV and PF. The histopathological appearance of pemphigus is characterized by intraepidermal acantholysis caused by loss of adhesion between keratinocytes. In PV, blistering occurs suprabasally, with acantholytic cells and basal keratinocytes still attached to the basement membrane showing a tombstone-like morphology. In contrast, PF lesional skin shows superficial, subcorneal blisters without

apparently acantholytic cells. DIF staining of perilesional skin presents deposition of IgG autoantibodies on the surface of epidermal keratinocytes in a reticular pattern in PV and PF. Circulating autoantibodies in the blood of pemphigus patients can be detected by IIF staining typically using monkey esophagus as substrate demonstrating reactivity of IgG autoantibodies with the surface of epithelial cells [129]. The implementation of ELISAs allows the quantitative detection of anti-Dsg1 and anti-Dsg3 antibodies in patients' sera using recombinant Dsg protein [129, 130]. In general, autoantibody levels fluctuate in line with clinical disease activity and can therefore be useful for the monitoring of disease course [131, 132].

1.10. Treatment of pemphigus diseases

The initial therapy of pemphigus aims to control disease activity without new blister formation and to support the healing of existing blisters and erosions. According to the recent recommendations by an international panel of experts, the first-line treatment of pemphigus is immunosuppression with systemic corticosteroids in combination with immunosuppressive adjuvants [133]. However, several severe side effects of long-term therapy with corticosteroids have been reported, such as osteoporosis, hyperglycemia, hypertension, and increased overall susceptibility to infections [134]. In addition, about half of patients experience a relapse during corticosteroid therapy, and the remaining patients reach complete remission off therapy within an average of three years of treatment [135]. For severe cases or for patients without clinical remission upon immunosuppression, depletion of B cells by anti-CD20 monoclonal antibodies (rituximab) may be administered. Rituximab has been proven to be highly effective in pemphigus treatment and, referring to only one of many studies, showed remission off-therapy in 89 % of patients after two years compared to 34 % of patients treated with corticosteroids alone [136]. Meta-analyses revealed complete clinical remission within 6 months in 76 – 90 % of pemphigus patients with a mean duration of 16 months [137, 138]. Yet, a relapse occurs in at least half of the patients and severe side effects linked to infections may appear [138]. In addition, there are patients not responding to rituximab treatment or even experiencing exacerbation of the disease [139-142]. Therefore, understanding of pemphigus pathogenesis is essential to investigate novel therapeutic strategies targeting involved factors, cells and autoantibodies in order to avoid general immune suppression.

1.11. Aim of the study

PV and PF are rare blistering skin diseases mediated by autoantibodies directed against the desmosomal cadherins Dsg3 and Dsg1. While the cellular immune response that results in autoantibody formation presumably initiates at distant sites from the target organ, the disease itself manifests at mucosa and skin. Binding of pathogenic autoantibodies to the desmosomes causes inflammatory response, loss of epithelial cell adhesion, blister formation and extensive erosions. As in other autoimmune diseases, the development of autoantibody production is based on specialized Th cells, which upon activation may stimulate autoreactive B cells [143]. For many years it was assumed that autoantibody-mediated diseases like PV and PF were driven by classical type 2 Th cells producing the lineage-characteristic cytokine IL-4. However, both Th2- as well as Th1-associated cytokines have been found in lesional skin of PV patients. Moreover, Dsg-reactive Th2 and Th1 cells were detected in peripheral blood of pemphigus patients. Nevertheless, the exact phenotype of the T cells responsible for the development of pemphigus needs to be identified. The discovery of new T cell subtypes and associated cytokines has advanced our understanding of inflammation and autoimmunity. For instance, $CD4^+$ IL-17-producing Th17 cells were shown to be the key players in the pathogenesis of psoriasis, an inflammatory autoimmune skin disease with epithelial hyperproliferation [144]. First reports suggest that IL-17 may also be involved in other skin diseases like pemphigus. Further, Dsg3-specific IL-21^+ T cells as well as circulating Tfh cells seem to be overrepresented in the blood of pemphigus patients. Of note, IL-21 is also implicated in the promotion of Th17 cell responses. Based on these recent developments, it is possible that a Th17 cell response could play a more prominent role in pemphigus than Th2 or Th1 cells. In the present study, the aim was to analyze the dominant cytokines and disease-inducing $CD4^+$ T cell subsets in a large cohort of patients suffering from pemphigus by performing large-scale gene expression studies, T cell phenotyping and quantitative analysis of cytokines in the skin and peripheral blood.

New therapeutic options for the treatment of pemphigus are needed. In recent years, JAKs have emerged as an attractive target for specific immune blockade and JAKi are currently approved for autoimmune diseases such as rheumatoid arthritis or psoriatic arthritis. Due to the high immunological activity in pemphigus, JAKi could also provide high efficacy in the therapy of this disease. In addition, due to the limited expression of JAK3 to hematopoietic

and lymphoid cells, the identification of a selective JAK3 inhibitor should have limited but precise effects on immune cells and would not affect other cell types, promoting a novel therapeutic approach in the treatment of pemphigus and other inflammatory autoimmune diseases. In order to identify novel selective compounds, the dose-dependent inhibition of STAT phosphorylation in human $CD4^+$ T cells was determined. In addition, selected JAKi were further characterized for their ability to abrogate Th cell lineage associated cytokine signaling. Furthermore, the effect of JAKi on autoantibody-induced acantholysis in keratinocyte monolayers was investigated.

The main aims and objectives of this study were as follows (illustrated in Figure 7):

(1) Identification of the disease-relevant Th and Tfh cell subsets in pemphigus disease by immunophenotyping of peripheral blood from pemphigus patients.

(2) Detection of relevant cytokines involved in pemphigus pathogenesis by gene expression analysis of lesional skin from pemphigus patients.

(3) Investigation of selective JAK inhibitors and their potential role as therapeutics in pemphigus disease.

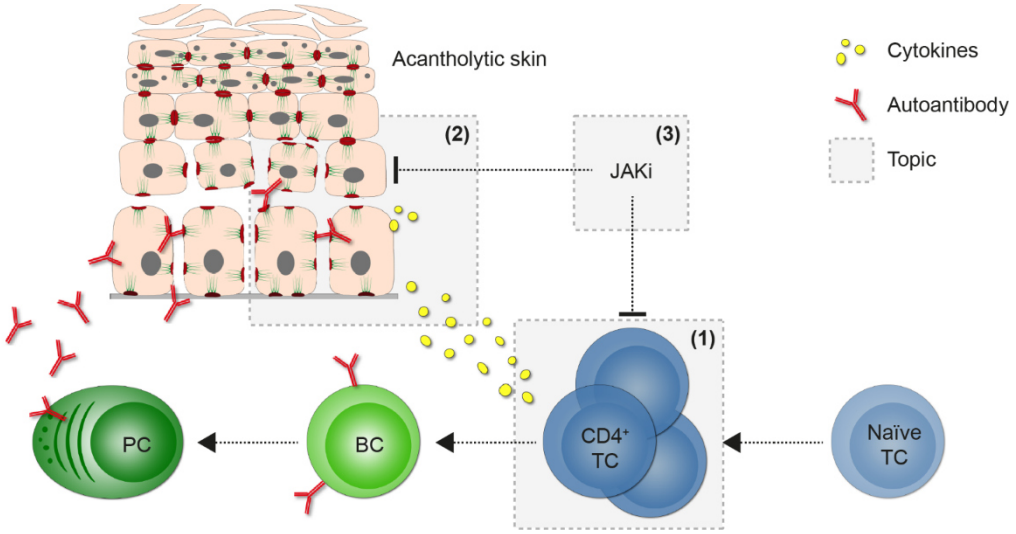

Figure 7: Illustration of topics addressed in the immune pathogenesis of pemphigus. Cytokine producing $CD4^+$ effector T cells (TC) activate autoreactive B cells (BC) and thereby initiate the formation of autoantibody-secreting plasma cells (PC). Binding of the autoantibodies to desmosomes leads to acantholysis and manifests with blisters and erosions of skin and mucosa. **(1)** The exact phenotype of the T cells responsible for disease development, **(2)** the cytokine signature of lesional skin from pemphigus patients and **(3)** a potential role of Janus kinase inhibitors (JAKi) in the treatment of pemphigus was investigated.

2. MATERIALS

2.1. Laboratory equipment

Centrifuge 5417C with rotor F45-30-11	Eppendorf, Hamburg, Germany
Centrifuge Multifuge 3 S-R with rotor 75006445	Heraeus, Hanau, Germany
E1-ClipTip™ Electronic Single Channel Pipette 12.5 µl	Thermo Fisher Scientific, Waltham, USA
Electrode BlueLine 18 pH	SI Analytics, Mainz, Germany
FACSAria Cellsorter	BD, Franklin Lakes, USA
Freezer	Liebherr, Bulle, Switzerland
Freezing Container Mr. Frosty™	Thermo Fisher Scientific, Waltham, USA
Heracell 240 CO_2 Incubator	Heraeus, Hanau, Germany
Herasafe HS 18 Safety Cabinet	Heraeus, Hanau, Germany
Inverted Laboratory Microscope DM IL LED	Leica, Wetzlar, Germany
LightCycler® 480 II Real-Time PCR Instrument	Roche, Basel, Switzerland
LightCycler® 480 Real-Time PCR Instrument	Roche, Basel, Switzerland
LSR II FACS-Analyzer	BD, Franklin Lakes, USA
MACSmix™ Tube Rotator	Miltenyi, Bergisch Gladbach, Germany
Mastercycler gradient thermal cycler	Eppendorf, Hamburg, Germany
Millipore Elix® 3 UV Water Purification system	Merck, Darmstadt, Germany
Mini-PROTEAN® Tetra Cell Casting Module with 15-well combs, 1.5 mm gel casting modules, casting stands and casting frames	Bio-Rad, Hercules, USA
Mini-PROTEAN® Tetra Vertical Electrophoresis Cell	Bio-Rad, Hercules, USA
Multiskan EX Microplate Reader	Thermo Fisher Scientific, Waltham, USA
NanoDrop 1000 Spectrophotometer	Thermo Fisher Scientific, Waltham, USA
Nanozoomer digital slide scanner	Hamamatsu, Hamamatsu City, Japan
Odyssey® Sa Infrared Imaging System	LI-COR, Lincoln, USA
pH meter CG842	Schott, Mainz, Germany
PIPETBOY acu Pipette Controller	Integra, Zizers, Switzerland
Power supply EV243	Consort, Turnhout, Belgium

QuadroMACS™ Separator	Miltenyi, Bergisch Gladbach, Germany
Refrigerator	Liebherr, Bulle, Switzerland
Repeater® M4 multipette	Eppendorf, Hamburg, Germany
Research® plus 0.1-2.5 µl pipette	Eppendorf, Hamburg, Germany
Research® plus 0.5-10 µl pipette	Eppendorf, Hamburg, Germany
Research® plus 100-1,000 µl pipette	Eppendorf, Hamburg, Germany
Research® plus 10-100 µl pipette	Eppendorf, Hamburg, Germany
Research® plus 20-200 µl pipette	Eppendorf, Hamburg, Germany
Research® plus 2-20 µl pipette	Eppendorf, Hamburg, Germany
Self-Contained Ice Machine AF124	Scotsman Ice Systems, Vernon Hills, USA
Thermomixer comfort	Eppendorf, Hamburg, Germany
TissueLyser Adapter Set 2 x 24	Qiagen, Hilden, Germany
TissueLyser MM300 Bead Mill	Retsch, Haan, Germany
Ultra-low temperature freezer	Thermo Fisher Scientific, Waltham, USA
Vortex Mixer	Neolab, Heidelberg, Germany
Western blot incubation box, black	LI-COR, Lincoln, USA
Wet/Tank electroblotting module	Biostep, Burkhardtsdorf, Germany
Xplorer® 50-1,000 µl electronic pipette	Eppendorf, Hamburg, Germany

2.2. Consumables

96-MicroWell Plates, Nunc-Immuno™	Thermo Fisher Scientific, Waltham, USA
96-well PCR plate, colorless	Biozym, Hessisch Oldendorf, Germany
BioCoat™ Flask T75 Collagen I coated	Corning, Corning, USA
C-Chip Counting Chamber, Neubauer improved	Merck, Darmstadt, Germany
Cell culture dish 60/15 mm, PS, sterile	Greiner Bio-One, Kremsmünster, Austria
Cell culture plate 24-well, PS, clear, with lid, sterile	Greiner Bio-One, Kremsmünster, Austria
Centrifuge Tube 15 ml, sterile	Greiner Bio-One, Kremsmünster, Austria
Centrifuge Tube 50 ml, sterile	Greiner Bio-One, Kremsmünster, Austria
ClipTip 12.5 µl, filter, sterile	Biozym, Hessisch Oldendorf, Germany
Column 2.5 ml, 35 µm filter pore size	MoBiTec, Göttingen, Germany

Combitips advanced® 0.1 ml, PCR clean	Eppendorf, Hamburg, Germany
Combitips advanced® 5 ml, sterile	Eppendorf, Hamburg, Germany
Cryo vials 2 ml, PP, round bottom	Greiner Bio-One, Kremsmünster, Austria
Falcon® 5 mL Round Bottom Polystyrene Test Tube	Corning, Corning, USA
Falcon® 5 mL Round Bottom Polystyrene Test Tube, sterile with snap-cap	Corning, Corning, USA
Injekt®-F solo fine dosage syringe 1 ml	B. Braun, Melsungen, Germany
LS Columns	Miltenyi, Bergisch Gladbach, Germany
Microplate 96-well, PS, F-bottom, clear	Greiner Bio-One, Kremsmünster, Austria
PCR 12-well CapStrips	Biozym, Hessisch Oldendorf, Germany
PCR 12-well SoftStrips	Biozym, Hessisch Oldendorf, Germany
Polyvinylidene difluoride (PVDF) membrane Immobilon-FL	Merck, Darmstadt, Germany
qPCR adhesive plate seals	Genaxxon, Ulm, Germany
Safe-Lock Tube 0.5 ml	Eppendorf, Hamburg, Germany
Safe-Lock Tube 1.5 ml	Eppendorf, Hamburg, Germany
Safe-Lock Tube 2.0 ml	Eppendorf, Hamburg, Germany
SafeSeal SurPhob Tips 1,250 µl, filter, sterile	Biozym, Hessisch Oldendorf, Germany
SafeSeal SurPhob Tips 200 µl XL, filter, sterile	Biozym, Hessisch Oldendorf, Germany
SafeSeal Tips Premium 10 µl, filter, sterile	Biozym, Hessisch Oldendorf, Germany
SafeSeal Tips Premium 2.5 µl, filter, sterile	Biozym, Hessisch Oldendorf, Germany
S-Monovette® 8.5 ml, CPDA1	Sarstedt, Nümbrecht, Germany
Stainless Steel Beads, 5 mm	Qiagen, Hilden, Germany
Sterican® single-use hypodermic needles 20 gauge	B. Braun, Melsungen, Germany
Stripette™ Serological Pipets 10 ml, sterile	Corning, Corning, USA
Stripette™ Serological Pipets 2 ml, sterile	Corning, Corning, USA
Stripette™ Serological Pipets 25 ml, sterile	Corning, Corning, USA
Stripette™ Serological Pipets 5 ml, sterile	Corning, Corning, USA
UltraPoint Graduated Filter Tip 100 µl, sterile	Starlab, Hamburg, Germany
Whatman Cellulose Chromatography Paper	GE Healthcare, Chicago, USA

2.3. Chemicals

1,4-Dithiothreitol (DTT)	Carl Roth, Karlsruhe, Germany
2-Propanol	Honeywell, Charlotte, USA
Acrylamide ROTIPHORESE®Gel 30 (37.5:1)	Carl Roth, Karlsruhe, Germany
Ammonium persulfate (APS)	Sigma-Aldrich, St. Louis, USA
Aqua ad injectabilia	B. Braun, Melsungen, Germany
AutoMACS Rinsing Solution (contains 2 mM EDTA in PBS pH 7.2)	Miltenyi, Bergisch Gladbach, Germany
Biocoll Separating Solution	Merck, Darmstadt, Germany
Bovine Serum Albumin (BSA), lyophilized	Sigma-Aldrich, St. Louis, USA
BSA, 10 % in PBS (MACS Stock Solution)	Miltenyi, Bergisch Gladbach, Germany
Bromophenol blue sodium salt	Carl Roth, Karlsruhe, Germany
CnT-Prime Basal Medium	CELLnTEC, Bern, Switzerland
cOmplete™ Protease Inhibitor Cocktail	Roche, Basel, Switzerland
Crystal violet	Carl Roth, Karlsruhe, Germany
CD4 MicroBeads	Miltenyi, Bergisch Gladbach, Germany
Dimethyl sulfoxide (DMSO) Cell culture grade	AppliChem, Darmstadt, Germany
Dispase II (neutral protease, grade II)	Roche, Basel, Switzerland
Dulbecco's Phosphate Buffered Saline (PBS)	Sigma-Aldrich, St. Louis, USA
Ethylenediamine tetraacetic acid (EDTA) disodium salt dihydrate, Titration complex III	Carl Roth, Karlsruhe, Germany
Ethanol absolute for analysis	AppliChem, Darmstadt, Germany
Fetal Bovine Serum (FBS)	Sigma-Aldrich, St. Louis, USA
Formaldehyde solution 37 %	Carl Roth, Karlsruhe, Germany
Gentamycin / Amphotericin B Solution (500x)	CELLnTEC, Bern, Switzerland
Glycerol	Sigma-Aldrich, St. Louis, USA
Glycine	Carl Roth, Karlsruhe, Germany
Hanks' Balanced Salt Solution (HBSS) with calcium and magnesium	Gibco, Karlsruhe, Germany
Hydrochloric acid fuming 37 % (HCl)	Carl Roth, Karlsruhe, Germany
Intercept® (PBS) Blocking Buffer	LI-COR, Lincoln, USA

Ionomycin calcium salt from *Streptomyces conglobatus*	Sigma-Aldrich, St. Louis, USA
MACS BSA Stock Solution	Miltenyi, Bergisch Gladbach, Germany
Methanol	VWR, Radnor, USA
MTT (3-(4,5-Dimethylthiazol-2-yl)-2,5-Diphenyl-tetrazolium Bromide)	Thermo Fisher Scientific, Waltham, USA
PageRuler™ Plus Prestained Protein Ladder, 10-250 kDa	Thermo Fisher Scientific, Waltham, USA
Penicillin/Streptomycin 10,000 U/10,000 µg/ml	Merck, Darmstadt, Germany
Phorbol 12-myristate 13-acetate (PMA)	Sigma-Aldrich, St. Louis, USA
PhosSTOP™	Roche, Basel, Switzerland
Protein G Sepharose® 4 Fast Flow	GE Healthcare, Chicago, USA
Protein Transport Inhibitor GolgiStop™	BD, Franklin Lakes, USA
RNAlater RNA Stabilization Reagent	Qiagen, Hilden, Germany
Roswell Park Memorial Institute (RPMI) 1640 Medium with L-alanyl-glutamine and sodium bicarbonate	Sigma-Aldrich, St. Louis, USA
Saponin	Carl Roth, Karlsruhe, Germany
SDS pellets	Carl Roth, Karlsruhe, Germany
Sodium carbonate (Na_2CO_3)	Carl Roth, Karlsruhe, Germany
Sodium fluoride (NaF)	Sigma-Aldrich, St. Louis, USA
Sodium hydroxide pearls (NaOH)	Carl Roth, Karlsruhe, Germany
Sodium hydroxide solution 4 N (NaOH)	Carl Roth, Karlsruhe, Germany
Supernatant from AK23 hybridoma cell line	Ritva Tikkanen, Giessen, Germany
Tetramethylethylenediamine (TEMED)	Carl Roth, Karlsruhe, Germany
Tris(hydroxymethyl)aminomethane (TRIS)	Carl Roth, Karlsruhe, Germany
tri-Sodium citrate dihydrate ($Na_3C_6H_5O_7$ x $2H_2O$)	Carl Roth, Karlsruhe, Germany
Triton® X 100	Carl Roth, Karlsruhe, Germany
Trypan Blue Solution 0.4 %	Thermo Fisher Scientific, Waltham, USA
Trypsin/EDTA Solution 0.05 %/0.02 % w/v	Merck, Darmstadt, Germany
Tween® 20 for synthesis	Merck, Darmstadt, Germany
UltraComp eBeads	eBioscience, San Diego, USA

Urea	Carl Roth, Karlsruhe, Germany
X-VIVO 15, serum-free, hematopoietic cell medium	Lonza, Basel, Switzerland

2.4. Kits

LightCycler® 480 Probes Master	Roche, Basel, Switzerland
Maxima First Strand cDNA Synthesis Kit for RT-qPCR	Thermo Fisher Scientific, Waltham, USA
peqGOLD MicroSpin Total RNA Kit (Safety-Line)	VWR, Radnor, USA
peqGOLD Total RNA Kit (Safety-Line)	VWR, Radnor, USA
ROTI®Quant universal Biuret solutions	Carl Roth, Karlsruhe, Germany
TURBO DNA-*free*™ Kit	Thermo Fisher Scientific, Waltham, USA

2.5. Antibodies

Table 2: Antibodies used for the stimulation of $CD4^+$ cells (BioLegend, San Diego, USA)

Antigen	**Clone**	**Coating concentration**
CD3	UCHT1	5 µg/ml
CD28	CD28.2	5 µg/ml

Table 3: Antibodies used for immunohistochemical staining (Cell Signaling, Danvers, USA)

Antibody	**Dilution**
Rabbit anti-Phospho-STAT1 (Tyr701), clone 58D6	1:500
Rabbit anti-Phospho-STAT3 (Tyr705), clone D3A7	1:400

Table 4: Antibodies used for multiparameter flow cytometry (BioLegend, San Diego, USA)

Antigen	Fluorochrome	Clone	Dilution
Isotype controls			
Mouse IgG1, κ	BV421	MOPC-21	1:20
Mouse IgG1, κ	BV510	MOPC-21	1:40
Mouse IgG2b, κ	FITC	MPC-11	1:100
Mouse IgG1, κ	PE	MOPC-21	1:200
Mouse IgG1, κ	PerCP-Cy5.5	MOPC-21	1:100
Mouse IgG1, κ	PE-Cy7	MOPC-21	1:40
Mouse IgG2b, κ	APC	MPC-11	1:200
Mouse IgG1, κ	APC-Cy7	MOPC-21	1:33
Mouse IgG1, κ	FITC	MOPC-21	1:125
T cell panel			
CXCR3	BV421	G025H7	1:20
CD4	BV510	RPA-T4	1:20
CD45RA	FITC	HI100	1:100
CXCR5	PE	J252D4	1:100
CD3	PerCP-Cy5.5	SK7	1:50
CD25	PE-Cy7	M-A251	1:20
CCR6	APC	G034E3	1:100
CD127	APC-Cy7	A019D5	1:50
Intracellular staining			
IL-17A	PE-Cy7	BL168	1:20
IFN-γ	APC-Cy7	4S.B3	1:20
IL-21	PerCP-Cy5.5	3A3-N2	1:20
IL-4	PE-Cy7	MP4-25D2	1:20
B cell panel			
CD19	FITC	HIB19	1:100
CD27	PE-Cy7	M-T271	1:50

Table 5: Primary and secondary antibodies used for immunoblot

Antibody	Dilution	Company
Mouse anti-Actin, clone C4	1:5,000	Merck, Darmstadt, Germany
Rabbit anti-Actin, clone 13E5	1:1,000	Cell Signaling, Danvers, USA
Rabbit anti-Phospho-STAT1 (Tyr701), clone 58D6	1:1,000	Cell Signaling, Danvers, USA
Rabbit anti-Phospho-STAT3 (Tyr705), polyclonal	1:1,000	Cell Signaling, Danvers, USA
Rabbit anti-Phospho-STAT4 (Tyr693), clone D2E4	1:1,000	Cell Signaling, Danvers, USA
Rabbit anti-Phospho-STAT5 (Tyr694), clone C71E5	1:1,000	Cell Signaling, Danvers, USA
Rabbit anti-Phospho-STAT6 (Tyr641), polyclonal	1:1,000	Cell Signaling, Danvers, USA
Rabbit anti-STAT1, polyclonal	1:1,000	Cell Signaling, Danvers, USA
Rabbit anti-STAT3, clone 79D7	1:1,000	Cell Signaling, Danvers, USA
Rabbit anti-STAT5, clone D2O6Y	1:1,000	Cell Signaling, Danvers, USA
Rabbit anti-Phospho-p38 MAPK (Thr180/Tyr182), clone D3F9	1:1,000	Cell Signaling, Danvers, USA
Rabbit anti-p38 MAPK, polyclonal	1:1,000	Cell Signaling, Danvers, USA
Mouse anti-Desmoglein 3, clone 5H10	1:1,000	Bio-Techne, Minneapolis, USA
IRDye® 680RD Goat anti-Mouse IgG	1:14,000	LI-COR, Lincoln, USA
IRDye® 800CW Goat anti-Rabbit IgG	1:14,000	LI-COR, Lincoln, USA

2.6. Recombinant proteins

Recombinant human Dsg3-Alexa Fluor 647	Robert Pollmann, Marburg, Germany
Recombinant human IFN-α (Roferon®-A)	Roche, Basel, Switzerland
Recombinant human IL-2 (PROLEUKIN® S)	Novartis, Basel, Switzerland
Recombinant human IL-21	PeproTech, Rocky Hill, USA
Recombinant human IL-4	Bio-Techne, Minneapolis, USA
Recombinant human IL-6	PeproTech, Rocky Hill, USA

2.7. Primers and probes

Table 6: Sequences of human primer and probes (TIB MOLBIOL, Berlin, Germany)

Gene	Primer	Probe
ACTB	for AgCCTCgCCTTTgCCgA rev CTggTgCCTggggCg	CCgCCgCCCgTCCACACCCgCC
POLR2A	for gTggAgATCTTCACggTgCT rev gTgCggCTgCTTCCATAA	TACCACgTCATCTCCTTTgATggCTCCTAT
IL1A	for gAAggCTgCATggATCAATCTgT rev gTgAggTACTgATCATTggCTCg	CgggAAggTTCTgAAgAAgAgACggT
IL1B	for CAgggACAggATATggAgCAA rev ATgTACCAgTTggggAACTg	AgAATCTgTACCTgTCCTgCgTgTTgAA
IL4	for ACAgAgCAgAAgACTCTgTgCA rev CCTTCTCAgTTgTgTTCTTggA	AgATgTCTgTTACggTCAACTCggT
IL10	for gCTACggCgCTgTCATCgA rev AgATgCCTTTCTCTTggAgCTTA	ACCTgCTCCACggCCTTgCT
IL12B	for CTgATATTTTAAAggACCAgAAAgAAC rev gTCAAATCAgTACTgATTgTCgTCA	CTggACgTTTCACCTgCTggTgg
IL17A	for AACCTgAACATCCATAACCggAA rev gTCCTCATTgCggTggAgA	CCAATACCAATCCCAAAAggTCCTCAgA
IL19	for CTgCggCAATgTCAggAAC rev CgTggACCTCCAgCTgATCATA	ATgACTCTggTggCATTggTggC
IL21	for gACACTggTCCACAAATCAAgC rev CTgACCACTCACAgTTTgTCTCTAC	TCAAgATCgCCACATgATTAgAATgCgTC
IL22	for TgATgACCTgCATATCCAgAggAAT rev ATCCAgTTCTCCAATTgCTTTgATC	TgCAAAAgCTgAAggACACAgTgAAAAA
IL23A	for TAgTgggACACATggATCTAAg rev gCAAgCAgAACTgACTgTTg	CCATCTCCACACTggATATggggA
IL24	for AgCATTCAAACAgTTggACgTA rev TCTAgACATTCAgAgCTTgTAgAATTT	CAAgggCTTTggTCAgAgCTgC
IFNG	for gCATCCAAAAgAgTgTggAg rev ggACATTCAAgTCAgTTACCgA	ATCAAggAAgACATgAATgTCAAgTTTTTCAA
CXCR5	for TgCAgTCATCTTgACCAAgCA rev TCACgCTTCCTCAggTCACT	CTggCTCTgACCgAAACAgCg

2.8. Inhibitors (stock solution 10 mM in DMSO)

Selective JAK3 inhibitors and Skepinone-L were kindly provided by Michael Forster from the group of Stefan Laufer from the Pharmaceutical Chemistry Department of the Tübingen University.

Tofacitinib Citrate (pan-JAK)	Selleck Chemicals, Houston, USA
FM-409 (JAK3)	Michael Forster, Tübingen, Germany
FM-381 (JAK3)	Michael Forster, Tübingen, Germany
FM-492 (JAK3)	Michael Forster, Tübingen, Germany
NIBR3049 (JAK3)	Michael Forster, Tübingen, Germany
FM-481 (JAK3)	Michael Forster, Tübingen, Germany
FM-392 (JAK3)	Michael Forster, Tübingen, Germany
PF-04965842 (JAK1)	Sigma-Aldrich, St. Louis, USA
Skepinone-L (p38 MAPK)	Michael Forster, Tübingen, Germany

2.9. Buffers, media and solutions

70 % Ethanol	Ethanol	70 %
	Aqua ad injectabilia	
APS solution	APS	10 % (w/v)
	H_2O	
CnT complete medium	Gentamycin	10 µg/ml
	Amphotericin B	0.25 µg/ml
	CnT-Prime Basal Medium	
CnT differentiation medium	$CaCl_2$	1.8 mM
	CnT complete medium	

Crystal violet staining solution	Crystal violet	0.5 % (w/v)
	Methanol	20 %
	H_2O	
Dispase II (dissociation assay)	Dispase II	2.5 U/ml
	HBSS	
Dispase II (primary keratinocyte isolation)	Dispase II	12 U/ml
	CnT complete medium	
EDTA buffer pH 8.0	EDTA	0.5 M
	H_2O	
	Adjust pH to 8.0 with NaOH.	
Elution buffer	tri-Sodium citrate dihydrate	20 mM
	H_2O	
	Adjust pH to 2.4 with HCl.	
Fixation buffer (dissociation assay)	Formaldehyde	8 %
	HBSS	
Fixation buffer (intracellular flow cytometry)	Formaldehyde	2 %
	PBS	
Freezing medium	DMSO	10 %
	CnT Prime Basal Medium	
MACS buffer	BSA (MACS Stock Solution)	0.5 %
	AutoMACS Rinsing Solution	
MTT staining solution	MTT	5 mg/ml
	HBSS	

Neutralization buffer	Sodium carbonate	2 M
	H_2O	
	Adjust pH to 9.0 with HCl.	
PBST	Tween® 20	0.1 %
	PBS	
Permeabilization buffer	Saponin	0.5 % (w/v)
	MACS buffer	
Protein lysis buffer	EDTA	1 mM
	Tween® 20	0.005 %
	Triton® X 100	0.5 %
	Sodium fluoride	5 mM
	Urea	6 M
	cOmplete™	1x
	PhosSTOP™	1x
	H_2O	
Resolving gel buffer	TRIS	1.5 M
	SDS	0.4 % (w/v)
	H_2O	
	Adjust pH to 8.8 with HCl.	
RPMI complete medium	FBS	10 %
	Penicillin	100 U/ml
	Streptomycin	100 µg/ml
	RPMI 1640 Medium	

SDS-PAGE running buffer	TRIS	25 mM
	Glycin	200 mM
	SDS	0.1 % (w/v)
	H_2O	
	Adjust pH to 8.3 - 8.5 with HCl.	
SDS-PAGE sample buffer 5x	Glycerol	50 %
	DTT	250 mM
	SDS	5 % (w/v)
	Bromophenol blue	0.05 % (w/v)
	TRIS buffer pH 6.8	125 mM
	H_2O	
Stacking gel buffer	TRIS buffer pH 6.8	0.5 M
	SDS	0.4 % (w/v)
	H_2O	
Standard for protein quantification	BSA, lyophilized	2 mg/ml
	PBS	
Stripping buffer	NaOH	0.5 M
	H_2O	
TE buffer pH 8.0	TRIS buffer pH 8.0	10 mM
	EDTA buffer pH 8.0	1 mM
	H_2O	
TRIS buffer pH 8.0	TRIS	1 M
	H_2O	
	Adjust pH to 8.0 with HCl.	

TRIS buffer pH 6.8	TRIS	1 M
	H_2O	
	Adjust pH to 6.8 with HCl.	
Western blot transfer buffer	TRIS	250 mM
	Glycin	200 mM
	Methanol	20 %
	H_2O	
	Adjust pH to 8.5 with HCl.	

2.10. Software

Table 7: Software versions used for data analysis

Software	Version	Company
Adobe Illustrator CS6	16.0.3	Adobe Inc., San Jose, USA
Adobe Photoshop CS6	13.0.1	Adobe Inc., San Jose, USA
Ascent Software for Multiskan	2.6	Thermo Fisher Scientific, Waltham, USA
BD FACSDiva™	6.1.3	BD, Franklin Lakes, USA
FastQC	0.11.8	Babraham Institute, Cambridge, UK
FlowJo	10.0.7	BD, Franklin Lakes, USA
GraphPad Prism	8.1.0	GraphPad Software, San Diego, USA
Image Studio™ Lite	3.1.4	LI-COR, Lincoln, USA
ImageJ Fiji	1.53c	Wayne Rasband, NIH, Bethesda, USA
LightCycler® 480 Software	1.5.1.62	Roche, Basel, Switzerland
MultiQC	1.7	Phil Ewels, Stockholm, Sweden
NanoDrop 1000 Software	3.7.1	Thermo Fisher Scientific, Waltham, USA
NDP.view2	2.7.39	Hamamatsu, Hamamatsu City, Japan
Odyssey® Sa Software	1.1.7	LI-COR, Lincoln, USA
R	3.5.1	CRAN
Salmon	0.12.0	Rob Patro, Stony Brook, USA

2.11. Patient samples

A total of 76 PV and 16 PF patients were included in this study. 47 of the patients were recruited in Tübingen and 45 in Marburg. Diagnosis of pemphigus was determined by clinical evidence of blisters or erosions and direct immunofluorescence microscopy of perilesional skin biopsies for demonstration of intercellular IgG and complement deposition. Furthermore, serum autoantibodies were detected by indirect immunofluorescence microscopy of monkey esophagus as well as by Dsg1/Dsg3-specific ELISA. Patient cohorts were classified depending on their status of disease according to Pfütze et al. into acute (onset with ≤ 3 month duration), chronic (active disease with a duration of ≥ 3 months) and patients in remission (no appearance of new clinical lesions for ≥ 1 month) [145]. Detailed data on epidemiology, clinical status and desmoglein levels at the time of analyses are shown in Table A1, Table A2, Table A3 and Table A4 in the appendix.

Punch biopsies of 4 mm diameter were taken from lesional or perilesional skin of pemphigus patients. Perilesional skin for RNA analysis was taken 1-2 cm distant from the corresponding lesion, while perilesional skin for immunohistochemical (IHC) stainings was obtained at the interface of the lesion, eventually including a part of the blister. For the remission group, biopsies from lesional skin were taken only from patients presenting chronic non-debilitating erythematous lesions in which disease remission was achieved either under or off treatment. Healthy skin samples were obtained from adult control patients, who underwent surgical procedures for non-inflammatory diseases. For RNA isolation, all skin samples were incubated over night at 4 °C in RNAlater, transferred into fresh 2.0 ml tubes and stored at -80 °C. Tissue samples from patients recruited in Marburg were shipped to Tübingen for analysis. Tissue for IHC staining were fixed with paraformaldehyde and embedded in paraffin. Peripheral blood from patients and control individuals (healthy individuals or patients with non-inflammatory disease and no immunosuppressive therapy) was collected in citrate-phosphate-dextrose-adenine (CPDA) containing tubes and processed directly. Flow cytometric measurement of 40 patients and 14 control individuals recruited in Marburg was performed by Farzan Solimani, Carolin Baum, Robert Pollmann and Manuel Schulze-Dasbeck from the group of Christian Möbs at the Philipps-University Marburg and raw data was analyzed in Tübingen. The study was approved by the Ethics Committees of the Eberhard Karls University Tübingen (protocol

759/2016BO2) and the Medical Faculty of the Philipps-University Marburg (Az.: 20/14) and patients gave their written informed consent for participating in this study.

Tissue samples of seven individuals suffering from psoriasis vulgaris were collected and proceeded for IHC staining as described above for pemphigus and healthy skin. Each patient signed an informed consent and ethical approval was obtained by the ethics committee of the Eberhard Karls University Tübingen (protocol 309/2017BO2).

2.12. Human cell culture

Primary normal human epidermal keratinocytes (NHEK) were isolated from discarded healthy foreskin tissue. The isolation of primary human cells was approved by the medical ethical committee of the Eberhard Karls University (protocol 331/2010BO2) and performed in accordance with the Declaration of Helsinki principles.

Peripheral blood cells for $CD4^+$ cytokine stimulation assays were isolated from leukoreduction system chambers, which were obtained from the Centre for Clinical Transfusion Medicine in Tübingen, where they are typically discarded after platelet donations.

3. METHODS

3.1. RNA isolation

Total RNA from human skin was isolated using PeqGOLD Total RNA Kit. Frozen tissue was placed into a 2.0 ml tube containing one frozen stainless steel bead with 5 mm diameter. The tube was placed into the TissueLyser Adapter and the TissueLyser was operated for 40 s at 30 Hz. All following steps were performed at room temperature (RT). 600 µl RNA Lysis Buffer T was added to the tube and the tissue was homogenized two more times for 40 s at 30 Hz followed by centrifugation for 3 min at full speed to remove debris. The lysate was transferred directly into a DNA Removing Column placed in a 2.0 ml collection tube and the further procedure was performed according to the manufacturer's protocol [146]. To elute the RNA, the column was placed into a fresh 1.5 ml tube, 50 µl RNase-free H_2O was added directly to the binding matrix in the column and incubated for 5 min followed by centrifugation for 1 min at 5,000 x g. The column was discarded, RNA concentration was quantified using the NanoDrop 1000 spectrophotometer system and the RNA was stored at -80 °C.

Total RNA from sorted cells was isolated using peqGOLD MicroSpin Total RNA Kit. The sorted cells were transferred from the collection tubes into 1.5 ml tubes and centrifuged at 400 x g for 5 min at RT. The supernatant was carefully removed and 300 µl RNA Lysis Buffer T was added. By passing the lysate through a 20 gauge needle ten times with a 1 ml syringe the pellet was homogenized. The lysate was transferred into a DNA Removing Column placed in a 2.0 ml collection tube and the protocol was proceeded according to the manufacturer's instructions [147] with the PerfectBind MS RNA Column and 20 µl elution volume.

To assess all transcript variants of *CXCR5*, the TaqMan assay had to be designed on one exon, so that it was not possible to span or flank introns. For this reason, remaining contaminating genomic DNA was removed from the isolated RNA using TURBO DNA-*free*™ Kit containing the DNase enzyme, buffer and inactivation reagent. The procedure was performed following the manufacturer’s protocol [148].

3.2. Next-generation sequencing and bioinformatics

Total RNA from healthy and patient skin was isolated and submitted to the NGS Competence Center Tübingen (NCCT) for next-generation sequencing (NGS) analysis, a high throughput technology allowing transcriptome profiling and quantification. Sequencing data was produced on Illumina NextSeq 500 system in single-end sequencing mode (sequence length = 75 bp). Raw data was analyzed with the help of Tobias Tekath from the Biomedical Informatics group of the Institute of Medical Informatics at the University of Münster. Thorough quality control for the sequenced data was performed with FastQC [149] and MultiQC [150]. Read-mapping and quantification was performed with Salmon [151] using the Gencode [152] human reference transcriptome v29. The Salmon quasi-index was created with a default k-mer length of 31 and the *--gencode* flag. Subsequent quantification was performed while accounting for sequence-specific biases like random hexamer priming, which often results in lower base-call quality of the first few bases of a read. Additional parameters included *--validateMappings* and *--rangeFactorizationBins 4* to potentially improve the quantification accuracy. The mean transcriptomic mapping rate was 89.2 % with a standard deviation of 2 %. The transcript counts were summarized to gene-level with tximport [153] and supplementary annotation data from Ensembl [154] through the biomaRt-package [155, 156]. During this summarization step, allosomal and mitochondrial genes were excluded to decrease (sex-specific) biases. The differential expression analysis between pemphigus and healthy skin samples was performed on the gene-level counts by DESeq2 [157]. The requirement for a valid differentially expressed gene (DEG) was an absolute $\log_2$ fold change significantly greater than 1 with an adjusted *p*-value below 0.05. Furthermore, independent hypothesis weighting (IHW) was used to increase the statistical power [158]. Gene-set enrichment analysis was performed for the DEGs with goseq [159], both for Gene Ontology [159, 160] terms and KEGG [161, 162] pathways. The goseq enrichment is accounting for selection bias via the median transcript length of a gene. The association of a gene with a specific pathway/term was directly pulled from the KEGG online resource or Ensembl biomart, respectively. Results were visualized with the help of cowplot [163], ggplot2 [164], ggpubr [165], GOplot [166], Pathview [167] and pheatmap [168]. For visualization purposes, shrunken $\log_2$ fold change values have been computed using the *adaptive t prior shrinkage estimator* from the apeglm [169] package and expression values have been variance stabilized with the *rlog*-function of DESeq2. R session information can be found in the appendix.

3.3. cDNA synthesis

Reverse transcription from RNA into cDNA was performed with Maxima First Strand cDNA Synthesis Kit for RT-qPCR. Maxima Enzyme Mix contained M-MuLV reverse transcriptase and RNase inhibitor. 5x Reaction Mix contained the reaction buffer, dNTPs, oligo$(dT)_{18}$ and random hexamer primers to prime synthesis of first strand cDNA. The template RNA was denatured for 5 min at 65 °C and cooled on ice before pipetting the following reaction into a 0.5 ml tube:

Reaction Mix (5x)	4 µl
Maxima Enzyme Mix	2 µl
Template RNA	1,000 ng
Nuclease-free water	to 20 µl
Total volume	20 µl

If there was less RNA than 1,000 ng, the maximum volume of template RNA (14 µl) was used. This reaction was incubated for 10 min at 25 °C for primer extension followed by synthesis of cDNA for 30 min at 50 °C. Heating at 85 °C for 5 min terminated the reaction by inactivating the enzyme. The product was stored at -80 °C.

3.4. Quantitative real-time PCR (qPCR)

The polymerase chain reaction (PCR) is a method for the specific in vitro multiplication of any DNA section. First, the DNA double strand is separated by heating to 95 °C in two single strands (denaturation). Thereafter, the hybridization of the primer (annealing) takes place at reduced temperature. Starting from the primers, complementary DNA strands are synthesized in the next step (elongation). By repeating this reaction sequence, there is an exponential increase in the DNA fragment that lies between the primers. The quantitative real-time PCR (qPCR) allows in addition to the duplication the quantification of the DNA. By using fluorescent dyes, the increase of the amount of PCR product can be detected in real time during each PCR cycle.

Relative mRNA expression was determined by qPCR using Probes Master and TaqMan® probes for the Roche LightCycler® 480 system. According to the fluorescence resonance energy transfer (FRET) principle the PCR product was detected by specific hydrolysis probes, which

were marked with a fluorescent reporter (fluorescein, FAM) and a quencher of fluorescence (BlackBerry® Quencher, BBQ). While the probe was intact, the quencher was close to the reporter and any fluorescence signal was suppressed. During amplification, the probe was cleaved by the 5'-3'-exonuclease activity of the Taq polymerase (contained in Probes Master) and the reporter was released. An increase of PCR product caused a proportional increase in fluorescence signal. The fractional PCR cycle where the amplification curve met the threshold line was used for quantification (quantification cycle, C_q).

In duplicates, the following reaction was pipetted per well of a 96-well PCR plate:

Probes Master (2x)	5.0 µl
Nuclease-free water	2.5 µl
Forward primer (20x)	0.5 µl
Reverse primer (20x)	0.5 µl
Hydrolysis probe (20x)	0.5 µl
cDNA template	1.0 µl
Total volume	10 µl

The plate was sealed with sealing foil and centrifuged for 5 min at 400 x g. The following PCR parameters were programmed for the LightCycler® 480 system PCR run:

Table 8: qPCR parameters

Step		Temperature	Time	Cycles	Analysis Mode
Enzyme activation		95 °C	10 min	1	None
Amplification	Denaturation	95 °C	10 s	50	Quantification
	Annealing and elongation	60 °C	20 s		
Cool		40 °C		1	None

ACTB and *POLR2A* were used as reference genes for the analysis of human skin samples. A pool of healthy skin cDNA (n=10) served as control and was set to 1 for normalization. For gene expression analysis of T cell subsets, the reference gene *POLR2A* was used.

Relative gene expression was calculated according to the $2^{-\Delta\Delta Cq}$ method [170]:

$\Delta C_q = C_q$ (target gene) - C_q (reference gene)

$\Delta\Delta C_q = \Delta C_q$ (treatment) - ΔC_q (control)

Relative expression = $2^{-\Delta\Delta Cq}$

3.5. PBMC isolation

Peripheral blood mononuclear cells (PBMCs) were isolated from whole blood by density gradient centrifugation. Peripheral blood was collected in CPDA-monovettes, transferred into a 50 ml tube and diluted 1:2 with PBS. 12 ml Biocoll separating solution were pipetted in a 50 ml tube and carefully overlaid with 20 ml of blood-PBS mixture. The tube was centrifuged with the acceleration and brake set to the lowest level for 30 min at 400 x g and RT. Cells with higher densities (granulocytes and erythrocytes) sedimented at the bottom of the tube during centrifugation. The PBMCs (lymphocytes and monocytes) settled at the interface between the density gradient medium and the plasma, from which they were carefully collected into a 15 ml tube and washed twice with PBS: the tube was filled up with PBS, centrifuged at 400 x g for 5 min at RT, the supernatant was discarded and the pellet was resuspended in PBS. After the second wash step, the cells were resuspended in 1 ml MACS buffer, the cell number was determined and the cells were kept on ice until further use.

3.6. Determination of cell number

Cell number was determined using Neubauer improved counting chambers. The cells were diluted with trypan blue to selectively stain dead cells and pipetted into the counting chamber. The unstained vital cells in the four corner squares were counted and the cell number was calculated as follows:

$$\frac{\text{number of cells}}{\text{ml}} = \frac{\text{number of counted cells}}{\text{number of squares}} \text{ x dilution factor x } 10{,}000$$

3.7. Flow cytometry

Detection of antigen expression on cell surfaces was performed by immunofluorescent staining of cells for flow cytometric analysis. In the process, the cells are characterized based on the forward and side scattering of light with respect to their size and granularity. At the same time, the expression of antigens is determined with fluorochrome-labeled antibodies by excitation of the fluorochrome by a laser and detection of the emitted fluorescent light.

After determination of the cell number, the concentration of PBMCs was set to 1×10^7 cells/ml. Per test, 1×10^6 cells in 100 µl volume were pipetted into 5 ml round bottom polystyrene tubes and antibodies were added as indicated in Table 4. The optimal antibody dilution was determined by titration of each antibody and isotype controls were used to ensure the detected signal was due to specific binding. After incubation for 30 min at 4 °C in the dark the cells were washed with 1 ml MACS buffer, the supernatant was discarded and cells were resuspended in 100 µl MACS buffer. Stained cells were kept on ice until measurement by BD LSR II cytometer with BD FACSDiva™ software and compensation was set up using UltraComp eBeads. Analysis of generated data was performed with FlowJo software.

Characterization of the T cell subsets in blood samples was determined based on the expression of surface receptors in an 8-color flow cytometry analysis adapted from Morita et al. [171]. Combination of these surface markers allowed for subdivision of $CD3^+$ $CD4^+$ $CD45RA^-$ $CXCR5^-$ T helper (Th) and $CD3^+$ $CD4^+$ $CD45RA^-$ $CXCR5^+$ follicular T helper (Tfh) cells. The expression of CXCR3 and CCR6 helped to further distinguish between Th1 ($CXCR3^+$ $CCR6^-$), Th2 ($CXCR3^-$ $CCR6^-$), Th17 ($CXCR3^-$ $CCR6^+$) and Th17.1 cells ($CXCR3^+$ $CCR6^+$). $CXCR5^+$ Tfh cell subsets were subdivided according to their Th-like profile and regulatory T (Treg) cells and T follicular regulatory (Tfr) cells were identified by the markers CD25 and CD127 (Figure 8).

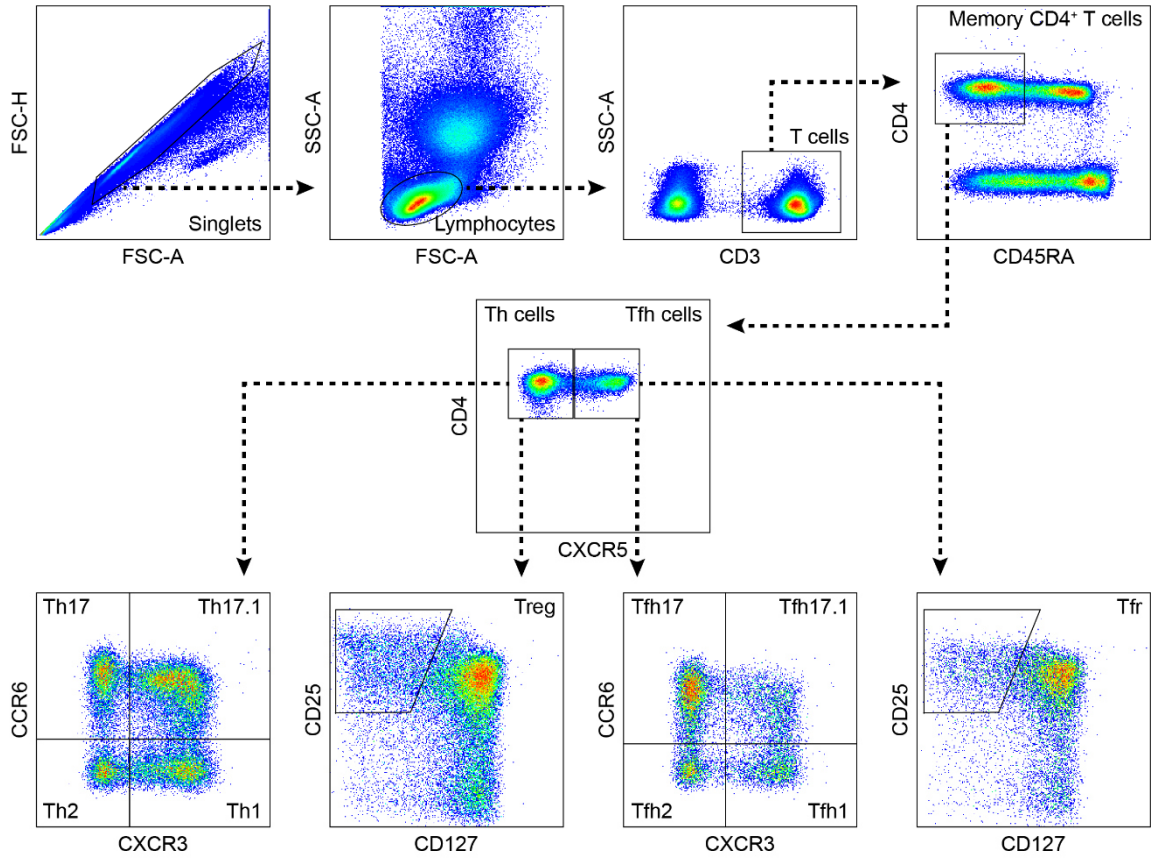

Figure 8: Gating strategy for multi-color flow cytometric analysis of both conventional CD3⁺ CD4⁺ CXCR5⁻ T helper and CD3⁺ CD4⁺ CXCR5⁺ follicular T helper cell subsets. Further characterization of T cell subpopulations: CXCR3⁺ CCR6⁻ for Th1 and Tfh1, CXCR3⁻ CCR6⁻ for Th2 and Tfh2, CXCR3⁻ CCR6⁺ for Th17 and Tfh17, CXCR3⁺ CCR6⁺ for Th17.1 and Tfh17.1, CD127$^{low/-}$ CD25⁺ for Treg and Tfr.

Identification of autoreactive B cell populations was performed by using 2 µl/test (1:50) of fluorochrome-labeled recombinant human Dsg3 protein, which was kindly provided by Robert Pollmann from the Philipps-University Marburg [143]. CD19⁺ Dsg3⁺ autoreactive B cells and CD19⁺ CD27⁺ Dsg3⁺ autoreactive memory B cells were distinguished by 3-color flow cytometric analysis following the gating strategy shown in Figure 9.

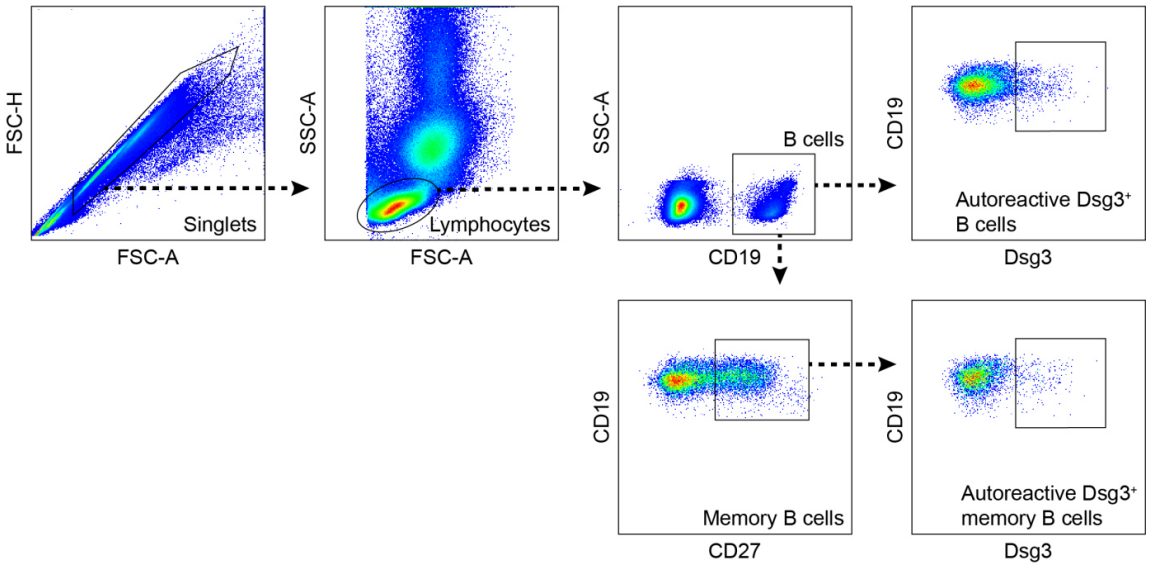

Figure 9: Gating strategy for the identification of Dsg3-reactive B cells. Characterization of autoreactive CD19$^+$ Dsg3$^+$ B cells and autoreactive CD19$^+$ CD27$^+$ Dsg3$^+$ memory B cells using fluorochrome-labeled recombinant Dsg3 protein.

3.8. Intracellular flow cytometry

For analysis of intracellular cytokine expression, 4 x 10^6 cells were stained with the surface markers CD4, CD45RA, CXCR5, CCR6 and CXCR3 as described before in sterile 5 ml round bottom polystyrene tubes. After antibody incubation, the cells were washed with 2 ml PBS, the cell pellet was resuspended in 2 ml RPMI complete medium and pipetted into a 24-well cell culture plate with 1 ml/well. In order to induce cytokine production, the cells were stimulated with 50 ng/ml PMA and 1 µg/ml Ionomycin for 4 h at 37 °C and 5 % CO_2. Secretion of cytokines was blocked by adding 1 µl/ml protein transport inhibitor. After stimulation, the cell suspension was transferred into a 15 ml tube and washed with 2 ml PBS. The cell pellet was resuspended in 2 ml fixation buffer and incubated for 10 min at RT in the dark followed by washing with 2 ml permeabilization buffer. The supernatant was discarded, the fixed cells were resuspended in 200 µl permeabilization buffer and divided into two tubes containing 100 µl/tube. Antibodies for IL-17A and IFN-g were added to one tube and antibodies for IL-4 and IL-21 were added to the other tube. After incubation for 30 min at RT in the dark, the cells were washed with 1 ml MACS buffer, resuspended in 100 µl MACS buffer, and stained cells were kept at 4 °C in the dark until measurement. The cytokine production of distinct T cell populations was determined by including the indicated markers to the gating strategy for Th and Tfh cell subsets as shown in Figure 8. A representative analysis of cytokine-producing Th

cells is demonstrated in Figure 10 for $CD4^+$ $CXCR5^-$ T cell subsets. Analysis of $CXCR5^+$ Tfh cell subgroups was performed accordingly.

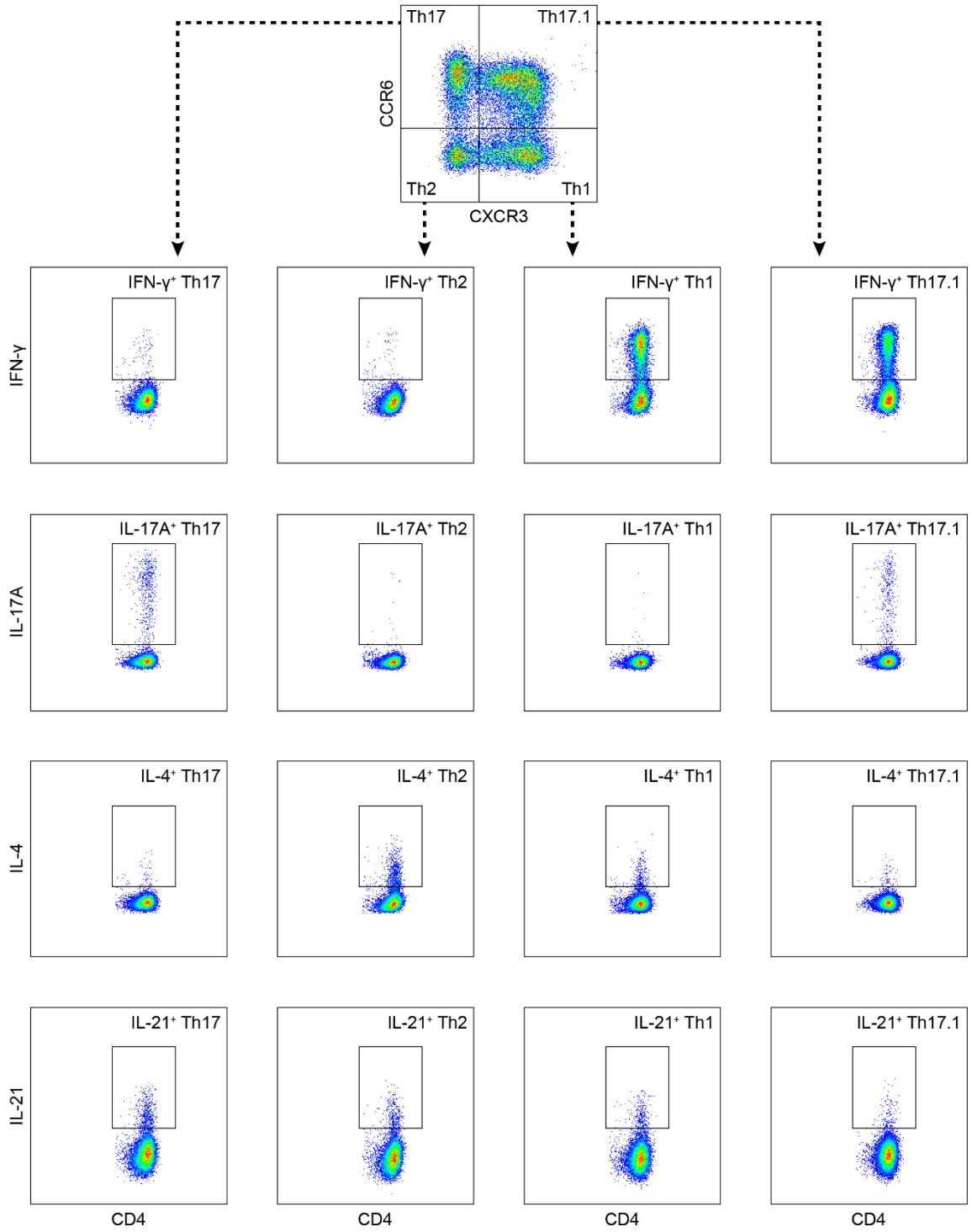

Figure 10: Representative analysis of cytokine-producing $CXCR5^-$ T helper cell subsets by intracellular flow cytometry. Distinct $CD4^+$ Th subsets were identified according to the gating strategy shown in Figure 8, and cytokine-producing cells were gated within the respective subsets. $CXCR5^+$ follicular T helper cell populations were analyzed accordingly.

3.9. Cell sorting

Fluorescence-activated cell sorting (FACS) was used for isolation of different T cell populations from PBMCs. FACS is a subform of flow cytometry where the cells can be sorted by size, granularity and fluorescence. Individual drops of liquid, ideally with one cell per drop, are analyzed by flow cytometry and based on the measured parameters electrically charged. Deflection plates attract or repel the single drops accordingly into different collection tubes.

To achieve an appropriate number of sorted cells, 10 x 10^6 cells (≙ 10 tests) were stained for the sorting experiments in 1 ml MACS buffer as previously described for flow cytometry. The cells were sorted into 5 ml round bottom polystyrene tubes containing 500 µl MACS buffer and the tubes with sorted cells were kept on ice until RNA isolation.

3.10. Preamplification of cDNA for qPCR

Due to low amounts of RNA obtained from sorted cells, preamplification of cDNA was performed before quantitative real-time PCR. Selected forward and reverse primers were pooled and diluted with TE buffer to a final concentration of 0.2x per primer. The following preamplification reaction was prepared in 0.2 ml PCR strips:

Probes Master (2x)	25.0 µl
Pooled primer mix (0.2x)	12.5 µl
cDNA template	12.5 µl
Total volume	50 µl

The thermal cycling conditions were set up for the preamplification reaction as shown in Table 9 and the product was diluted 1:20 in TE buffer. To ensure that all amplicons were amplified uniformly without bias, preamplification uniformity check was performed for each gene by comparing amplification of non-preamplified cDNA to amplification of preamplified cDNA. Gene expression was determined as described for skin samples. *POLR2A* was used as reference gene.

Table 9: Thermal cycler setup for the preamplification reaction

Step		Temperature	Time	Cycles
Enzyme activation		95 °C	10 min	1
Amplification	Denaturation	95 °C	15 s	14
	Annealing and elongation	60 °C	4 min	
Enzyme inactivation		99 °C	10 min	1
Cool		4 °C		Hold

3.11. CD4⁺ T cell cytokine stimulation assay

PBMCs were isolated from leukoreduction system chambers as described before. Th cells were purified from PBMCs by magnetic cell separation (MACS) technology using CD4 MicroBeads and LS columns following the manufacturer's instructions [172]. In this method, the $CD4^+$ cells were magnetically labeled and then loaded on a column, which was placed in a magnetic field. The labeled cells retained within the column, while all unlabeled cells ran through. After removing the column from the magnetic field, the $CD4^+$ cells were eluted as the positively selected fraction. The purity of isolated cells was >98 % as determined by CD4 staining and flow cytometry. Isolated cells were counted followed by centrifugation for 5 min at 400 x g and RT and the supernatant was discarded. The pellet was resuspended in X-VIVO 15 medium and cell number was set to 2 x 10^6 c/ml. 24-well cell culture plates were coated with 5 µg/ml of each anti-CD3 and anti-CD28 antibody in 300 µl PBS over night at 4 °C or for at least 2 h at 37 °C. The liquid was removed from the wells and 2 x 10^6 $CD4^+$ cells (1 ml cell suspension) were added per well. After three days of activation with the plate-bound anti-CD3 and anti-CD28 antibodies at 37 °C and 5 % CO_2 the cells were further expanded for three days by transferring the cells from one well into two wells each containing 500 µl fresh medium supplemented with 6 ng/ml IL-2, resulting in a final concentration of 3 ng/ml IL-2 per well. If required, the cells were expanded with 3 ng/ml IL-2 for three more days. After expansion, the T cells were washed three times with medium, the cell number was set to 2 x 10^6 c/ml and 2 x 10^6 T cells per well were rested in fresh medium overnight. For each condition, at least two wells were incubated with the indicated concentrations of JAKi in DMSO or DMSO alone (control condition) for 1 h and then stimulated with either 50 ng/ml IL-2, 50 ng/ml IL-4, 50 ng/ml IL-6, 1,000 U/ml IFN-α or 50-ng/ml IL-21 for 30 min. After stimulation, the cells of each condition

were pooled and washed with PBS followed by lysis of the cell pellet in 100 µl protein lysis buffer. Further homogenization was achieved by freezing the lysate in liquid nitrogen and thaw at RT for a total of three freeze/thaw cycles. The lysates were centrifuged at full speed for 3 min, the protein containing supernatant was transferred into fresh tubes, protein concentration was determined and lysate was kept at -80 °C until Western Blot analysis. For investigation of mRNA expression, the cells were isolated, pre-incubated for 1 h with JAKi and subsequently transferred into wells coated with CD3/CD28. The cells were further stimulated with 50 ng/ml IL-21 for 24 h followed by washing with PBS and lysis in 400 µl RNA Lysis Buffer T. The lysates were stored at -80 °C until RNA isolation using the PeqGOLD Total RNA Kit.

3.12. Keratinocyte culture

NHEK were isolated from healthy foreskin tissue by separating the epidermal layer from the dermis. Therefore, the tissue was cut into small pieces and placed into a 6 cm cell culture dish with the epidermis facing upwards. The cell culture dish was flooded with dispase II solution so that the dermis was submerged and the epidermis remained at the air surface. After incubation over night at 4 °C, the epidermal layer was stripped off, placed into a 6 cm cell culture dish containing 5 ml trypsin/EDTA, cut into smaller pieces and incubated for 30 min at 37 °C. Trypsin activity was stopped by adding 10 ml RPMI complete medium to the cell culture dish and the epidermis was passed through a 100 µm cell strainer to achieve a single cell suspension. After centrifugation for 5 min at 400 x g and RT, the cell pellet was resuspended in 10 ml CnT complete medium, transferred into a T75 collagen coated cell culture flask and cultured at 37 °C and 5 % CO_2. When 90 % confluence was reached, the cells were subcultured or frozen. The medium was discarded and keratinocyte monolayer was rinsed with PBS. In order to detach cells from the surface and obtain single cells, 3 ml trypsin/EDTA was added to the flask and incubated for 5 to 10 min at 37 °C while observing the detachment under the microscope. When >90 % of the cells have detached, 7 ml RPMI complete medium was added to the flask to stop enzyme activity and cell suspension was transferred into a 50 ml centrifuge tube. After centrifugation at 400 x g and RT for 5 min, the cell pellet was resuspended in 5 ml CnT complete medium for further cultivation and 1 ml was pipetted into a T75 collagen coated cell culture flask containing 9 ml CnT complete medium (passage 1). For cryopreservation, the

cell pellet was resuspended in 3 ml ice cold freezing medium. Portions of 1 ml were frozen in cryovials at -80 °C using a freezing container to provide a freezing rate of 1 °C per minute. Keratinocytes were thawed by warming the cryovial at 37 °C for 1 minute and transferring the cells into a 50 ml centrifuge tube containing 9 ml CnT complete medium. The cells were centrifuged at 400 x g for 5 min at RT, pellet was resuspended in 10 ml CnT complete medium and cell suspension was transferred into a T75 collagen coated cell culture flask (passage 1). Experiments were performed at passages 2 to 4.

3.13. Purification of AK23 from hybridoma cell culture supernatants

AK23 is a mouse monoclonal anti-Dsg3 antibody with pathogenic activities produced by the cultivation of the AK23 hybridoma cell line [96]. IgG containing supernatants from this cell line were kindly provided by the laboratory of Ritva Tikkanen from the Giessen University [173]. The purification of the AK23 antibodies was performed by protein G affinity chromatography, which separates proteins based on reversible interactions between the protein (AK23) and a specific ligand (protein G) coupled to a chromatography matrix (sepharose). To 25 ml supernatant 1 ml protein G sepharose was added and incubated with rotation over night at 4 °C to allow the Fc regions of the antibodies to bind to the protein G. The 2.5 ml column was primed with 2 ml ethanol, washed with 5 ml PBS and then packed with the supernatant-sepharose mix. The flow through was discarded and the column matrix was washed with 20 ml PBS. 60 µl neutralization buffer was pipetted to ten 1.5 ml tubes and 5 ml elution buffer was added to the column to elute the antibodies from the protein G sepharose matrix. 500 µl fractions were collected to each tube, the protein concentration was determined using the NanoDrop 1000 spectrophotometer system and the purified AK23 was stored at -20 °C.

3.14. Dispase-based dissociation assay

NHEK were seeded in triplicates with 500 µl/well in a 24-well cell culture plate and grown until complete confluent. Upon confluence, CnT complete medium was exchanged by CnT differentiation medium for 24 h. Cells were pre-incubated for 1 h with indicated inhibitors at indicated concentrations in DMSO or DMSO alone (control condition) followed by incubation with 20 µg/ml AK23 or neutralization/elution buffer mix (control condition) for further 4 h at

37 °C and 5 % CO_2. The keratinocytes were washed with HBSS and incubated with 250 µl dispase II solution at 37 °C until all monolayers were completely detached (approx. 30 min). The dispase II solution was removed from the wells and 250 µl HBSS was pipetted to the monolayers. For better visualization and to ensure the cells were alive, the monolayers were stained with 10 µl MTT solution for 15 min. By pipetting up and down with an electronic pipette set to 230 µl, mechanical stress was applied to the monolayers, which caused fragmentation. For all replicates and conditions of one experiment, the same number of pipetting steps was applied. The fragments were fixed by adding 250 µl fixation buffer, stained with 1 µl crystal violet solution over night at 4 °C and subsequently counted.

3.15. Keratinocyte AK23 stimulation assay

Keratinocytes were seeded and treated with AK23 with or without inhibitors as described for dissociation assay for the indicated time points. After incubation with AK23, the supernatant was discarded and cells were washed with PBS. Subsequently, 100 µl/well protein lysis buffer was applied and lysates were collected into 1.5 ml tubes. Further homogenization was achieved by freezing the lysate in liquid nitrogen and thaw at RT for a total of three freeze/thaw cycles. The lysates were centrifuged at full speed for 3 min, the protein containing supernatant was transferred into a fresh tube and protein concentration was determined.

3.16. Protein quantification and sample preparation for SDS-PAGE

Determination of the protein concentrations for immunoblotting was performed using the ROTI®Quant universal kit, which is based on a biuret reaction. The peptide bonds of tripeptides and larger polypeptides react with Cu^{2+} ions in an alkaline environment and reduce them to Cu^{+} ions. The resulting complex is stained blue and the color intensity is proportional to the amount of peptide bonds in the sample. The faint color is then enhanced by chelation of the Cu^{+} ions with PCA and the resulting chelate complex is strongly stained greenish-blue.

The BSA stock solution was diluted in PBS to a standard curve with the following concentrations: 2,000, 1,500, 1,000, 750, 500, 250, 125, 50, 25, 5 and 0 µg/ml. The samples were diluted 1:10 with PBS. 50 µl of standard and samples was pipetted in duplicates into the

wells of a 96-well microplate. A working solution was prepared by mixing 15 parts of Reagent 1 with 1 part of Reagent 2 and 100 µl working solution was added to each well. After incubation for 30 min at 37 °C, the optical density was determined using a microplate reader set to 492 nm and the sample protein concentration was calculated based on the standard curve. Samples were diluted with sample buffer (5x) to a final amount of 20 µg protein per well and heated for 5 min at 95 °C before loading on the SDS gel.

3.17. SDS-PAGE

Sodium dodecyl sulfate polyacrylamide gel electrophoresis (SDS-PAGE) is a method for the analysis of protein mixtures and determination of molecular weights based on the discontinuous SDS-containing tris-glycine buffer system according to Laemmli [174]. The samples are incubated with the anionic detergent SDS at 95 °C, thereby the secondary and tertiary structures of the proteins are dissolved, resulting in a linear conformation. Furthermore, negatively charged SDS-protein complexes are formed with a constant mass-to-charge ratio, which differ only in size and have comparable hydrodynamic properties. Addition of reducing agents such as 1,4-Dithiothreitol (DTT) disrupts the disulfide bonds of the proteins and results in complete unfolding and maintenance of the proteins in fully reduced states. Applied on the gels, the samples are first focused in the neutral, wide-pored stacking gel and then separated according to their molecular weight in the narrow-pored alkaline resolving gel. The SDS-protein complexes migrate in the electric field to the anode, where the molecular sieve effect of the polyacrylamide matrix separates the proteins according to their molecular weight. By using a protein ladder with marker proteins of known sizes, the molecular weight of the sample proteins can be determined.

Gel casting was performed with the Mini-PROTEAN® casting module. The 12 % acrylamide resolving gel was poured into the assembled gel sandwich and overlaid with 2-propanol. Polymerization was initiated by ammonium persulfate (APS) with tetramethylethylenediamine (TEMED). Upon polymerization of the resolving gel, 5 % acrylamide stacking gel was poured on top, the comb was placed in the cassette and the gel was allowed to polymerize. The composition of the gels is listed in Table 10. The polymerized gel was placed in the Mini-PROTEAN® cell and the cell was filled with 1x running buffer. The

comb was removed from the gel, the wells were rinsed and the samples containing equal protein amounts and protein ladder were loaded to the wells. The separation was first performed at 80 V for 30 min (focusing of the samples), then the voltage was raised to 120 V for approx. 90 min. After electrophoresis, the stacking gel was removed and the separation gel was used for Western blotting.

Table 10: Recipes for resolving and stacking gels.

	Resolving gel 1.5 mm (10 ml)	**Stacking gel 1.5 mm (4 ml)**
Corresponding gel buffer	2.55 ml	1.00 ml
Acrylamide	4.00 ml	0.67 ml
H_2O	3.45 ml	2.33 ml
TEMED	6.25 µl	5 µl
APS 10 %	50 µl	40 µl

3.18. Western blot and immunodetection

In a Western blot, the proteins from the SDS gel are transferred electrophoretically to an adsorbing membrane. During this process, the negatively charged SDS-protein complexes migrate out of the gel and stick to the membrane. The proteins on the membrane can then be specifically identified by immunodetection.

The PVDF membrane was first activated by placing it in methanol for 1 min and then equilibrated in transfer buffer. The filter paper and SDS gel were also equilibrated in transfer buffer. The blotting tank was filled with transfer buffer and the transfer sandwich was assembled as follows: The PVDF membrane and the gel were layered between buffer-soaked filter papers and sponges and then placed between two electrodes submerged in transfer buffer, while the gel side faced the cathode and the membrane side faced the anode. When the electric field was applied, the negatively charged proteins moved out of the gel and onto the surface of the membrane. Protein transfer was performed at a constant current of 200 mA for 2 h. To prevent antibodies from non-specific binding to the membrane, it was subsequently placed into a dark incubation box containing 10 ml LI-COR blocking buffer and blocked for 1 h at RT and shaking. For specific protein identification, the membrane was incubated with

primary antibodies diluted in 10 ml PBST/blocking buffer (1:2) using the indicated dilutions (Table 5) over night at 4 °C and shaking. Pan-actin was co-detected as reference protein. After washing three times with PBST for 10 min at RT the membrane was incubated with IRDye-labeled secondary antibodies diluted 1:14,000 in PBST/blocking buffer (1:2) for 1 h at RT and shaking followed by another three times washing with PBST. The membrane was placed in PBS and visualization of protein bands and semi-quantitative analysis of signal intensity was performed with the Odyssey Sa infrared imaging system and Image Studio Lite software. Relative signal intensity was calculated using the following formula:

$$\text{relative signal} = \frac{\text{signal (target protein)}}{\text{signal (reference protein)}}\text{(treatment)} \times \frac{\text{signal (reference protein)}}{\text{signal (target protein)}}\text{(control)}$$

Control condition was set to 1 for normalization.

After detection of phospho-proteins, the respective total non-phosphorylated protein was determined. For this purpose, the primary and secondary antibodies were removed from the membrane by 10 min incubation with stripping buffer, the stripped membrane was then washed two times with PBST, blocked and restained with the respective antibodies as described before.

3.19. Immunohistochemical staining of skin

Formalin-fixed paraffin embedded (FFPE) punch biopsies of the skin were cut into 4 µm sections and IHC staining was performed in the Institute of Pathology and Neuropathology at the Tübingen University using an automated immunostainer (Ventana Medical Systems, Tucson, USA) according to the manufacturer's protocol. During this process, specific binding of the pSTAT1 and pSTAT3 antibodies was visualized with 3,3-Diaminobenzidine (DAB) and the tissue was counterstained with hematoxylin. Appropriate positive and negative controls were used to confirm the adequacy of the staining. Stained tissue slides were digitized using the Hamamatsu Nanozoomer system and images were taken with the NDP.view2 software with 100x magnification. Semi-quantitative analysis of the stained skin was performed using the color deconvolution plugin of ImageJ Fiji software according to Crowe et al. [175]. Application

of the vector Hematoxylin & DAB (H DAB) to the images resulted in the separation of the brown DAB staining, representing the protein of interest, and the blue hematoxylin stain, depicting cell nuclei. The threshold of DAB staining was set the same for all images, only the epidermis was selected with the freehand selection tool, and the area fraction of positive pixels within the selection was measured in %.

3.20. Statistics

All data except for RNA-seq were analyzed and plotted using GraphPad Prism software. Statistical analyses were performed by using the Spearman correlation (two groups, nonparametric, two-tailed *p*-value), One-sample Wilcoxon test (two groups, nonparametric, two-tailed *p*-value), Mann-Whitney test (two groups, unpaired, nonparametric, two-tailed *p*-value), Wilcoxon matched-pairs signed rank test (two groups, paired, nonparametric, two-tailed *p*-value), Dunn's multiple comparisons test after Friedman test (≥ three groups, paired, nonparametric) and Dunn's multiple comparisons test after Kruskal-Wallis test (≥ three groups, unpaired, nonparametric) as indicated. Values of $p<0.05$ were considered significant. For statistical analysis of RNA-seq data, see *3.2 Next-generation sequencing and bioinformatics.*

4. RESULTS

The data presented in *4.1* to *4.6* were published by Holstein et al. [176] with some modifications. Further, part of the Western blot images shown in *4.7* were reported by Forster et al. [177, 178].

4.1. Whole mRNA expression analysis reveals a profound impact of pemphigus disease on gene expression

For decades, Th2 cells have been considered to be primarily involved in the pathogenesis of pemphigus. However, data on large-scale next-generation sequencing (NGS) analysis of lesional pemphigus skin is limited. For this reason, whole transcriptome shotgun sequencing (RNA-seq) of lesional skin of six patients with pemphigus vulgaris was compared to the transcriptome of six healthy skin samples (control). Thorough quality control for the sequenced data revealed no remarkable quality issues with 94.7 % of the reads having a quality score above Q30. Figure A1 to Figure A4 in the appendix illustrate the results of quality control analyses. Many genes were found overexpressed in the samples of PV patients, which have not been described before as involved in pemphigus pathogenesis. Of 53,903 genes examined, 216 genes showed significantly altered expression in lesional pemphigus skin compared to healthy skin. Of these differentially expressed genes (DEGs), 167 were significantly upregulated and 49 downregulated in pemphigus patients (Figure 11A). A considerable number of the genes identified were related to Th17 immune responses. Pemphigus lesions showed significant overexpression of *IL19*, *IL20* and *IL24* (Figure 11B), cytokines typically expressed in Th17-mediated psoriatic skin inflammation [179]. Furthermore, other Th17-associated factors like the IL-1 family cytokines *IL36A* and *IL1B* and the cytokine receptors *IL1RL1* and *IL21R* were also among the 167 genes significantly overrepresented in pemphigus. Consequently, *IL17A* itself was strongly upregulated. Furthermore, the expression of genes encoding chemokines, neutrophil-attractants and inflammasome activators like the CXC chemokine ligands (CXCL) *CXCL1*, *CXCL5*, *CXCL8*, *CXCL10*, absent in melanoma 2 (*AIM2)* and caspase 5 (*CASP5)*, genes involved in tissue remodeling like the matrix metalloproteinases (MMP) *MMP1*, *MMP10* and *MMP13*, and genes encoding defensive and antimicrobial factors like *S100A8*, *S100A9*, *S100A12*, and the beta-defensins *DEFB103B*, *DEFB4A*, *DEFB4B* were enhanced in pemphigus (Figure 11B). Among the

downregulated genes were *WFIKKN2*, a serine- and metalloproteinase inhibitor, the muscarinic receptor 4 encoding gene *CHRM4*, and *MATN4*, encoding the extracellular space component matrilin 4. In addition, *MYC*, *ADAMTS9-AS2* (A disintegrin and metalloproteinase with thrombospondin motifs 9, antisense RNA 2) and cell adhesion molecule 2 (*CADM2)*, which encode proteins linked to cancer development, were underrepresented.

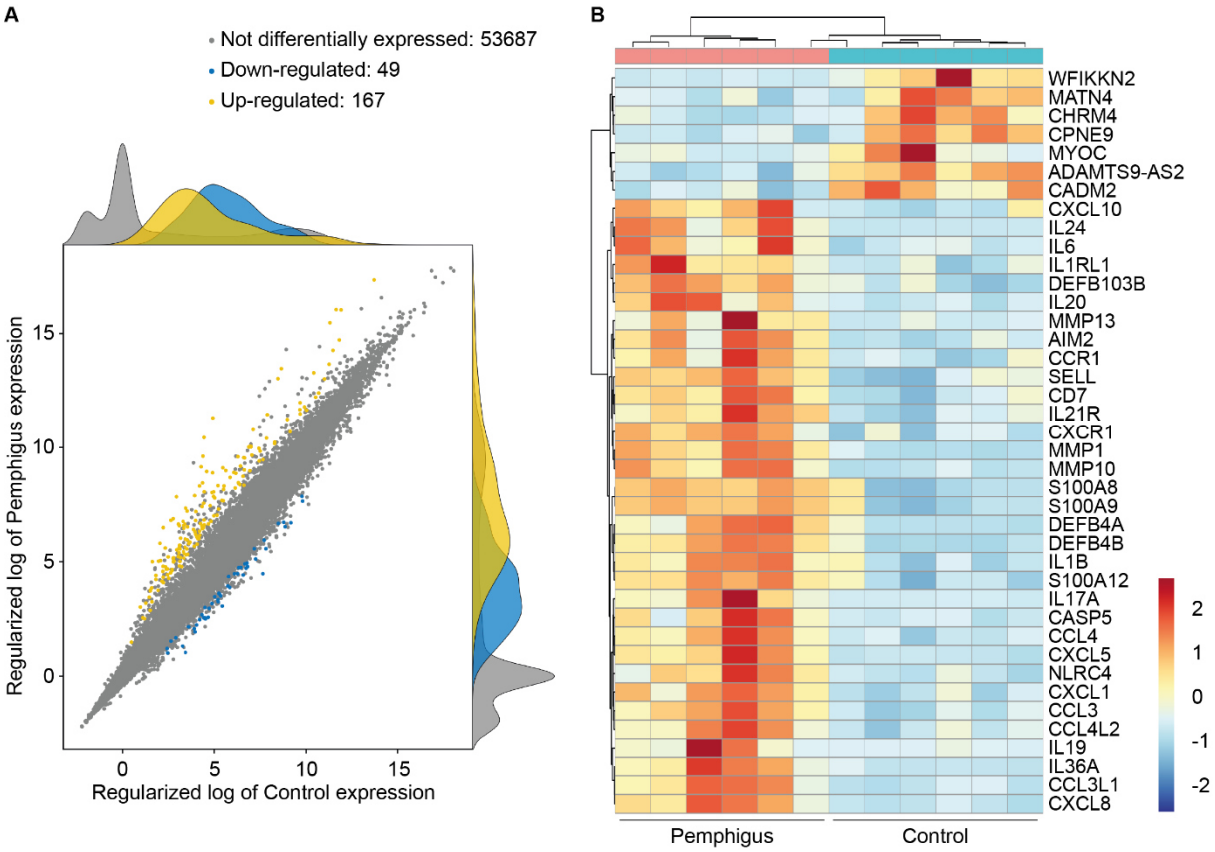

Figure 11: Transcriptome analysis reveals overexpression of *IL17A* and related genes in pemphigus. Whole transcriptome shotgun sequencing (RNA-seq) was performed in pemphigus lesional skin (n=6) and in healthy control skin (n=6). **(A)** Scatter plot of all expressed genes comparing control and affected skin. **(B)** Selected differentially expressed genes (DEGs) are shown as a heat map. Figure was published with minor modifications in [176].

Gene Ontology (GO) enrichment analysis of the DEGs [159, 160] revealed that the majority of overexpressed genes were involved in biological processes (n=71), while only a minority in either formation of cellular components (n=12) or molecular function (n=13), as shown in Figure A5 in the appendix. The most significant enrichment of DEGs in biological process was in the terms immune response, immune system process and inflammatory response. In the cellular component category extracellular region, extracellular space and immunoglobulin

complex had the most significant enrichment of DEGs, and for molecular function the terms cytokine activity, antigen binding and chemokine activity were the most significantly enriched GO-terms (Figure 12A). Genes related to Th17 immune response like *IL19, IL1B* or *IL17A* itself were mostly involved in the terms extracellular space, extracellular region, cytokine-mediated signaling pathway and cytokine activity (Figure 12B).

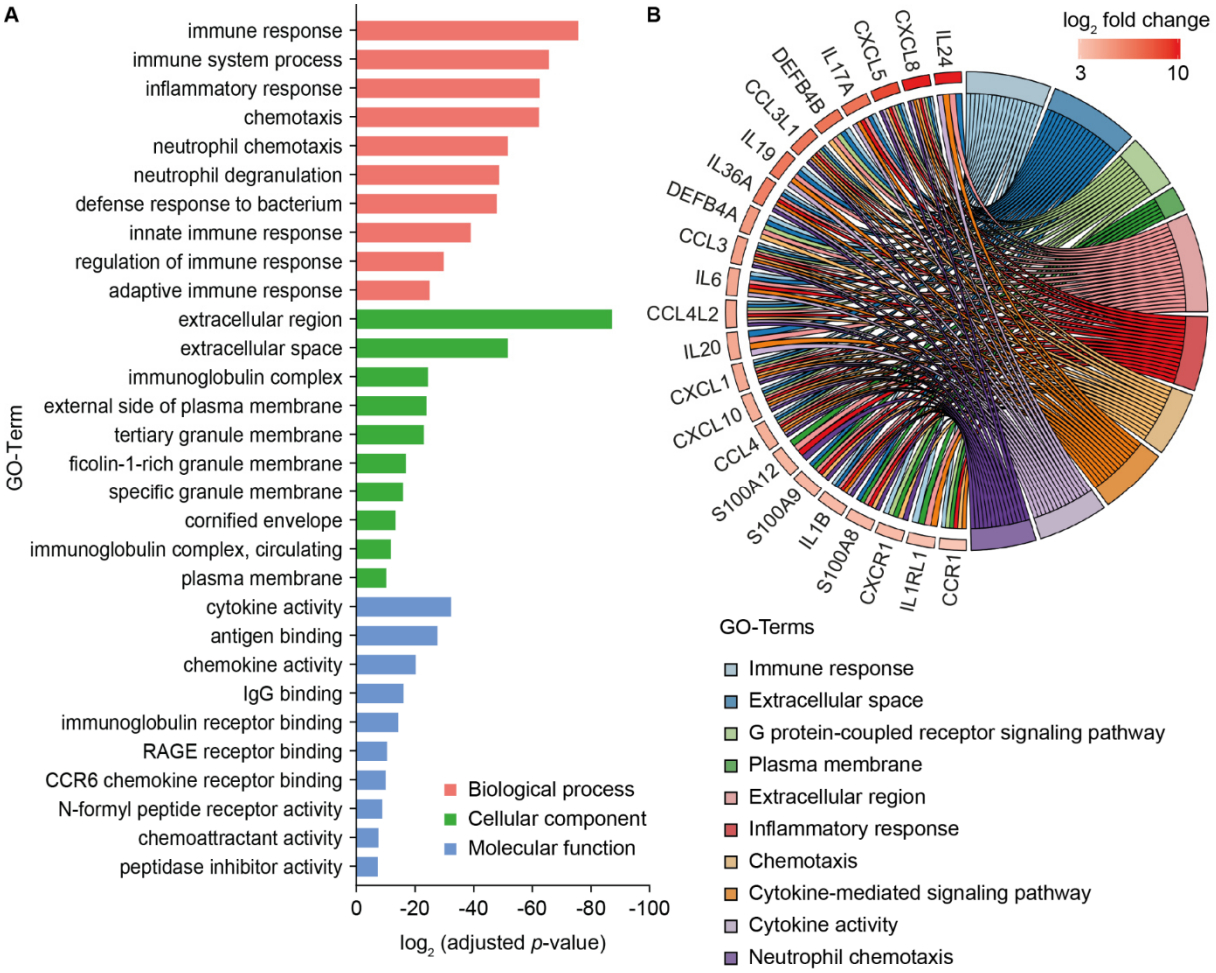

Figure 12: Gene Ontology (GO) enrichment analysis of upregulated DEGs. RNA-seq analysis of lesional skin biopsies from pemphigus patients (n=6) was compared to healthy skin biopsies (n=6). **(A)** GO-terms were classified into biological process, cellular component and molecular function. The top ten GO-terms with the lowest *p*-values of each category are shown. **(B)** Circle plot depicts selected regulated DEGs in relation to GO-terms. Part (B) of this figure was published by Holstein et al. [176].

4.2. Altered processes in pemphigus skin are shaped by the IL-17 signaling pathway

To identify pathways involved in pemphigus pathogenesis, the Kyoto Encyclopedia of Genes and Genomes (KEGG) analysis [161, 162] of the RNA-seq data was performed. Pathway

analysis revealed that several pathways like the *Staphylococcus aureus* infection, rheumatoid arthritis, B cell receptor signaling pathway and the Janus kinase (JAK)/signal transducer and activator of transcription (STAT) signaling pathway were significantly overrepresented in pemphigus (Figure 13A).

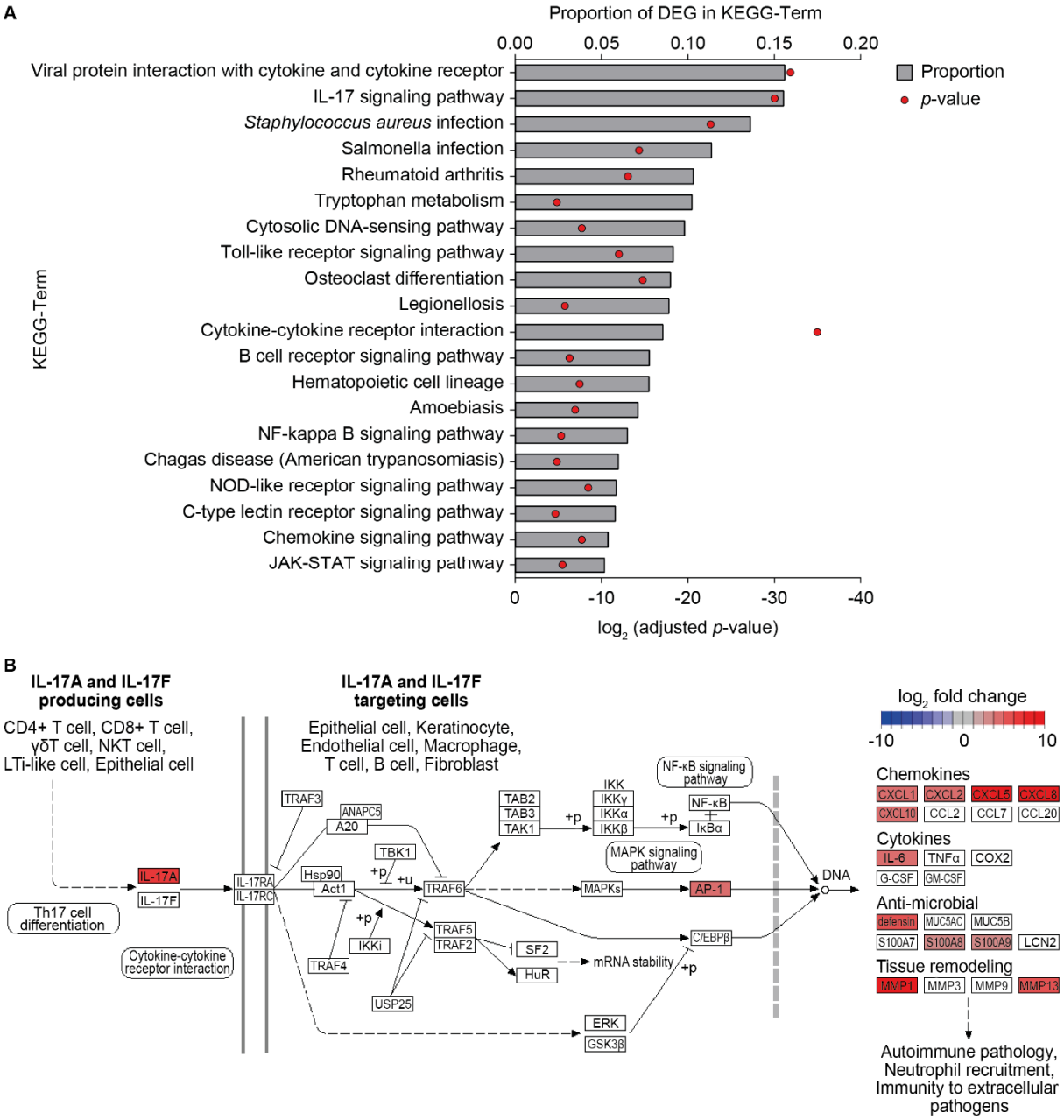

Figure 13: IL-17 signaling pathway is overrepresented in pemphigus skin biopsies. KEGG pathway enrichment analysis of DEGs in lesional skin from pemphigus patients (n=6) compared to healthy skin biopsies (n=6) was performed. **(A)** Significantly upregulated KEGG pathways in pemphigus skin biopsies are presented. **(B)** KEGG analysis shows significantly altered gene expression in the IL-17 signaling pathway. Figure was published with minor modifications by Holstein et al. [176].

Further, the activation of the IL-17 signaling pathway was confirmed as supported by the expression of chemokines, cytokines, anti-microbial peptides and tissue remodeling proteins as described above (Figure 13B, Figure 11B). Taken together, these data showed that *IL17A* and related genes seem to play a more prominent role in pemphigus than previously reported.

4.3. Cytokine signature of pemphigus skin is defined by IL-17A and associated interleukins

The whole transcriptome analysis of six patients indicated that pemphigus pathogenesis was driven by an IL-17 dominated immune response. To further address this issue, mRNA expression in skin samples from a large patient collective with pemphigus vulgaris (PV, n=18) and pemphigus foliaceus (PF, n=11) were investigated by quantitative real-time PCR (qPCR). First, the gene expression analysis from RNA-seq data was validated by qPCR analysis of 12 selected genes (*IFNG*, *IL1A*, *IL1B*, *IL4*, *IL10*, *IL12B*, *IL17A*, *IL19*, *IL21*, *IL22*, *IL23A* and *IL24*) for the pemphigus patients (n=6) and healthy controls (n=6) studied in Figure 11. Comparison of $\log_2$ fold change of these genes showed a positive linear relationship between the RNA-seq and qPCR data (Spearman's correlation coefficient r=0.8951 and p=0.0002). Thus, the mRNA expression data obtained by qPCR largely confirmed the transcriptome analysis generated by RNA-seq (Figure 14).

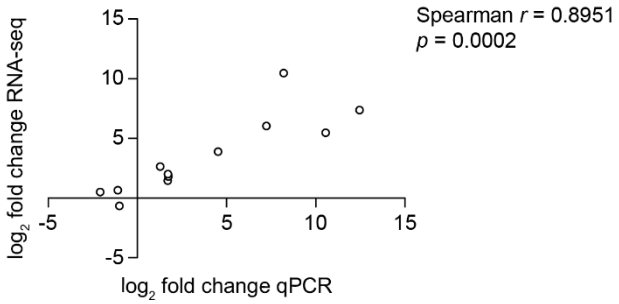

Figure 14: Positive linear correlation between RNA-seq and qPCR data. Spearman correlation analysis of data obtained from RNA-seq and qPCR of 12 genes (*IFNG*, *IL1A*, *IL1B*, *IL4*, *IL10*, *IL12B, IL17A*, *IL19*, *IL21, IL22*, *IL23A* and *IL24*) expressed in the same samples from pemphigus patients (n=6) and healthy controls (n=6). Data were published by Holstein et al. [176].

Gene expression levels of the 12 selected genes were then analyzed in the whole patient cohort. In agreement with previous reports [118], *IL4* cytokine levels were slightly elevated in PV and significantly increased in PF lesional skin (p<0.01). The expression of *IFNG* and *IL10*

were also enhanced in pemphigus lesional skin compared to control skin (both $p<0.05$). Several genes directly associated with the Th17 pathway showed significantly elevated expression levels including the IL-1 cytokines *IL1A* and *IL1B* (both PV and PF $p<0.05$) as well as *IL23A* (PV $p<0.001$), *IL21* (PV and PF $p<0.01$) and *IL17A* itself (PV $p<0.05$). Other related cytokines like *IL19* and *IL24* were also found overexpressed in both PV and PF ($p<0.05$). *IL12B* revealed no significantly altered expression and of all analyzed Th17-associated cytokines, *IL22* was the only one showing significantly decreased expression levels compared to healthy skin (PF $p<0.01$). There was no significant difference in gene expression between PV and PF lesional skin, although *IL1A* showed a trend towards increased expression in PV compared to PF (Figure 15).

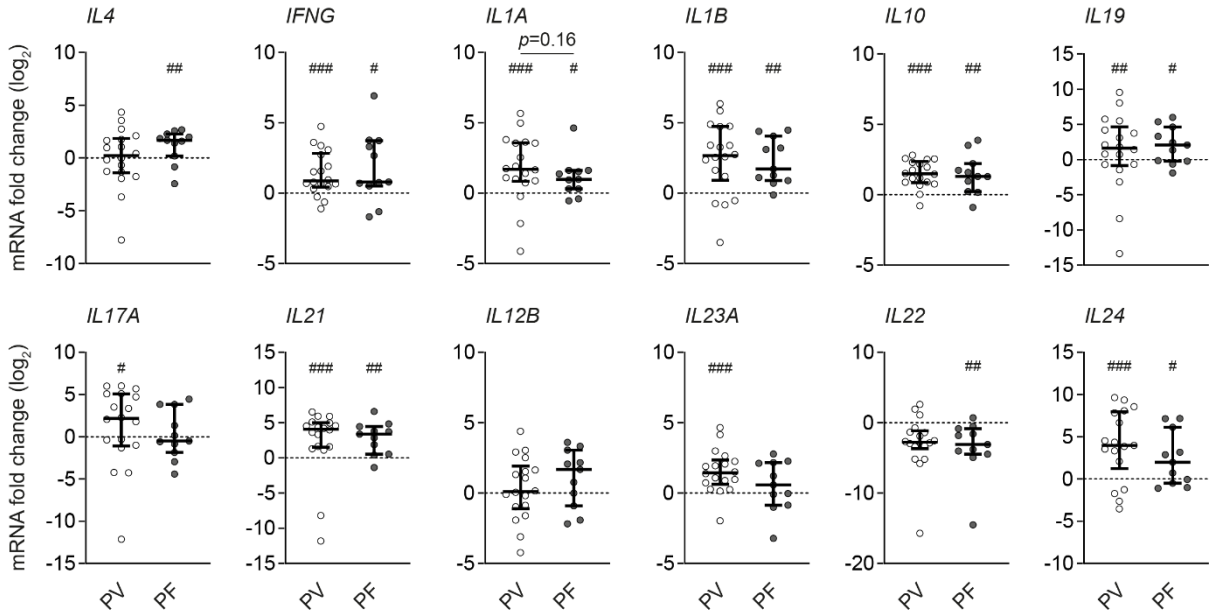

Figure 15: Increased expression of Th17 associated cytokines in pemphigus lesions compared to healthy skin. Relative cytokine expression in lesional skin from patients with pemphigus vulgaris (PV, n=18) and pemphigus foliaceus (PF, n=11) was determined by qPCR and compared to healthy skin (pool of n=10, set to 1). Single patients and median with IQR are shown. Data were normalized to *ACTB* and *POLR2A*. One-sample Wilcoxon test (# $p<0.05$, ## $p<0.01$, ### $p<0.001$) for comparison to healthy skin; Mann-Whitney test for comparison between PV and PF ($p<0.2$ as indicated). Data were published in [176].

The pemphigus patients were stratified according to their clinical disease stage [145] in active (acute: onset with ≤ 3 month duration, n=8 and chronic: active disease with a duration of ≥ 3 months, n=15) and remittent group (no appearance of new clinical lesions for ≥ 1 month, n=6).

While *IL4* was only slightly enhanced (p<0.05), levels of *IFNG*, *IL21*, *IL23A*, *IL1A*, *IL1B*, *IL10*, *IL19* and *IL24* were strongly expressed (p<0.001) in the active group. *IL17A* was exclusively increased in the active group (p<0.01) compared to healthy skin. In remittent patients only levels of *IFNG*, *IL23A* and *IL10* were elevated (p<0.05). Again, *IL12B* showed no statistically significant differences, and levels of *IL22* mRNA were suppressed in both the active and remittent group (p<0.05). There was no altered mRNA expression between the active and remittent group, but there was a trend towards higher *IFNG* expression in affected skin of patients in remission. In contrast, *IL19* expression was elevated in active disease compared to remittent group (Figure 16).

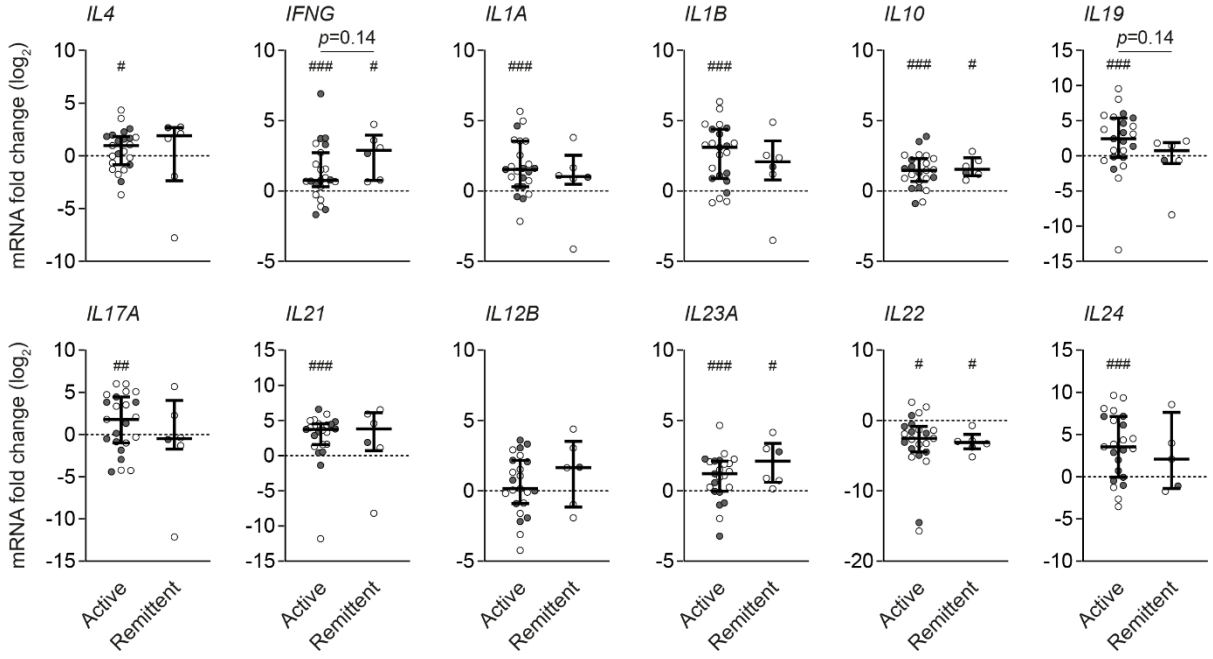

Figure 16: Upregulation of *IL17A* and *IL21* as well as suppressed expression of *IL22* in lesional skin of patients with active pemphigus disease. Patients were clinically classified according to their disease activity. The stages were defined as active (acute and chronic, n=23) and patients in remission (n=6). Single patients and median with IQR are shown. One-sample Wilcoxon test (# p<0.05, ## p<0.01, ### p<0.001) for pemphigus vs. healthy skin; Mann-Whitney test for comparison between active and remittent group (p-values <0.2 are indicated). Data were published in [176].

In addition, the mRNA levels of the selected cytokines in lesional and perilesional skin of six pemphigus patients were compared, whereas the perilesional biopsy of the respective patient was obtained from unaffected skin distant from the lesion. Despite the small sample size, *IL10*

and *IL21* were significantly increased in perilesional skin compared to normal skin (p<0.05). In contrast, *IL19*, *IL22* and *IL24* mRNA levels were suppressed in unaffected skin of pemphigus patients when comparing it with unaffected healthy skin. A marked, but not statistically significant increase of *IL17A* mRNA was found in lesional tissue (p=0.16) and significantly higher levels of *IFNG*, *IL21*, *IL19* and *IL24* (p<0.05) were detected compared to perilesional skin (Figure 17).

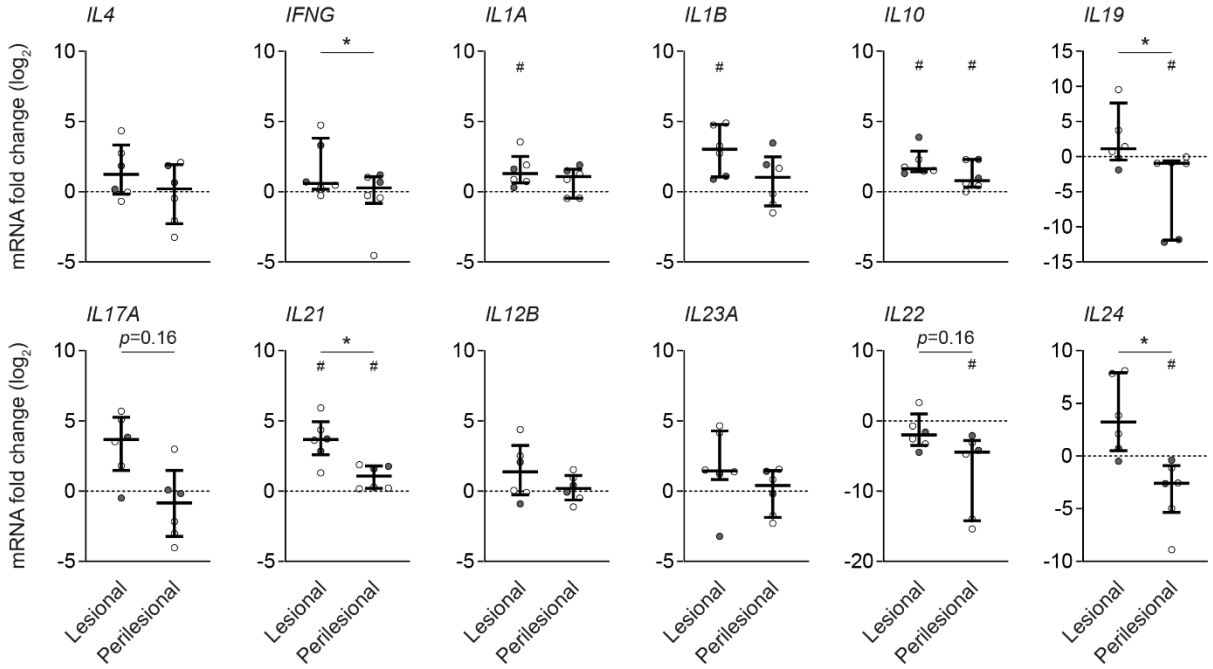

Figure 17: Overexpressed cytokines mainly accumulate in lesional skin rather than in perilesional tissue of pemphigus patients. Lesional and perilesional skin biopsies were taken at the same time point from six patients and mRNA expression was analyzed by qPCR compared to healthy skin (set to 1). Single patients and median with IQR are shown. Data were normalized to *ACTB* and *POLR2A*. One-sample Wilcoxon test (# p<0.05) for comparison to healthy skin; Wilcoxon matched-pairs signed rank test (* p<0.05, p<0.2 as indicated) for lesional vs. perilesional skin. Data were published in [176].

4.4. Higher frequencies of circulating IL-17-producing T cell subsets in active disease

After characterization of the local cytokine signature in the skin, the systemic immune response in pemphigus disease was investigated by performing flow cytometric analysis of T cell subsets in the peripheral blood from 79 pemphigus patients (PV n=68 and PF n=11) and 28 control individuals. The amounts of $CD3^+$ T cells, $CD45RA^-$ $CD4^+$ memory T helper (Th) cells, $CXCR5^-$ Th cells and $CXCR5^+$ follicular T helper (Tfh) cells were similar in pemphigus and control

group. Further, frequencies of Th and Tfh cell subsets type 1 (CXCR3$^+$ CCR6$^-$), type 2 (CXCR3$^-$ CCR6$^-$), type 17 (CXCR3$^-$ CCR6$^+$) and type 17.1 (CXCR3$^+$ CCR6$^+$) were investigated. In peripheral blood mononuclear cells (PBMCs) of pemphigus patients, significantly lower levels of Th17.1 cells (p<0.05) were found than in control blood, but no other Th populations. Compared to the distribution of Tfh cell subsets in control individuals, pemphigus patients showed similar amounts of circulating Tfh cells (Figure 18).

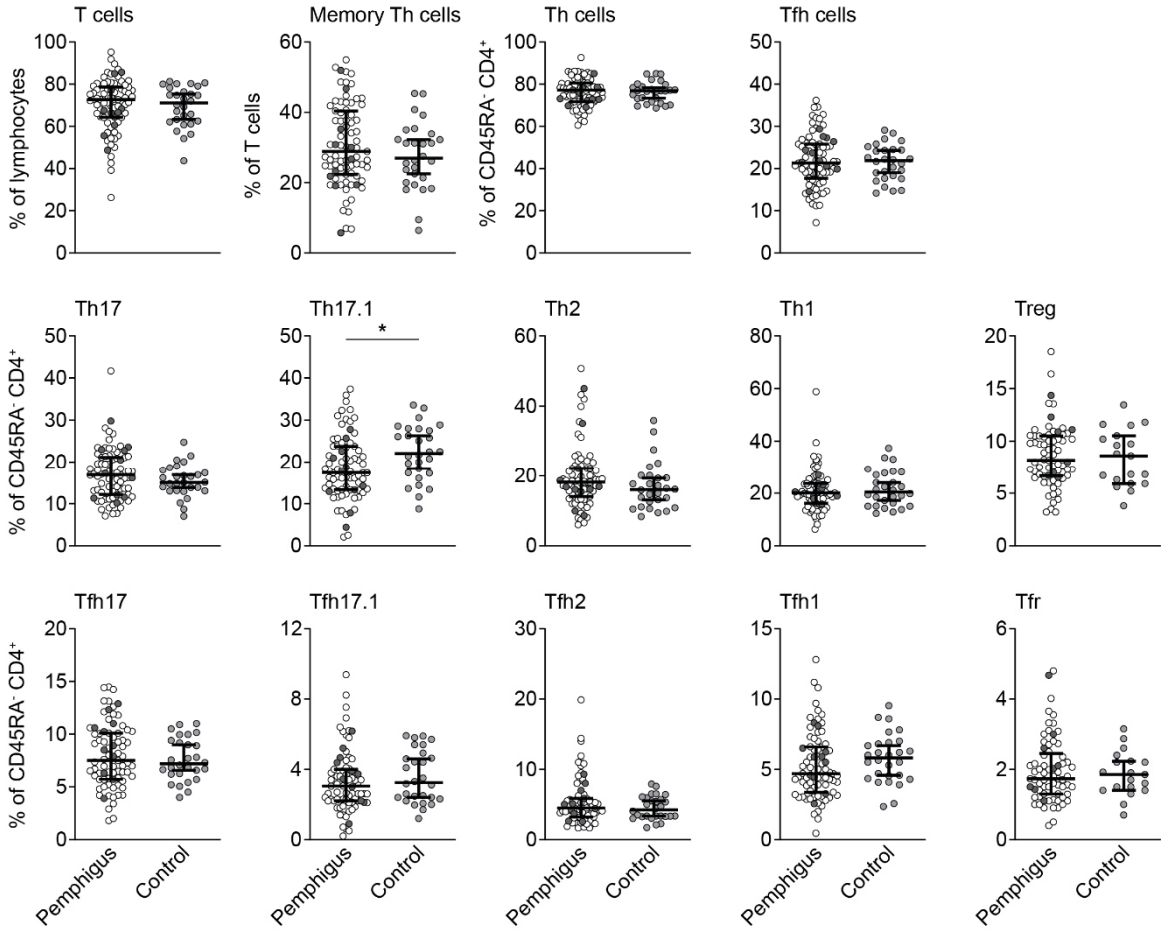

Figure 18: Lower proportions of Th17.1 cells in peripheral blood of pemphigus patients. Comparison of circulating levels of T cell populations in peripheral blood mononuclear cells of patients with pemphigus (clear dots: PV n=68, full dots: PF n=11; Treg/Tfr PV n=61, PF n=8) and control individuals (n=28; Treg/Tfr n=19). Single patients and median with IQR are shown. Mann-Whitney test (* p<0.05). Part of the data was published by Holstein et al. [176].

To determine if the distribution of T cell subtypes within the cohort of pemphigus patients depended on disease activity, the patients were divided into active (acute n=9; Treg/Tfr n=7 and chronic n=32; Treg/Tfr n=26) and remittent group (n=38; Treg/Tfr n=36) as described

before. Again, percentages of T cells, memory Th cells, CXCR5$^-$ Th cells and CXCR5$^+$ Tfh cells were similar in active and remittent disease stage. In contrast, pemphigus patients with active disease activity displayed higher frequencies of circulating Th17 and Th17.1 cells compared to patients in remission (p<0.05). Remittent patients showed higher numbers of Th2 and Th1 cells than patients in the active group (p<0.05), while Treg subsets were comparable in both groups. Furthermore, patients with active disease had significantly higher amounts of Tfh17 (p<0.01) and Tfh17.1 (p<0.05) cells than patients in remission, whereas frequencies of Tfh2, Tfh1 and Tfr cells were similar (Figure 19).

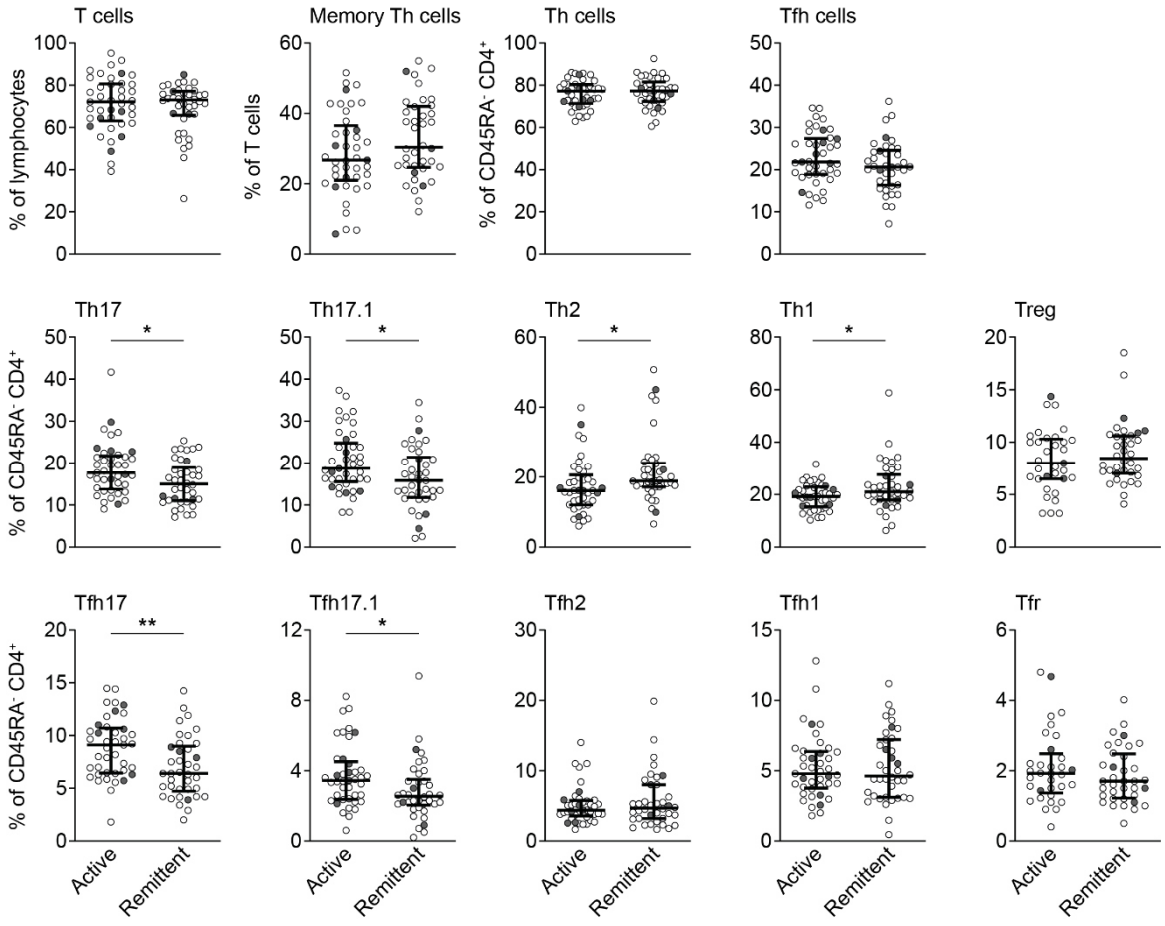

Figure 19: Circulating T cell subsets in patients with active disease are dominated by IL-17-producing Th and Tfh cells. Levels of Th and Tfh cell populations in peripheral blood mononuclear cells of patients with pemphigus vulgaris (clear dots, n=68; Treg/Tfr n=63) and pemphigus foliaceus (full dots, n=11; Treg/Tfr n=8) divided by their clinical disease stage: patients with either active disease (n=41; Treg/Tfr n=33) or patients in remission (n=38; Treg/Tfr n=36). Single patients and median with IQR are shown. Mann-Whitney test (* p<0.05, ** p<0.01). Part of the data was published by Holstein et al. [176].

Due to the increasing evidence for the involvement of Tfh cells in pemphigus pathogenesis, the mRNA expression of the Tfh marker CXCR5 in pemphigus skin was assessed. No significant differences between PV and PF were detected by qPCR (Figure 20). However, biopsies of patients in remission showed slightly elevated *CXCR5* mRNA expression compared to patients with active disease stage (p<0.05). There also was a trend towards increased *CXCR5* expression in perilesional skin compared to lesional skin. Nevertheless, the expression levels compared to healthy skin were not meaningful.

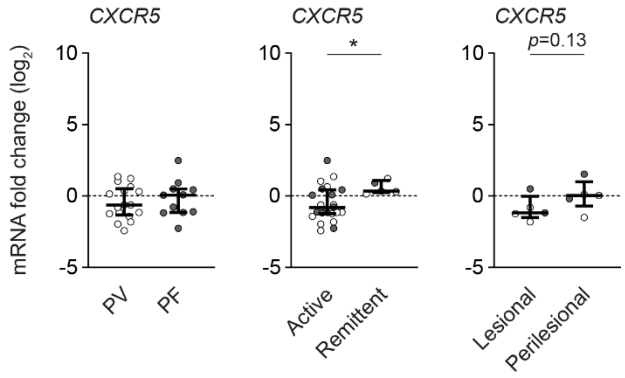

Figure 20: Expression of *CXCR5* mRNA in skin of pemphigus patients is not altered compared to healthy skin. Skin biopsies from pemphigus patients (clear dots: PV n=17, full dots: PF n=11) and control individuals (pool of n=10, set to 1) were analyzed by qPCR. Expression data were normalized to *ACTB* and *POLR2A.* Single patients and median with IQR are shown. Mann-Whitney test for comparison of PV with PF and for active (n=23) vs. remittent (n=5) group (* p<0.05). Wilcoxon matched-pairs signed rank test (p<0.2 as indicated) for comparison between lesional and perilesional skin (both n=6). Data were published in [176].

4.5. Verification of the gating strategy

Circulating T cell subsets in peripheral blood of pemphigus patients were identified by their expression patterns of chemokine receptors. Although the link between cytokine and chemokine receptor expression in human $CD4^+$ cells was reported before, it was unclear if this link was also valid for pemphigus patients' cells [41]. To connect the cytokine expression to the chemokine receptor pattern of the defined Th and Tfh subsets, the distinct populations were purified by flow cytometry-based cell sorting according to the indicated gating strategy and the mRNA expression levels of the lineage-associated cytokines *IL17A* (Th17 and Tfh17), *IL4* (Th2 and Tfh2), *IFNG* (Th1 and Tfh1) and *IL21* (Tfh) were determined in each individual subtype in PV patients (n=6) and control individuals (Co, n=5). *IL17A* expression was almost

exclusively found in Th17, Th17.1, Tfh17 and Tfh17.1 cell subsets in pemphigus and control group with significantly elevated levels in Th17 cells compared to Th1 cells for both groups (p<0.01) and to Th2 cells for PV (p<0.05). Further, *IL17A* was increased in Tfh17 cells compared to Tfh1 cells in control individuals (p<0.01). A predominant expression of *IL4* was detected in type 2 cells with significantly higher levels in Th2 compared to Th17 for PV (p<0.01) and Co (p<0.05). However, some *IL4* was also detected in type 1 cells. Th1 subsets from PV patients showed significantly higher *IL4* expression than Th17 cells (p<0.01). A similar phenomenon was described for chronic asthma or during helminth infection, where Th subsets different than classical type 2 cells were capable of producing IL-4 [180, 181]. The Th1 cytokine *IFNG* was mainly expressed by Th1 as well as Tfh1 cells and to a lower extent by Th17.1 and Tfh17.1 cell subsets. *IFNG* mRNA was significantly enhanced in Th1 cells compared to Th17 cells in both PV (p<0.001) and Co (p<0.01), in Tfh1 cells compared to Tfh17 in PV (p<0.05) and in Tfh1 (p<0.01) and Tfh17.1 (p<0.05) subsets compared to Tfh17 in the control group. The Tfh associated cytokine *IL21* was mainly present in all Tfh subsets in both groups, but also in Th1 subsets. In PV, the *IL21* mRNA level in Th1 cells was significantly higher than in Th17.1 (p<0.05) and in Th2 (p<0.05) cell subsets (Figure 21). These mRNA expression data confirmed the relationship between chemokine receptor and cytokine expression in each T helper cell subpopulation.

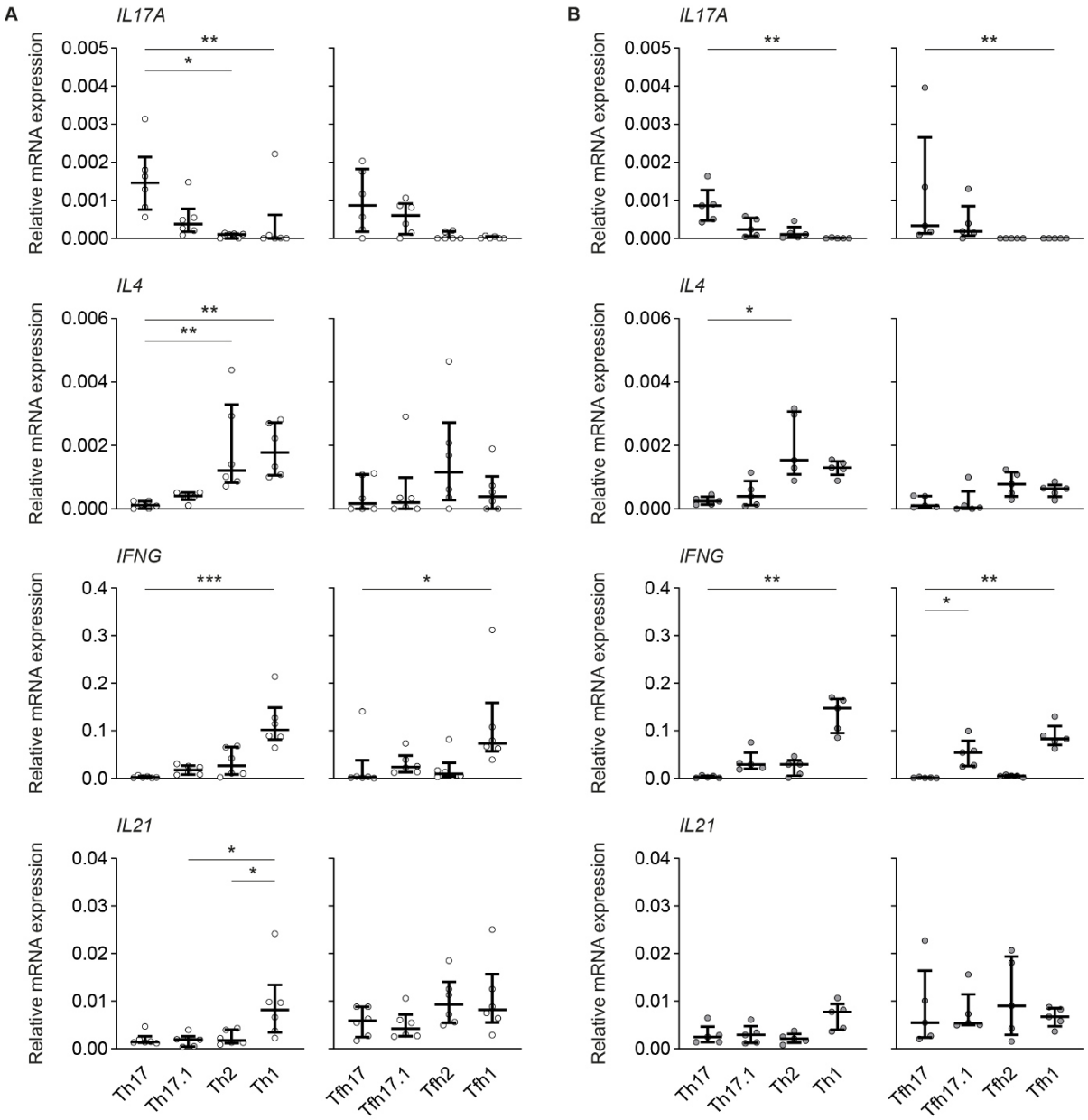

Figure 21: *IL17A* mRNA is expressed by CCR6$^+$ CXCR3$^-$ and CCR6$^+$ CXCR3$^+$ T cell subsets. Gene expression analysis of Th subset related cytokines was performed in sorted T cells from **(A)** pemphigus vulgaris patients (n=6) and **(B)** control individuals (n=5). Single patients and median with IQR are shown. Data were normalized to *POLR2A*. Dunn's multiple comparison test after Friedman test (* p<0.05, ** p<0.01, *** p<0.001). Data were published in [176].

In addition to the mRNA validation, the Th and Tfh subtypes in peripheral blood of pemphigus patients (PV n=8 and PF n=1) and control individuals (Co, n=11) were also analyzed for the expression of their associated cytokines at protein levels by intracellular cytokine staining of stimulated cells and flow cytometry. Again, IL-17A production was limited to Th17, Th17.1, Tfh17 and Tfh17.1 cells. In pemphigus patients, Th17 and Tfh17 cells produced significantly

higher amounts of IL-17A than Th2 and Tfh2 (p<0.05) as well as Th1 and Tfh1 (p<0.01) cells. In control individuals, IL-17A was significantly elevated in Th17 and Tfh17 cell subsets compared to Th2 and Tfh2 (p<0.01) or Th1 and Tfh1 (p<0.001). Further, Th17.1 and Tfh17.1 subsets showed higher IL-17A levels than Th1 and Tfh1 cells (p<0.01). The type 2 cytokine IL-4 was mainly produced by Th2 and Tfh2 cells and to a lesser extent by Th1 in both pemphigus and Co. Percentages of IL-4 positive cells were significantly increased in Th2 and Tfh2 cells compared to Th17 and Tfh17 (p<0.01) as well as to Th17.1 and Tfh17.1 (p<0.05) for pemphigus and control group. In addition, Tfh2 cells from control individuals showed more IL-4 than Tfh1 (p<0.05). Similar to the mRNA expression data of *IL4* in distinct T cell subsets, protein levels of IL-4-producing Th1 cells were elevated in Co compared to Th17.1 (p<0.05) and also in pemphigus, although to a lesser extent. IFN-γ was exclusively detected in Th1 and Tfh1 as well as in Th17.1 and Tfh17.1 populations in both groups, whereas the difference between type 1 and type 17 cells was statistically significant (p<0.01). Th1 and Tfh1 cell subsets also produced more IFN-γ than Th2 and Tfh2 cells (p<0.01). Th17.1 and Tfh17.1 cells showed higher IFN-γ levels than Th17 and Tfh17 (p<0.05) as well as Th2 and Tfh2 cells (p<0.05) in both pemphigus and Co. IL-21 positive T cells were found throughout all populations, although cells from pemphigus patients showed higher levels of IL-21 in $CXCR5^+$ Tfh cells than in $CXCR5^-$ Th cells. Significantly higher IL-21 amounts were detected in Th17 subsets than in type 2 cells for pemphigus and Co (both p<0.05). Further, more IL-21-producing cells were identified in the Tfh17.1 subset than in Tfh2 for both groups (p<0.05). Moreover, T cells from control individuals expressed significantly higher levels of IL-21 in Tfh1 subsets compared to Tfh2 (p<0.05) and in Th17 subgroups compared to Th17.1 (p<0.01). Altogether, lower cytokine production was detected in peripheral blood lymphocytes of pemphigus patients than in the cells of control individuals (Figure 22). Due to the systemic immunosuppressive therapies of the pemphigus patients, the cells were presumably less responsive to stimulation. Nevertheless, cytokine analysis at protein levels by intracellular flow cytometry confirmed mRNA expression data on cytokine patterns of distinct T cells subsets. Taken together, these data clarified the connection between chemokine receptor expression and cytokine profile in each $CD4^+$ subpopulation and verified the reliability of the applied gating strategy for T helper cell types.

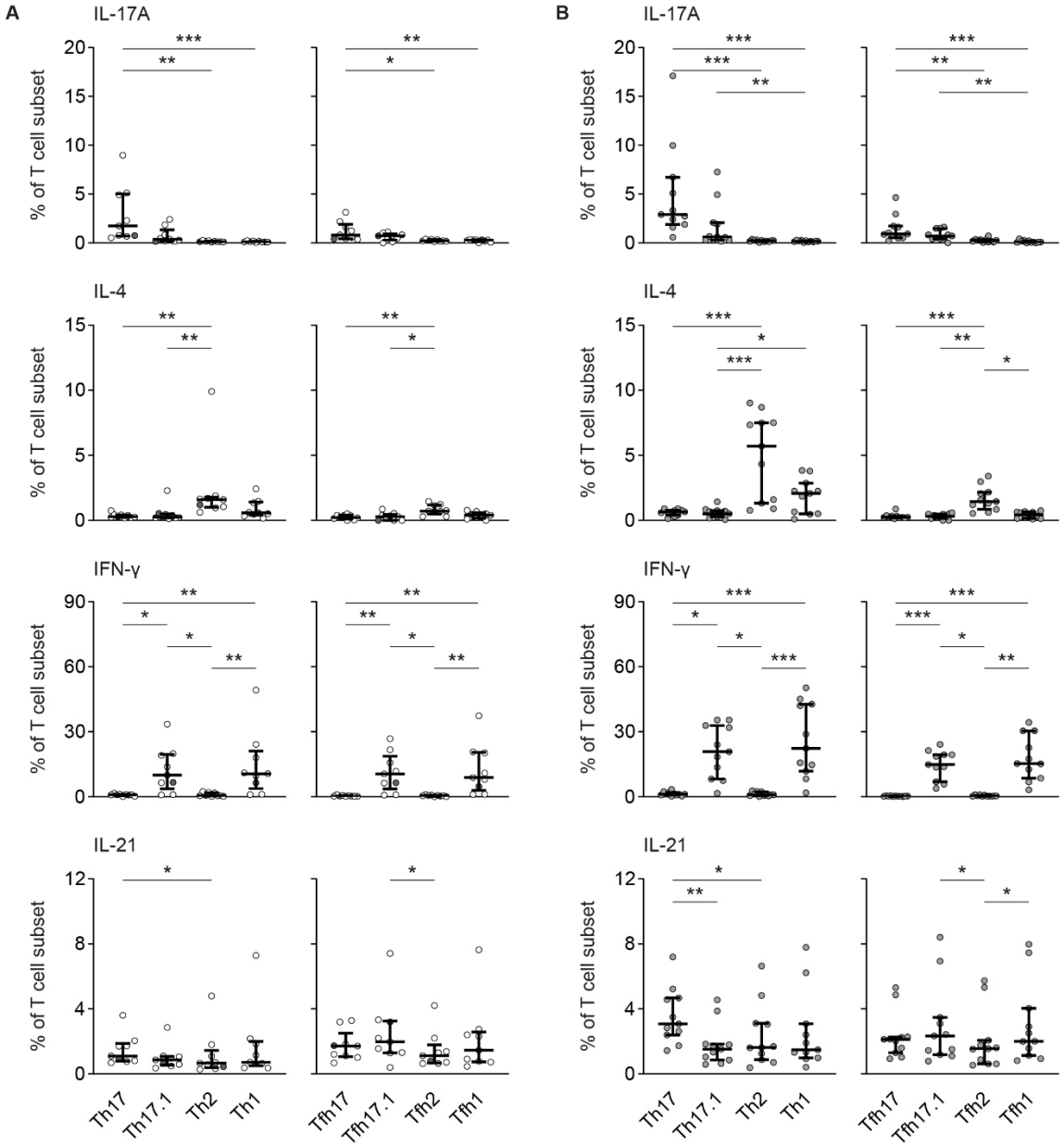

Figure 22: Production of IL-17A protein by CCR6$^+$ CXCR3$^-$ and CCR6$^+$ CXCR3$^+$ T cell subsets. Intracellular flow cytometric analysis of cytokines produced by distinct T cell subsets was performed in peripheral blood mononuclear cells activated by PMA/Ionomycin from **(A)** pemphigus patients (clear dots: PV n=8, full dots: PF n=1) and **(B)** control individuals (n=11). Single patients and median with IQR are shown. Friedman test and Dunn's multiple comparison post-hoc test (* p<0.05, ** p<0.01, *** p<0.001). Data were published in [176].

4.6. Th17 and Tfh17 cell frequencies correlate with levels of Dsg3-specific memory B cells

To address the relevance of elevated Th17 and Tfh17 cell subsets in pemphigus pathogenesis, the frequencies of circulating Dsg3-specific B cells in pemphigus patients were determined and correlation analysis with distinct T cell subsets was performed. Autoreactive Dsg3$^+$ B cells

and Dsg3$^+$ memory B cells were identified by flow cytometric analysis of peripheral blood from PV patients in active (acute n=2 and chronic n=17) and remittent (n=20) disease stage and from control group (n=23). Elevated levels of Dsg3-specific CD19$^+$ B cells were found in PBMCs from patients with active disease compared to patients in remission (p<0.01) and control individuals (p<0.05). Additionally, frequencies of Dsg3-specific CD19$^+$ CD27$^+$ memory B cells were increased in active PV patients compared to both remittent (p<0.001) and control (p<0.01) group (Figure 23).

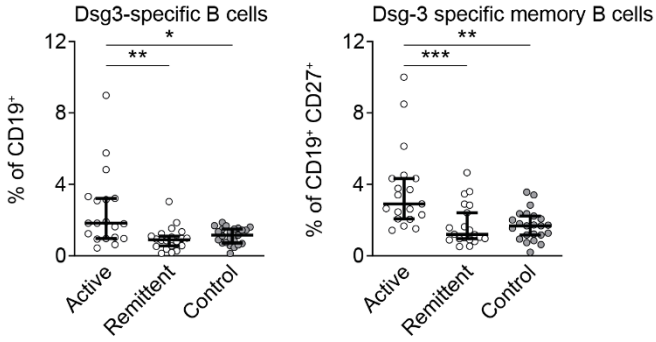

Figure 23: Circulating autoreactive Dsg3$^+$ B cells in blood of pemphigus patients with active disease. Flow cytometric analysis of Dsg3-specific B cells and Dsg3-specific memory B cells was performed in peripheral blood mononuclear cells of patients with pemphigus vulgaris in active (n=19) and remittent (n=20) disease stage and in control group (n=23). Single patients and median with IQR are shown. Dunn's multiple comparison test after Kruskal-Wallis test (* p<0.05, ** p<0.01, *** p<0.001).

Correlation analysis was performed and is summarized in Table 11 for memory B cells and in Table A5 in the appendix for total B cells. A positive correlation of total Dsg3-specific B cells with Tfh17 cell amounts was found in active PV disease (r=0.6523, p=0.0025). In the remittent and control group, no connection was determined between autoreactive Dsg3$^+$ B cells and T cell subsets. Correlation analysis of Dsg3-specific memory B cells with distinct T cell subsets in active PV revealed direct correlation for Th17 (r=0.4750, p=0.0399, Figure 24), Tfh17.1 (r=0.5538, p=0.0139) and Tfr (r=0.6744, p=0.0038) cell subsets. Furthermore, a strong positive relation between autoreactive Dsg3$^+$ memory B cells and Tfh17 cell numbers in active disease was found (r=0.8047, p<0.0001, Figure 24). Th1 cell frequencies negatively correlated with Dsg3-specific memory B cells in active patients (r=-0.6371, p=0.0033) and, as for total B cells, no correlation in remittent or control group was shown.

Table 11: Correlation analysis between Dsg3-specific memory B cells and distinct T cell subsets. Spearman's correlation coefficient *r* and *p*-values are indicated (ns not significant, * $p<0.05$, ** $p<0.01$, *** $p<0.001$).

	Th17	Th17.1	Th2	Th1	Treg	Tfh17	Tfh17.1	Tfh2	Tfh1	Tfr
Dsg3-specific memory B cells										
Active										
r	0.4750	0.0728	-0.2290	-0.6371	0.1754	0.8047	0.5538	0.1334	-0.0430	0.6744
p	0.0399	0.7670	0.3456	0.0033	0.4981	<0.0001	0.0139	0.5862	0.8612	0.0038
	*	ns	ns	**	ns	***	*	ns	ns	**
Remittent										
r	-0.3489	-0.0165	-0.1173	0.3008	-0.2144	-0.0962	0.0421	-0.1527	0.1369	-0.0459
p	0.1317	0.9448	0.6224	0.1976	0.3641	0.6865	0.8601	0.5204	0.5649	0.8476
	ns	ns	ns	ns	ns	ns	ns	ns	ns	ns
Control										
r	0.0969	0.1918	-0.2932	-0.0484	0.1975	-0.0371	-0.1513	-0.1985	-0.3436	-0.1469
p	0.6601	0.3807	0.1745	0.8263	0.4321	0.8666	0.4907	0.3640	0.1084	0.5607
	ns	ns	ns	ns	ns	ns	ns	ns	ns	ns

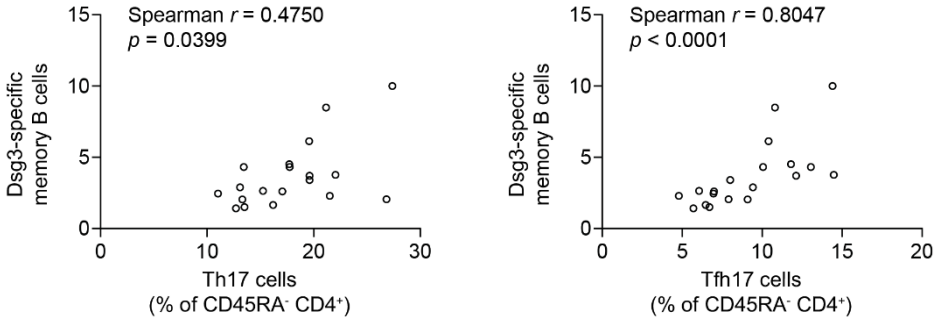

Figure 24: Positive correlation of Dsg3-specific memory B cells with Th17 and Tfh17 cell subsets in active pemphigus patients. Levels of autoreactive Dsg3$^+$ memory B cells were analyzed for correlation with Th17 and Tfh17 cell amounts. Spearman's correlation coefficient, *p*-values indicated.

4.7. Selective targeting of JAK3 with new small molecular compounds

KEGG pathway analyses suggested an involvement of the JAK/STAT signaling cascade in disease manifestation, as this pathway was overrepresented in lesional skin of pemphigus

patients. In addition, considering that the initiation and manifestation of various autoimmune disorders, including pemphigus, seem to be triggered by T lymphocytes and due to the largely restricted JAK3 expression to hematopoietic cells, a selective JAK3 inhibitor could provide benefits in the treatment of inflammatory autoimmune diseases without greatly affecting other types than immune cells. Moreover, a selective JAK3 inhibitor would presumably affect autoantibody production by B cells. For this purpose, novel JAK3 selective compounds were identified by the group of Stefan Laufer from the Pharmaceutical Chemistry Department of the Tübingen University and their functional selectivity was evaluated in a $CD4^+$ T cell cytokine stimulation assay. To study the effects of selective JAK inhibitors on cytokine signaling, the dose-dependent inhibition of STAT phosphorylation in human $CD4^+$ T cells was determined and inhibitory efficiency of new compounds was compared with the clinically established pan-JAK inhibitor Tofacitinib (Tofa) and the JAK3 selective NIBR3049 (NIBR).

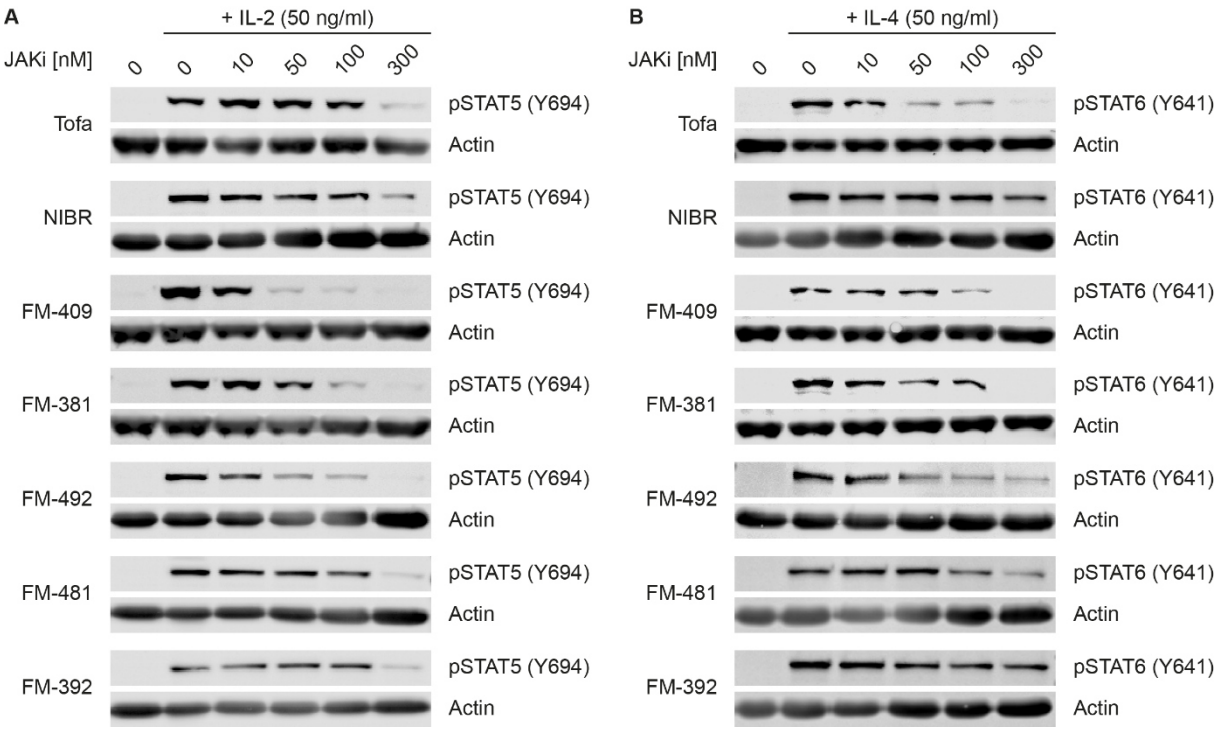

Figure 25: Inhibition of cytokine-induced STAT phosphorylation by JAK3-selective compounds. Human $CD4^+$ T cells were incubated with the indicated concentrations of Tofacitinib (Tofa), NIBR3049 (NIBR) or new JAK3-selective compounds (indicated) for 1 h followed by 30 min stimulation with respective cytokines. Levels of pSTAT5 and pSTAT6 were determined by phospho-specific antibodies and immunoblotting. **(A)** IL-2 activates JAK1/3 dependent STAT5 phosphorylation. **(B)** IL-4 initiates JAK1/3-mediated STAT6 activation. Western blot images were published in [177, 178].

Different cytokines using either combinations of JAK1 and JAK3 or combinations of JAK1, JAK2 and/or TYK2 were applied to stimulate $CD4^+$ T cells and activate the JAK/STAT signaling pathway. New compounds demonstrated JAK3 selectivity by inhibiting IL-2 as well as IL-4 receptor signaling cascades and blocking downstream STAT activation in a dose-dependent manner. Compared to treatment with Tofa or NIBR, some of the new compounds achieved JAK3 inhibition even at lower doses upon stimulation of T cells with these γc receptor using cytokines (Figure 25). The compounds FM-409, FM-381 and FM-492 blocked IL-2-mediated JAK1/JAK3 dependent STAT5 activation at lower concentrations, while FM-481 and FM-392 showed similar inhibitory potency like Tofa and NIBR. Inhibition of STAT6 phosphorylation via IL-4 signaling through JAK1/JAK3 was demonstrated for FM-409, FM-381, FM-492 and FM-481 comparable to Tofa, whereas compounds NIBR and FM-392 were not effective in blocking IL-4 induced STAT6 phosphorylation at the applied concentrations up to 300 nM.

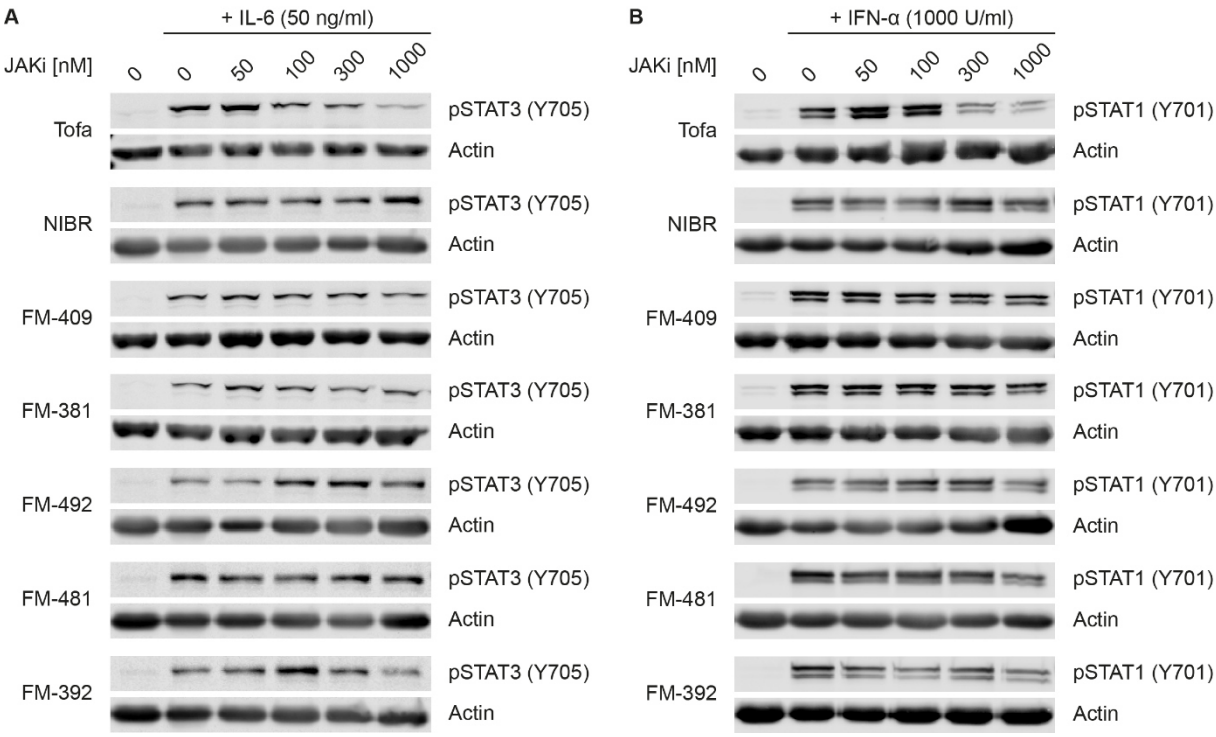

Figure 26: Cytokine-induced activation of STAT3 and STAT1 is not affected by JAK3 selective compounds. T cells were pre-incubated for 1 h with the indicated concentrations of Tofacitinib (Tofa), NIBR3049 (NIBR) or new compounds (as indicated) selective for JAK3 followed by 30 min stimulation with respective cytokines inducing phosphorylation of STAT3 and STAT1. **(A)** IL-6 induces JAK1/JAK2/TYK2 dependent STAT3 phosphorylation. **(B)** IFN-α promotes JAK1/TYK2-dependent STAT1 activation. Part of the images was published in [177, 178].

Since Tofa has been shown previously to inhibit not only JAK3 but also JAK1 and JAK2 activation [56], the impact of the new compounds on JAK3 independent JAK/STAT signal transduction, activated by cytokines like IL-6 or IFN-α, was investigated. As reported, Tofa inhibited IL-6 and IFN-α signaling in a dose-dependent manner as demonstrated by the activation of STAT3 through JAK1/JAK2/TYK2 and STAT1 through JAK1/TYK2 (Figure 26). In sharp contrast, NIBR and also the new compounds tested neither affected IL-6 nor IFN-α signaling cascade in T cells. However, a weak inhibition was demonstrated by FM-392 at 1,000 nM towards IL-6 induced, JAK1/JAK2/TYK2-mediated STAT3 phosphorylation.

4.8. Blockade of the IL-21 signaling cascade in CD4⁺ T cells by JAK inhibition

IL-21 induced signal transduction and activation of STAT3 via JAK1 and JAK3 play a crucial role in the differentiation of Tfh cells and thus also in the formation of autoantibodies [47, 50]. Therefore, the blockade of the IL-21 signaling pathway in $CD4^+$ cells using JAK inhibitors was assessed. For this purpose, the pan-JAK inhibitor Tofa, the JAK1 selective inhibitor PF-04965842 (PF-049) and the two JAK3 targeted compounds FM-481 and FM-381 were selected and investigated for their ability to abrogate the IL-21 signaling cascade. $CD4^+$ T cells were simulated with IL-21 in the presence or absence of inhibitors and subsequent phosphorylation of STAT3 (n=3) as well as induction of *IL21* mRNA expression (n=4) was measured. IL-21 strongly induced phosphorylation of STAT3 ($p<0.01$), which was blocked by all applied inhibitors in a dose dependent manner (Figure 27A and B). Tofa and the JAK3 selective compound FM-381 showed highly effective blockade of IL-21-mediated STAT3 activation, especially at 1 µM the activation was nearly completely abolished (both $p<0.05$). The JAK3 selective compounds showed more potent efficacy than the JAK1 targeted PF-049. Expression analysis revealed induction of *IL21* mRNA by IL-21 stimulation and, also suppressed *IL21* expression through JAK1 and JAK3 inhibition in a dose-dependent way (Figure 27C). Simultaneous blockade of both JAK1 and JAK3 signal transduction by Tofa was most effective ($p<0.01$ for 0.3 µM and $p<0.001$ for 1 µM) in suppressing *IL21* mRNA expression. Each of the selective compounds blocked the expression of *IL21* from 0.1 µM almost to the control level and fell below control expression at 0.3 µM. FM-481 and FM-381 showed significantly suppressed *IL21* mRNA levels at a concentration of 1 µM (both $p<0.01$).

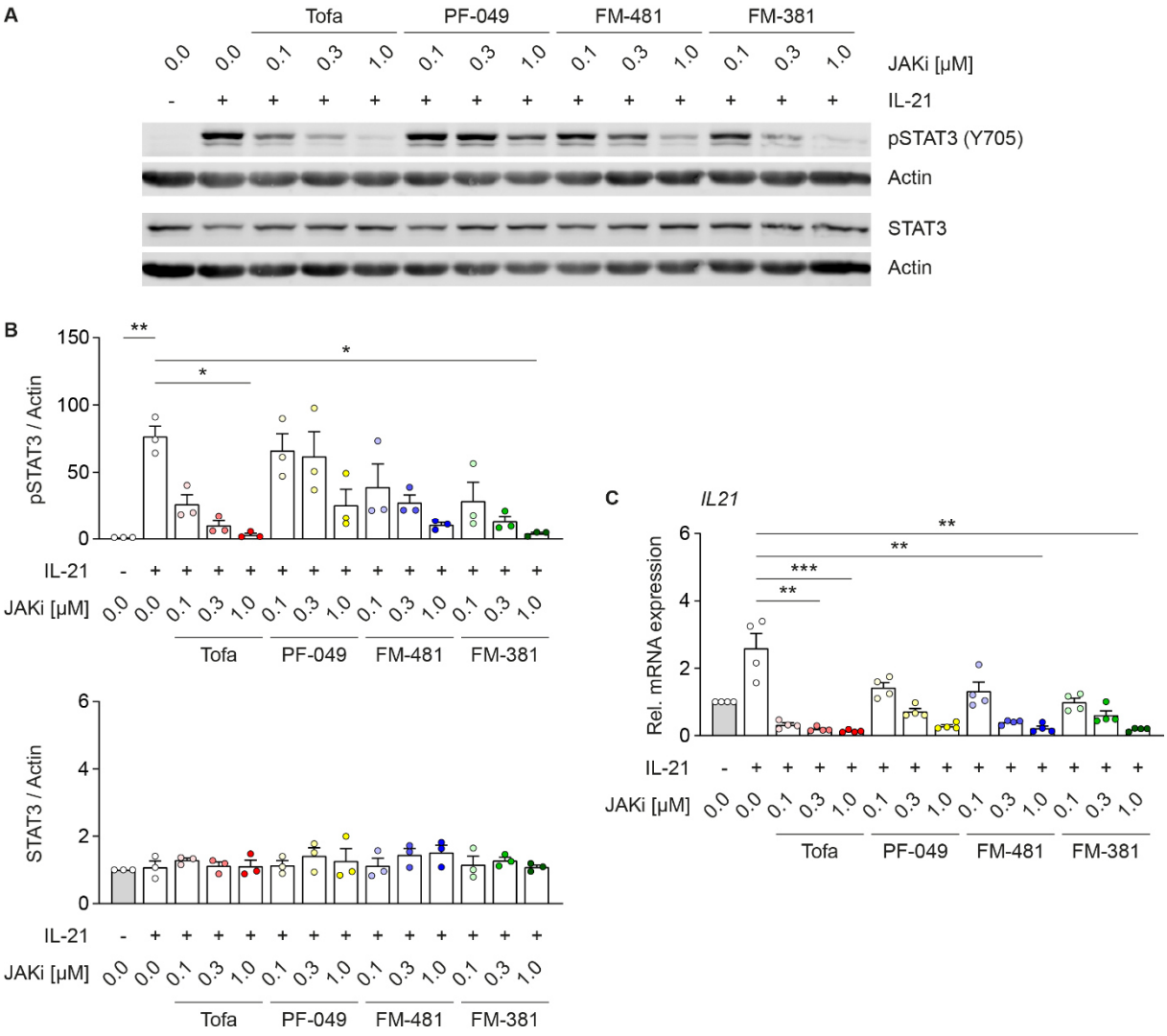

Figure 27: IL-21 signaling cascade is abrogated by JAK inhibitors in CD4⁺ T cells. CD4+ T cells were pre-incubated for 1 h with the indicated JAKi followed by stimulation with 50 ng/ml IL-21. STAT3 activation and *IL21* mRNA expression were determined by Western blot and qPCR, respectively. **(A)** Representative immunoblots for pSTAT3 and STAT3 after IL-21 stimulation of Th cells for 30 min. **(B)** Semi-quantitative analysis of specific bands relative to Actin (n=3). Single donors and mean with SEM are shown, control condition was set to 1. Friedman test and Dunn's multiple comparison post-hoc test (* p<0.05, ** p<0.01). **(C)** Relative *IL21* mRNA expression of CD4⁺ T cells pre-incubated with JAKi and stimulated with 50 ng/ml IL-21 in the presence of CD3/CD28 for 24 h (n=4). Data were normalized to *ACTB* and *POLR2A* and untreated control (DMSO only) was set to 1. Single donors and mean with SEM are shown. Dunn's multiple comparison test after Friedman test (** p<0.01, *** p<0.001).

4.9. Activation of STAT1 signaling pathway by monoclonal anti-Dsg3 IgG in keratinocytes

Besides immune cells, keratinocytes are also involved in the pathogenesis of pemphigus as they are the primary target cells of autoantibodies directed against desmosomal proteins. Binding of autoantibodies leads to the activation of several signaling pathways. Due to the finding of overrepresented JAK/STAT signaling pathway in lesions of pemphigus patients, the activation of STAT molecules by the monoclonal anti-Dsg3 IgG AK23 was investigated.

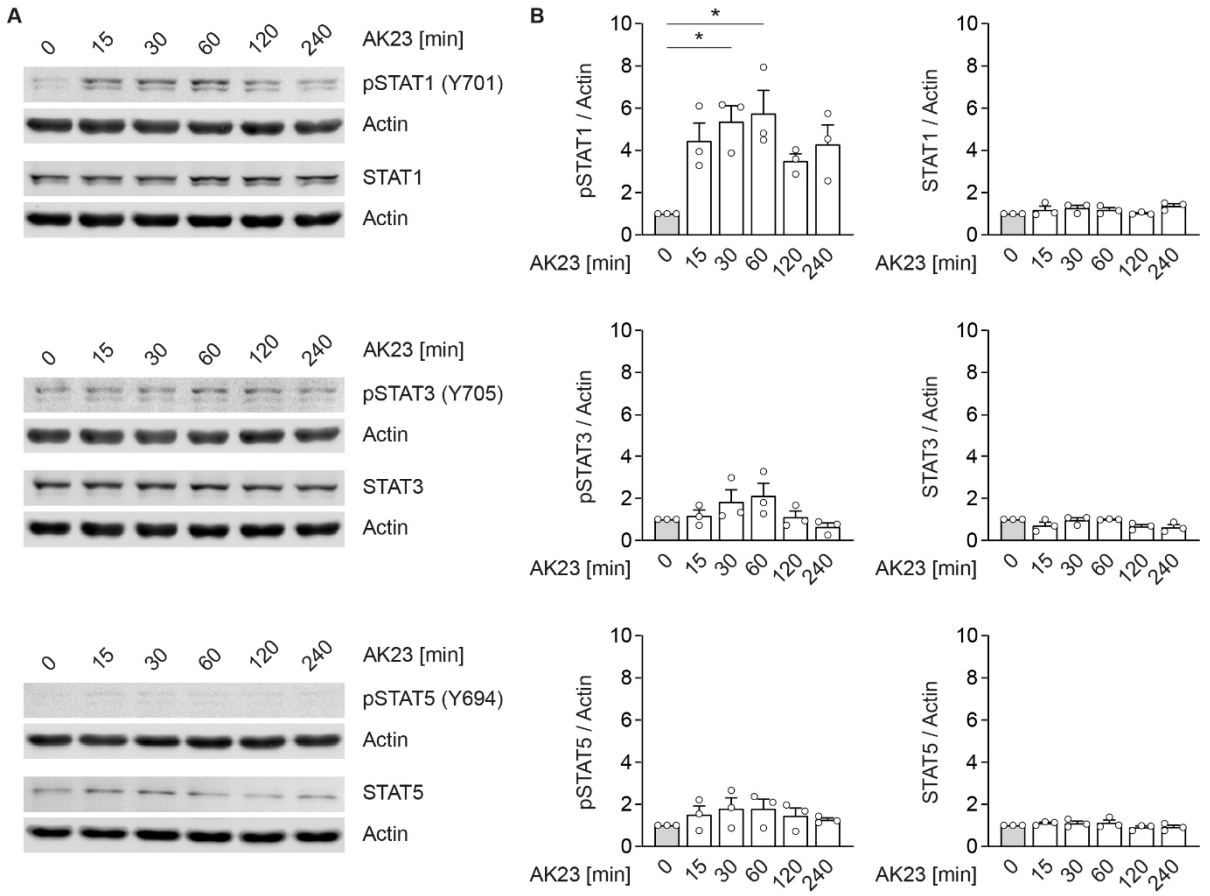

Figure 28: Activation of STAT1 by anti-Dsg3 antibody AK23 in human keratinocytes. Normal human epidermal keratinocytes (NHEK) were incubated with 20 µg/ml AK23 for 0 to 240 min (as indicated) and phosphorylation of STAT proteins was analyzed by immunoblotting. **(A)** Representative blots from one donor are shown for pSTAT1, STAT1, pSTAT3, STAT3, pSTAT5 and STAT5. **(B)** Semi-quantitative analysis of signal intensity was performed for specific bands (n=3 for each condition), data were normalized to actin and control was set to 1 (0 min, neutralization/elution buffer mix only). Single donors and mean with SEM are shown. Dunn's multiple comparison test after Friedman test (* p<0.05).

In order to analyze the phosphorylation of STAT1, STAT3, STAT4, STAT5 and STAT6 by immunoblot, primary normal human epidermal keratinocytes (NHEK) were treated with 20 µg/ml AK23 for 15, 30, 60, 120 and 240 min (n=3). STAT1 phosphorylation was detected from 15 min incubation on until the last time point of 240 min, whereas signal intensity first increased and then decreased over time. After 30 and 60 min of incubation with AK23, the relative pSTAT1 signal was significantly increased compared to untreated cells (p<0.05). There was also weak activation of STAT3 and STAT5 measured, but to a much lesser extent than STAT1 (Figure 28). However, no detectable signal for pSTAT4 and pSTAT6 was observed (n=2; representative immunoblot in Figure A6 in the appendix).

Next, immunoblots were performed to study the potential of JAK inhibitors to block AK23 induced STAT1 phosphorylation (n=5). The pan-JAK inhibitor Tofa, the JAK1 selective PF-049 and the JAK3 selective inhibitors FM-381 and FM-481 were tested. NHEK were pre-incubated with inhibitors for 1 h and treated afterwards with 20 µg/ml of anti-Dsg3 IgG for 4 h. Since AK23 has been reported to initiate p38 mitogen-activated protein kinase (MAPK) activation in the keratinocyte cell line HaCaT [182, 183], this protein was also assessed as a control downstream target (n=4). For this setting, the p38 MAPK inhibitor Skepinone-L [184] served as control compound. In agreement with the reports, p38 MAPK was phosphorylated upon AK23 incubation (p=0.09). This phosphorylation was completely abolished by Skepi-L (p<0.01), whereas JAK inhibitors had only slight effects on p38 MAPK activation. As expected due to the kinetics experiment, AK23 was able to induce the phosphorylation of STAT1 (p<0.05). The pan-JAK inhibitor Tofa blocked activation of STAT1 most successfully (p<0.01), while selective JAK1 as well as JAK3 compounds showed less effective inhibition. Skepi-L demonstrated only a minor inhibitory impact on STAT1 activation (Figure 29).

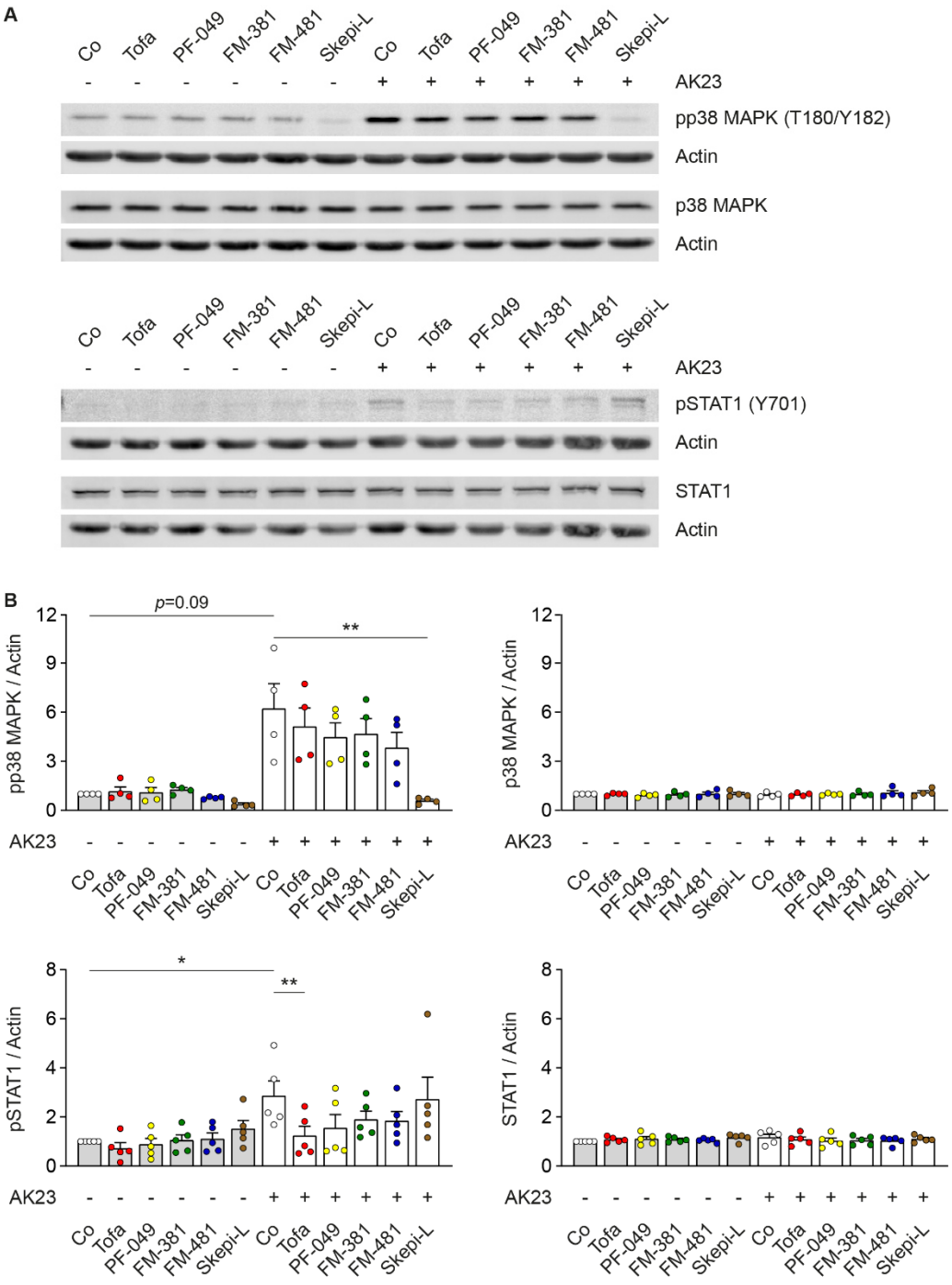

Figure 29: AK23 induced phosphorylation of STAT1 is inhibited by the pan-JAK inhibitor Tofacitinib. Keratinocytes were pre-incubated for 1 h with inhibitors (1 µM) and subsequently treated with 20 µg/ml of AK23 for 4 h. **(A)** Representative images of pp38 MAPK/p38 MAPK and pSTAT1/STAT1 detection are shown for one donor. **(B)** Quantification of detected signal intensity relative to actin (n=5 for pSTAT1/STAT1, n=4 for pp38 MAPK/p38 MAPK). Signals of keratinocytes treated with DMSO only (Co) were set to 1. Single donors and mean with SEM are shown. Dunn's multiple comparison test after Friedman test (* $p<0.05$, ** $p<0.01$, $p<0.2$ as indicated).

4.10. pSTAT1 and pSTAT3 expression in pemphigus skin

Since KEGG pathway analysis revealed a significant upregulation of the JAK/STAT signaling pathway in lesional skin of pemphigus patients and also STAT molecules were activated by AK23 in keratinocytes, IHC stains for pSTAT1 and pSTAT3 were performed in pemphigus skin (PV n=5, PF n=5). Healthy skin (Co, n=5) and lesional skin from patients with psoriasis vulgaris (Pso, n=7) served as control tissues, as it was demonstrated before, that STAT1 as well as STAT3 are activated in psoriatic skin [185, 186]. In both dermal infiltrate and epidermal keratinocytes, STAT1 was found phosphorylated in PV and in PF. As expected, psoriasis skin also presented a strong signal, whereas healthy skin showed no or very low protein expression of pSTAT1 (Figure 30A). Quantification of the specific signal in the epidermis revealed significant activation and overexpression of pSTAT1 in keratinocytes of diseased skin. Even though some patients had lower expression levels, it was still clearly increased compared to healthy skin, at least 10-fold in PV (p<0.05). The mean signals of PF and Pso were lower than those in PV, yet still significantly elevated compared to normal skin (PF p=0.12, Pso p<0.05). Similar to pSTAT1, activation of STAT3 was found in both epidermis and dermis, though there was a basal pSTAT3 expression in Co samples (Figure 30B). Overall, the level of pSTAT3 protein expression was lower than the pSTAT1 level in the epidermis. However, keratinocytes of PV patients showed significantly increased STAT3 activation compared to healthy skin (p<0.01). Furthermore, the expression of pSTAT3 in the epidermis of PF and Pso patients was also markedly elevated, though to a lesser extent than in PV. Nevertheless, the phosphorylated STAT3 protein levels in PF and Pso tended to be significantly higher than in Co (p=0.07 for PF and p=0.09 in Pso).

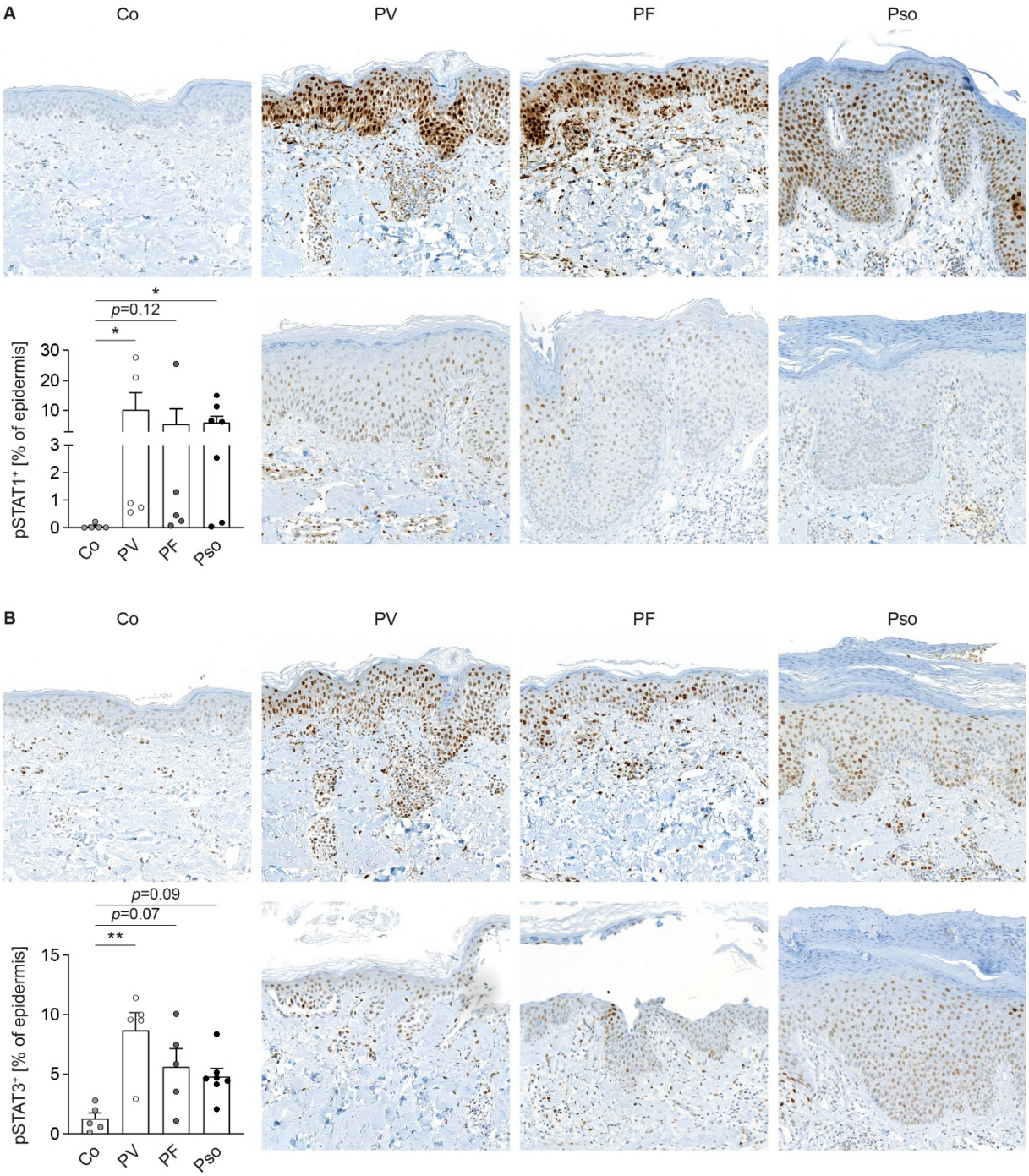

Figure 30: STAT1 and STAT3 are both activated in the skin of pemphigus patients. Formalin-fixed paraffin embedded tissue from normal skin (n=5), perilesional skin of pemphigus patients (PV and PF, both n=5) and lesional psoriatic skin (Pso, n=7) was stained using anti-pSTAT1 (Y701) and anti-pSTAT3 (Y705) antibodies. **(A)** Representative microscopic images of pSTAT1 stains are shown for Co, patient biopsies with high signal (upper row) as well as patient skin presenting low signal (lower images, original magnification 100x). Protein expression was determined by semi-quantitative analysis of the specific pSTAT signal in the epidermis. Single patients and mean with SEM are plotted. Dunn's multiple comparison test after Kruskal-Wallis test (* $p<0.05$, ** $p<0.01$, $p<0.2$ as indicated). **(B)** Representative images and analysis for pSTAT3 with the same setup as in (A).

4.11. JAK inhibitors protect keratinocyte monolayer from acantholysis in dispase-based dissociation assay

The JAK/STAT signaling pathway was found significantly overrepresented in pemphigus lesions by RNA-seq analyses, STAT molecules were activated in keratinocytes by the monoclonal anti-Dsg3 antibody AK23 and finally, phosphorylated STAT1 and STAT3 proteins were detected in perilesional skin of pemphigus patients as determined by IHC staining. For these reasons, JAK inhibitors were investigated for their ability to protect keratinocyte monolayers from anti-Dsg3 antibody induced fragmentation in a dispase-based dissociation assay. Four different JAK inhibitors were tested: the pan-JAK inhibitor Tofa, the JAK1 selective PF-049 and the JAK3 selective inhibitors FM-381 and FM-481. The p38 MAPK inhibitor Skepi-L served as control substance since modulation of p38 MAPK signaling prevents pemphigus skin blistering and abolishes loss of keratinocyte cohesion induced by AK23 [107, 182]. Therefore, monolayers of NHEK were pre-incubated with distinct inhibitors and acantholysis was induced with 20 µg/ml monoclonal anti-Dsg3 IgG and mechanical stress. Significantly increased loss of adhesion measured by the number of fragments was obtained in absence of any inhibitors ($p<0.05$). As expected, the fragmentation was reduced by the addition of the p38 MAPK inhibitor Skepi-L in a dose-dependent manner ($p<0.05$ for 0.1 µM and $p<0.01$ for 1 µM; Figure 31A and B). Interestingly, all four applied JAK inhibitors also significantly diminished AK23 induced acantholysis of the keratinocyte monolayers. While Tofa and PF-049 seemed to be most effective at 0.3 µM (both $p<0.01$), the JAK3 selective compounds FM-381 and FM-481 showed a dose-dependent effect with the highest efficacy at 1 µM ($p<0.001$ for FM-381 and $p<0.01$ for FM-481; Figure 31C and D).

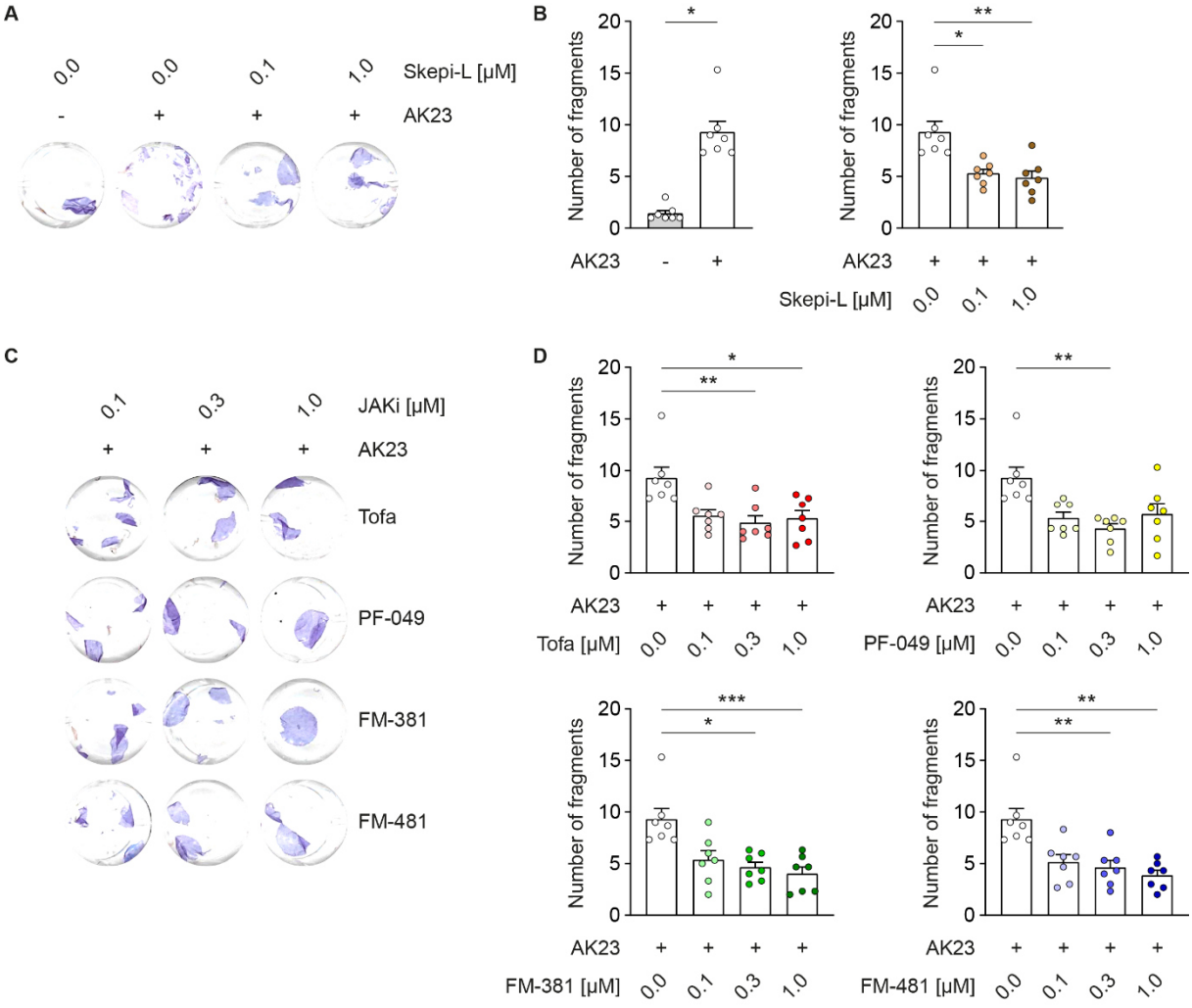

Figure 31: JAK inhibitors protect keratinocyte monolayer from acantholysis in dispase-based dissociation assay. Acantholysis was induced in primary human keratinocytes with 20 µg/ml AK23 for 4 h in the presence of indicated inhibitors in DMSO or DMSO alone (control). Quantification was achieved by counting the number of fragments obtained after application of mechanical stress to the monolayers (n=7). **(A)** Representative images showing AK23 induced monolayer fragmentation of one donor and the protective effect of Skepi-L. **(B)** Quantification of cell sheets after acantholysis as shown in (A). Fragment numbers of each experiment and mean with SEM are shown. Wilcoxon matched-pairs signed rank test (* p<0.05) for comparing control condition without AK23 and AK23 treatment. Friedman test and Dunn's multiple comparison test (* p<0.05, ** p<0.01) for comparison of Skepi-L with AK23 alone. **(C)** Representative results of JAK inhibitors Tofa, PF-049, FM-381 and FM-481 preventing loss of keratinocyte cohesion initiated by AK23**. (D)** Quantification of monolayer fragments after dissociation assay according to (C). Numbers of cell sheets counted in individual experiments and mean with SEM are shown. Friedman test and Dunn's multiple comparison test (* p<0.05, ** p<0.01, *** p<0.001) for comparison of each condition with AK23 alone.

5. DISCUSSION

In the present study, we aimed to analyze the immune signature in skin and peripheral blood of patients suffering from pemphigus. Especially, we were interested in identifying the cytokine targets implicated in pemphigus pathogenesis studying a large patient cohort from two clinical centers. Notably, the results revealed an IL-17A dominant signature in both skin lesions and peripheral blood of PV and PF patients. We found four distinct IL-17A-producing $CD4^+$ cell subsets circulating in active disease stage. Together with our collaborating group of Christian Möbs in Marburg we further demonstrated that of these subsets, only Tfh17 and to a lower level Tfh2 were able to induce the production of Dsg3-reactive autoantibodies by memory B cells of PV patients and Dsg1-reactive autoantibodies of PF patients, respectively [176]. These findings suggest that the hypothesis of pemphigus being a classical Th2-mediated disease should be reconsidered [92, 187]. Rather, our results indicate that IL-17A-producing Th/Tfh cells play a crucial role in pemphigus pathogenesis.

Immune reactions triggering disease manifestation are believed to initiate at distant sites of the body and as a consequence immune cells migrate to the skin, where autoantibodies bind to the desmosomes of epidermal keratinocytes [121]. This assumption is supported by the presence of autoantibodies circulating in peripheral blood of pemphigus patients [92]. In addition, overall systemic immunosuppression is more effective in improving disease activity than topical treatment of the lesions, for instance with rituximab, an anti-CD20 monoclonal antibody depleting B cells [188]. Furthermore, injection of Dsg3-reactive autoantibodies as well as the adoptive transfer of naïve splenocytes from $Dsg3^{-/-}$ mice in $Rag2^{-/-}$ immunodeficient mice resulted in a murine PV phenotype, which included weight loss, patchy hair loss and suprabasal acantholysis of the oral mucosa [96, 189]. Hence, the immunologic pattern in circulating $CD4^+$ T cells distant from the skin as well as at the site of disease manifestation and inflammation, the skin itself, was investigated.

Previous studies on skin of pemphigus patients reported the presence of Th1 and Th2 cytokines like IFN-γ and IL-4 [118]. These cytokines were also increased in our present study to some extent, but surprisingly, the transcriptome analysis revealed that Th17-associated cytokines were predominantly expressed in lesional pemphigus skin compared to healthy

control skin. The cytokines IL-17A, IL-21 and IL-23 have recently been reported in first small-sized cohorts to be elevated in pemphigus skin [120, 121]. In line with these studies, the data presented here confirm the overexpression of *IL17A*, *IL21* and *IL23A* in pemphigus skin, particularly in PV patients and in active disease stage. IL-21 may represent a key cytokine in pemphigus pathogenesis. Together with other cytokines, IL-21 promotes Th17 differentiation from naïve $CD4^+$ T cells and, in combination with IL-6, can trigger the development of Tfh17 cells. Both T cell subsets are capable of producing IL-21 themselves, resulting in a positive feedback mechanism and driving IL-17 production and Tfh induction [29, 47, 190]. In addition, IL-21 activates B cell responses to support the release of autoantibodies [191].

Moreover, numerous other factors were upregulated in lesional pemphigus skin compared to healthy skin samples. Amongst them was *IL1B*, a member of the IL-1 family, representing a group of cytokines primarily associated to innate immunity. IL-1β is essential to induce, together with IL-6 and IL-23, the differentiation of pathogenic Th17 cells and the production of IL-17A in mice [37]. Furthermore, IL-1β promotes the differentiation of $CCR6^+$ $CXCR3^+$ Th17.1 cells and, like IL-17, provokes the production of antimicrobial peptides by epithelial cells [42, 192, 193]. The major source of IL-1β are cells of the innate immune system, but epidermal keratinocytes are also capable of producing this protein upon IL-17A stimulation, thereby allowing the regulation of Th17 responses via a positive feedback mechanism. In addition, IL-17A as well as IL-1β both are similarly able to induce the expression of chemokines like CXCL1, CXCL5 or CXCL8 and also antimicrobial peptides such as S100A8 or S100A9 in keratinocytes [194]. These mediators were also found to be differentially expressed in pemphigus lesions compared to healthy skin by RNA-seq analysis in the present study. These findings further support the eminent role of IL-17 in disease initiation and maintenance.

Of note, the IL-20 subfamily members *IL19* and *IL24* within the IL-10 family of cytokines were also strongly induced in pemphigus lesional skin. These cytokines are typically overrepresented in inflammatory skin diseases dominated by IL-17, especially in psoriasis [195, 196]. However, neither IL-19 nor IL-24 have been associated with pemphigus diseases to date. Keratinocytes are able to express IL-19 upon IL-17A stimulation and the resulting amount of IL-19 can be further enhanced by the addition of IL-22 and TNF to IL-17A [195]. Besides keratinocytes, monocytes are capable of producing IL-19 upon treatment with

granulocyte macrophage colony-stimulating factor (GM-CSF), a cytokine also secreted by Th17.1 cells [40, 197]. Further, IL-19 has been reported to be expressed by B lymphocytes, which are also present in lesional pemphigus skin [121, 198]. Like IL-19, IL-24 is highly expressed in psoriatic lesions compared to normal skin [179]. The cellular sources of IL-24 are monocytes as well as T cells, predominantly Th2 cells [199]. Epidermal keratinocytes are also able to produce IL-24 upon stimulation with IL-17A or IL-1β, resulting in a positive feedback regulation of inflammation by expressing CXCL8 and MMP-1, mediators found to be upregulated in pemphigus skin by RNA-seq in this study [200]. All of these pro-inflammatory factors together form a network of highly cross-linked cytokines that display a robust IL-17 signature in pemphigus disease.

Considering this immunological profile of lesional pemphigus skin, there are similarities to psoriasis vulgaris, a chronic inflammatory autoimmune skin disorder driven by IL-17A-producing Th17 cells, although without an involvement of autoantibodies. In both diseases, IL-17-producing Th cells seem to play a pivotal role in disease pathogenesis and manifestation. Despite the similar cytokine signature, there are nonetheless important differences regarding morphological and molecular characteristics. Besides the clinical presentation and the absence of autoantibodies, high levels of IL-22 are detected in psoriasis patients [195]. This cytokine is essential for acanthosis, the epidermal thickening due to hyperproliferation of keratinocytes, characteristic for psoriasis [201]. In contrast, *IL22* was suppressed in pemphigus skin compared to healthy control and, consistent with this finding, decreased IL-22 serum levels were reported in blood of pemphigus patients [117, 202]. Further, IL-4, one characteristic Th2 defining cytokine of pemphigus diseases, is not detected in psoriasis patients. On the contrary, IL-4 therapy of psoriasis improves disease severity by inducing a Th2 response [203]. Although both psoriasis and pemphigus demonstrate a strong predominance of IL-17A, the cytokine profile in pemphigus presents more heterogeneic than that of psoriasis. Hence, selective inhibition of IL-17A and associated factors such as IL-21 or IL-23A might also be effective in treating blistering skin diseases like pemphigus. A recent case report demonstrates the successful therapy of a patient suffering from neutrophil-dominated PF with the anti-IL-17 antibody secukinumab. Neutralization of IL-17 led to a significant improvement of the clinical skin appearance and a marked decrease in anti-Dsg1 autoantibody amounts [204]. This first report supports the results described in the present study regarding the

pathogenic role of IL-17 secreting Th/Tfh cells in the production of anti-Dsg autoantibodies by autoreactive B cells in pemphigus diseases.

The multi-color flow cytometric analyses of T cell subsets circulating in the blood of pemphigus patients revealed higher numbers of IL-17-producing T cells in active stage of the disease compared to patients in remission. These cells were assigned to the $CXCR5^-$ Th17, $CXCR5^-$ Th17.1, $CXCR5^+$ Tfh17 and the $CXCR5^+$ Tfh17.1 subsets. However, no increased expression of *CXCR5* mRNA was detected in pemphigus skin when compared to normal control skin. Patients in remission even showed higher levels of *CXCR5* than those with active disease. Although the presence of $CD4^+$ cells capable of producing IL-17A and IL-21 was reported in lesions of active PV patients, these cells did not express CXCR5 or BCL6 [121]. This is consistent with the *CXCR5* mRNA expression data presented here. Nevertheless, Tfh cells are of crucial relevance for the secretion of pathogenic autoantibodies and the cytokines IL-6 and IL-21 are essential for the differentiation of Tfh cells [45, 47, 205]. In particular, IL-21 is crucial for the development of the Tfh lineage as well as the formation of GCs and is highly elevated in plasma of pemphigus patients [116]. It seems that IL-17-producing Th17 and Th17.1 as well as Tfh17 and Tfh17.1 cells are implicated in the pathogenesis of pemphigus diseases in different ways. While Th17 and Th17.1 cells are assumed to act as peripheral effector cells, Tfh17 and Tfh17.1 cells primarily maintain the autoantibody production through B cells in GCs [206].

The identification of $CXR3^+$ $CCR6^+$ Th17.1 and Tfh17.1 cells has improved the understanding of IL-17-producing Th cell populations [41]. These populations apparently play an important role within sustaining of inflammation in classical Th17-mediated autoimmune diseases like rheumatoid arthritis, multiple sclerosis or Sjogren's syndrome [40, 207, 208]. In active pemphigus patients who displayed high inflammatory parameters, also increased levels of these cell populations were observed compared to patients in remission showing diminished inflammation. Those $CXCR3^+$ $CCR6^+$ cells are able to secrete IFN-γ as well as IL-17A and to a certain extent GM-CSF [209].

Targeting autoreactive B cells with fluorescently labeled Dsg3 protein revealed significantly elevated levels of Dsg3-specific $CD19^+$ B cells and $CD19^+$ $CD27^+$ memory B cells from pemphigus patients with active disease compared to patients in remission as well as control

individuals. The detection of increased numbers of circulating Dsg3-reactive total B cells and memory B cells in PV patients compared to healthy individuals was reported before and is in line with these results [143]. Furthermore, activated autoreactive memory B cells with the ability to spontaneously produce anti-Dsg3 antibodies were exclusively found in patients with highly active disease, but not in remittent stage or in healthy donors. Moreover, increased numbers of total circulating Dsg3-reactive memory B cells was associated with enhanced disease activity [210]. Unexpectedly, a not negligible number of Dsg3-specific cells was also observed in the control group. In general, there is also a low prevalence of Dsg-reactive antibodies in healthy individuals. However, in contrast to autoantibodies from PV patients, the Dsg3-specific antibodies from healthy donors did not lead to internalization of Dsg3 *in vitro* [211]. The presence of Dsg3-specific B cells in blood of control individuals may indicate that IgM^+ B cells secrete potentially cross-reactive, non-pathogenic natural IgM autoantibodies [212]. Besides, the detected signal might also result from an unspecific binding of the fluorochrome-labeled Dsg3 to B cells.

Numbers of Th2 and Th1 cells were suppressed in active pemphigus disease compared to patients in remission. Moreover, correlation analysis revealed a negative correlation between Th1 cells and Dsg3-reactive memory B cells in active disease, suggesting that when Th1 cells increase, Dsg3-specific memory B cells decrease and vice versa. These findings are consistent with reports of suppressed IFN-γ levels and decreased numbers of IFN-γ-producing $CD4^+$ cells in the blood of active PV patients compared to patients in remission as well as healthy individuals [110, 114]. The decreased Th1 differentiation may result as a consequence of alterations in NK cells found in pemphigus patients, which led to impaired IL-12 signaling and subsequently abrogated Th1 cell activation [213]. NK cells are capable of instructing dendritic cells and thereby promoting the generation of Th1 cells [214, 215].

Remarkably, the numbers of Tfh17 cells from active PV patients correlated with total Dsg3-reactive B cells. Moreover, both Th17 and especially Tfh17 subsets demonstrated a strong positive relation to $CD19^+$ $CD27^+$ memory B cells in active stage of PV. These findings led to the investigation on the ability of distinct Th/Tfh subgroups to trigger B cells into producing autoantibodies. Our collaborators in Marburg finally demonstrated in co-culture experiments of T cell subsets together with memory B cells that primarily Tfh17 cells are responsible for

the formation of Dsg3- and Dsg1-reactive autoantibodies, respectively. Although all Th and Tfh cell types were able to induce IgG antibody production by memory B cells, the strongest induction of Dsg-specific autoantibody production was due to Tfh17 cells from patients with acute disease compared to chronic stage. However, T cells from patients in remission failed to elicit a specific autoantibody response. In addition, high levels of Dsg3-reactive Tfh17 cells were detected in acute PV patients, whereas the number of these cells was significantly decreased in chronic and remittent disease stages [176]. Very limited data is available addressing the role of Tfh17 cells as pathogenic subset in diseases driven by autoantibodies. However, these cells seem to be crucial for inducing T cell dependent IgA production in Peyer's patches [216]. Further, it has been reported that the IL-23-Th17 cell-dependent pathway defines autoantibody activity and thus determines the onset of the autoimmune disease rheumatoid arthritis [217]. Taken together, these outcomes underline a pivotal role of Th17 and more particularly Tfh17 cells in the development of autoantibody responses in patients with acute autoimmune diseases.

Th17 cells are believed to possess a dichotomous nature due to their roles in pro-inflammatory responses and also in barrier protection [218]. The findings presented in this study indicate that IL-17 also acts dichotomously in pemphigus. KEGG analysis revealed an induction of genes involved in tissue remodeling as well as in antimicrobial defense through the IL-17 signaling pathway, representing an advantageous outcome. On the other hand, various chemoattractants and cytokines are upregulated upon IL-17 stimulation, thereby promoting pathogenic inflammatory processes. Such opposing effects, simultaneously connected, have also been observed in atopic dermatitis, rheumatoid disorders and psoriasis, all diseases with elevated levels of IL-17 and related cytokines [218-220]. Prior to the development of effective medications for pemphigus diseases, infections, especially with *Staphylococcus aureus*, represented a major cause of death [221]. Therefore, the IL-17 signature found in pemphigus may be considered as a beneficial host defense mechanism against infections with bacteria, viruses and fungi. Consequently, genes associated with the staphylococcal infection pathway were overrepresented in RNA-seq analysis.

The investigation of gene expression by whole transcriptome sequencing in pemphigus reveals the broad impact of this disease on protein regulation. In this respect, the gene expression for

the oncogene suppressors *ADAMTS9-AS2* and *CADM2* were downregulated in the skin of pemphigus patients compared to control skin. These genes have been reported to inhibit tumor growth and are suppressed in various cancers, including esophageal squamous cell carcinoma [222-224]. This could explain the finding that pemphigus patients have a significantly higher prevalence for esophageal cancers than individuals, who never were diagnosed with pemphigus [225]. Furthermore, unraveling the contribution of the JAK/STAT signaling pathway in combination with the overexpression of cytokines activating this signaling cascade, including IL-4, IFN-γ and IL-21, could provide guidance for the application of novel therapeutic approaches by inhibiting JAK in pemphigus disease. Blockade of the JAK/STAT signal transduction through JAK1/JAK3 inhibitors would enable the interference with Th17, Th17.1, Tfh17, Tfh17.1 and also Th2 cells [56, 226].

In conclusion, the analyses of the skin cytokine signature and the immunophenotyping of peripheral blood cells have demonstrated that IL-17 and IL-17-producing cells may play a major role in pemphigus pathogenesis, manifestation and persistence. In particular, Tfh17 cells seem to act directly pathogenic during active disease stage, as their numbers significantly correlate with levels of memory B cells and they are able to induce the formation of autoreactive antibodies by memory B cells. These findings strongly suggest extending the consideration of pemphigus from being a classical Th2-derived disease towards a more complex condition dominated by Th17/Tfh17 cells. Taking this new insight into account, numerous new therapeutic options for pemphigus patients are emerging that may replace long-term treatment with corticosteroids. Specific biologics targeting, for instance, IL-21, IL-23 or IL-17A itself, thereby inactivating these cytokines, might be one therapy option. Another strategy could include the inhibition of cytokine signaling pathways, and thus impair T cell differentiation, GC formation, and production of autoantibodies by blocking molecules essential for downstream signal transduction.

In recent years, JAKs became attractive targets in the research and development of new therapeutic agents for the treatment of inflammatory responses. Aiming this family of cytoplasmic tyrosine kinases is attractive due to their participation in cytokine signal transduction. In particular, JAK3 seems to be critically involved in the development of immune cells as loss of function mutations of its gene may cause the SCID syndrome, an immunological

disorder characterized by the lack of NK cells, T cells and functional B cells [54]. Therefore, highly selective JAK3 inhibitors might be promising candidates for anti-inflammatory and immunosuppressive therapies. In the present study, a novel class of five covalent reversible JAK inhibitors was investigated for their ability to effectively and selectively block JAK3 signaling in primary human $CD4^+$ T cells by functional cytokine stimulation assays. All compounds were capable of blocking IL-2 signaling, whereas two compounds (NIBR and FM-392) failed to inhibit IL-4-mediated STAT6 activation at concentrations up to 300 nM. In addition, while the pan-JAKi Tofacitinib (which inhibits JAK3 and JAK1 and to some extent JAK2) clearly blocked JAK3 independent signaling cascades from 300 nM on, almost all inhibitors showed no effect even at a higher concentration, thus confirming their selectivity towards JAK3 in functional assays. However, the compound FM-392 weakly blocked IL-6 induced STAT3 activation at 1,000 nM. Determination of the cellular half maximal effective concentration (EC_{50}) revealed a similar potency of this substance for JAK2 (EC_{50}=630 nM) as for JAK3 (EC_{50}=678 nM), explaining its inhibitory effect on STAT3 phosphorylation [178].

The identification of NIBR led to debates, if the selective inhibition of JAK3 alone, without simultaneously blocking JAK1, is sufficient to suppress immune responses effectively, as JAK3 typically co-localizes with JAK1 for signaling through the γc receptor. There are studies claiming a dominant role for JAK1 over JAK3 due to a lower efficiency of JAK3 selective inhibitors [227, 228]. The rather low cellular activity of compounds NIBR and FM-392 are in conclusion with these findings. In contrast, another study demonstrated that fully abrogated downstream STAT5 phosphorylation was achieved by either JAK1 or JAK3 inhibition for the signal transduction of IL-15, a cytokine using the γc receptor for signaling [229]. This, together with the findings presented in this study, counters the assumption regarding the dominance of JAK1 and demonstrates that a potent, selective JAK3 inhibitor may also be able to achieve effective immunosuppression. Taken together, four of the five JAK inhibitors were identified as highly selective towards JAK3 in a functional $CD4^+$ cytokine stimulation assay. Furthermore, selective inhibition of JAK3 seemed to be sufficient to abrogate JAK1/JAK3 dependent STAT-phosphorylation without the need for concomitant JAK1 inhibition.

IL-21 contributes in the differentiation of Th17 as well as Tfh cells via activation of STAT3 and it is also essential for B cell responses and the release of autoantibodies. Hence it is not

surprising that this cytokine is overrepresented in blood and lesional skin of pemphigus patients, as previously described at protein level and found in the present study at mRNA level [116, 121]. Tofacitinib, but also JAK3 selective inhibitors were able to block IL-21-mediated signal transduction in $CD4^+$ cells determined by measurement of downstream STAT3 phosphorylation. This blockade led to suppressed *IL21* mRNA expression by these cells, which in pemphigus could result in prevention of Th17/Tfh17 cell differentiation and also autoantibody production by B cells. Depletion of IL-21 with neutralizing antibodies reduced both IL-17 protein and mRNA expression as well as blocked the formation of Th17 cells *in vitro* [190]. Experiments in mice have shown that Tofacitinib was very potent in blocking antigen specific production of antibodies and also impaired GC formation [230]. Furthermore, an essential role of STAT1 and STAT3 was revealed in the signal transduction of IL-6 and IL-21, cytokines crucial for the formation of GC. In the absence of IL-6 and IL-21 signaling, the generation of Tfh cells was impaired and thus levels of these cells were reduced. Consequently, the formation of GC was impaired and, due to the indispensable function of Tfh cells helping B cells to produce antibodies, the secretion of antibodies was also inhibited [231, 232].

Following binding of autoantibodies to desmosomes, both signal dependent as well as signal independent pathways seem to contribute to acantholysis and blister formation in pemphigus [106]. In the present study, besides activation of p38 MAPK, also STAT1 signaling was triggered upon stimulation of keratinocytes with the anti-Dsg3 IgG AK23. Further, this signaling cascade was effectively abrogated by Tofacitinib and, to a lesser extent, by the selective JAK1 inhibitor PF-049. Since the JAK/STAT pathway is typically used by various cytokines, it is reasonable to speculate that AK23 stimulates keratinocytes to produce cytokines leading to the phosphorylation of different JAKs and finally to the activation of primarily STAT1. These cytokines may further promote acantholysis as the blockade of JAK phosphorylation had a protective effect on cell fragmentation. The first cytokine group that comes to mind regarding STAT1 activation would be the interferons signaling via JAK1 and JAK2 or TYK2, and particularly, associated with inflammation, the type II interferon IFN-γ [233]. However, it is debatable whether keratinocytes are able to produce this cytokine as its production is thought to be mainly restricted to T cell and NK cell populations [234]. Moreover, a recent study showed undetectable or unaltered IFN-γ expression in HaCaT as well as NHEKs after

stimulation with IgG from PV patients or AK23 and subsequent cell sheet fragmentation. Besides, no increased release of IL-6, TNF and IL-1α has been demonstrated either [235]. Type I and type III interferons, on the other hand, are produced by almost all tissues, including epithelial cells, and may contribute to anti-Dsg3 IgG-mediated STAT activation [233]. Certainly, other cytokines might also be involved in AK23-induced acantholysis and further studies on this issue are necessary, although the identification of these factors could become challenging. First, the cytokine itself should be produced by keratinocytes, and second, the corresponding receptors need to be expressed on the cell surface. IL-22, for instance, activates STAT1, STAT3 and STAT5 in keratinocytes but is not secreted by these cells [236].

Of note, the JAK3 inhibitors also slightly interrupted the STAT1 activation by AK23, which may suggest less selectivity of these compounds in the keratinocyte setting. The active tyrosine kinase domains of all four JAK family molecules exhibit a high degree of homology, making it challenging to develop highly specific compounds and explaining why JAKi are selective but not that specific [237]. There are some inhibitors that initially claimed high JAK3 selectivity, yet later investigations revealed also inhibitory activity towards other JAK family proteins and only poor selectivity over JAK1, JAK2 or TYK2. A prominent example would be Tofacitinib, but also Decernotinib and Peficitinib only show a 4-fold and 5-fold potency, respectively, for JAK3 over other members of the JAK family [56, 238, 239]. Furthermore, selectivity and efficiency may vary amongst different cell types and depend on the particular activating cytokine and the applied inhibitor concentration.

Immunostainings of pemphigus patients' skin revealed a strong overexpression of pSTAT1 and pSTAT3 in epidermal keratinocytes compared to healthy skin. There are only limited data available on STAT molecules in blistering autoimmune diseases. JAK/STAT proteins were found to be overexpressed in lesions of bullous pemphigoid patients compared to perilesional skin as well as control skin [240]. A very recent report found increased levels of JAK3, STAT2 and STAT6 in perilesional and lesional epidermis of pemphigus patients compared to healthy skin [241]. Taking into account that numerous cytokines are overrepresented in the skin of pemphigus patients, it is reasonable to assume that various STAT molecules will be activated in keratinocytes. In particular, IFN-γ usually activates STAT1, but STAT3 has also been phosphorylated in primary human keratinocytes after IFN-γ stimulation, though to a lesser

extent [242]. In addition, anti-Dsg3 IgG, which is abundant in the lesions of pemphigus patients, also seem to activate STAT1 and, to a lesser extent, STAT3. The latter is typically activated by IL-6 or IL-23, both cytokines appearing among the overrepresented genes in pemphigus skin. Moreover, the IL-20 cytokine family members IL-19, IL-20 and IL-24 have been reported to induce phosphorylation of STAT3 in keratinocytes [196]. Interestingly, although IL-17 is not signaling through JAK associated receptors, but via a unique receptor family distinct from other known cytokine receptors, there are some reports indicating an involvement of the JAK/STAT pathway in the signal transduction of this cytokine [243-245]. Shi et al. for instance demonstrated that IL-17A is able to activate STAT1 and STAT3 in keratinocytes *in vitro* [246]. However, this can be an indirect effect. Moreover, JAK inhibition reversed the enhancement of antimicrobial peptides and chemokines induced by IL-17A in airway epithelia and airway smooth muscle cells, respectively [245, 247]. Again, other JAK/STAT using cytokines may be involved.

To investigate the functional role of the JAK/STAT pathway in pemphigus pathogenesis, acantholysis was induced in differentiated keratinocyte monolayers by the anti-Dsg3 IgG AK23 in the presence of JAKi. Interestingly, all applied inhibitors demonstrated a protective effect on cell fragmentation, suggesting a potential involvement of JAK/STAT molecules during blister formation in pemphigus disease. Data addressing the participation of JAK/STAT signaling in autoantibody-induced acantholysis are very scarce. Mao et al. assigned a role for STAT3 in the regulation of Dsg3 transcription and consequently the loss of keratinocyte adhesion. Inhibition of STAT3 led to increased Dsg3 levels, both for mRNA as well as protein expression. Furthermore, STAT3 inhibition prevented PV-IgG-mediated acantholysis in keratinocytes *in vitro* and autoantibody-induced blistering *in vivo* by inducing Dsg3 expression, while constitutive activation of STAT3 resulted in decreased Dsg3 levels and in enhanced cell sheet fragmentation, even in the absence of pathogenic autoantibodies [248]. In contrast, Dsg3 levels were not altered by JAKi in the present study (shown in Figure A7 in the appendix), but STAT3 was not directly inhibited either. Instead, JAKi only blocked the activation of STAT molecules without affecting total STAT protein levels. Nevertheless, a similar mechanism may be operating in this case, by regulating certain cell adhesion molecules through the modulation of JAK and thereby compensating for the impaired Dsg3-mediated cell adhesion.

Unexpectedly, the JAK3 selective compounds FM-381 and FM-481 also prevented keratinocyte monolayers from acantholysis in a dose-dependent manner. This might be explained by poor selectivity of the inhibitors for JAK3 over other JAK family members in the keratinocyte model, as mentioned above. On the other hand, although JAK3 is thought to be predominantly expressed in leukocytes, there is data supporting the presence of JAK3 in epithelial cells [51, 52]. Srivastava et al. investigated the expression of all four JAK family molecules in keratinocytes and demonstrated that, while the mRNA expression of JAK1, JAK2 and Tyk2 was comparable to PBMCs, JAK3 showed lower expression in keratinocytes, but was still expressed. Further, similar protein expression of all three JAKs was detected by Western blot in cultured keratinocytes [249]. By performing IHC staining in skin, JAK3 was detected in healthy epidermis as well as in keratinocytes of lesional and perilesional skin from pemphigus patients, whereas the number of JAK3 positive cells was increased in diseased skin [241, 250]. Another study also reported the presence of both JAK3 and pJAK3 in keratinocytes of cutaneous inflammatory diseases and healthy skin. Protein expression determined by IHC staining was elevated in affected samples. In addition, JAK3 was activated in keratinocytes *in vitro* upon stimulation with a mixture of proinflammatory cytokines and could subsequently be inhibited by Tofacitinib treatment [186]. Thus, there is some evidence that JAK3 is expressed in keratinocytes, both at mRNA and protein level and, that the protein is overrepresented under inflammatory conditions, making keratinocytes, along with lymphocytes, potential target cells for JAK3 inhibitors in the treatment of inflammatory skin diseases.

There are many studies aiming to investigate the efficacy of JAK inhibitors in autoimmune disorders of the skin, including atopic dermatitis, psoriasis or alopecia areata [251]. However, patients suffering from blistering autoimmune diseases such as bullous pemphigoid or pemphigus could also benefit from new therapeutic approaches regarding selective inhibition of JAKs. Considering the broad cytokine profile in the skin and blood of pemphigus patients, blocking JAKs as essential downstream cytokine signaling molecules could reduce inflammatory responses and autoantibody production. Such blockade may decrease blister formation, promote healing of blisters and erosions, as well as control the disease process. Even for maintenance therapy, the administration of highly selective inhibitors might be safe and effective. Furthermore, given that JAKi directly impact keratinocyte signaling, they could

be applied not only systemically but also topically. In contrast to the conventional treatment with topical steroids, which causes skin damage such as atrophy or telangiectasia upon long-term application, a topical formulation containing JAKi may be beneficial to prevent such side effects and further improve the safety profile of JAKi by avoiding the adverse reactions of a systemic therapy [252].

In conclusion, the findings presented in this study support the theory that, in addition to IL-4-producing Th2 cells and IFN-γ-producing Th1 cells, the immunological activity in pemphigus relies significantly on IL-17A-producing T cell subsets. Particularly, Tfh17 cells seem to act as potent inducers of autoantibody production by memory B cells in acute disease stage. Based on the profound immune activity, inhibition of JAKs might serve as a potential therapeutic approach and could improve the treatment of pemphigus disease.

6. REFERENCES

1. Burnet FM. A modification of Jerne's theory of antibody production using the concept of clonal selection. CA Cancer J Clin 26(2), 119-121 (1976).
2. Nossal GJ, Lederberg J. Antibody production by single cells. Nature 181(4620), 1419-1420 (1958).
3. Murphy K, Weaver C. Grundbegriffe der Immunologie. In: Murphy K, Weaver C. Janeway Immunologie. 9. Edition, Springer Spektrum, Berlin, Heidelberg (2018).
4. CHAN JKC, NG CS, HUI PK. A simple guide to the terminology and application of leucocyte monoclonal antibodies. Histopathology 12(5), 461-480 (1988).
5. de Rie MA, Schumacher TNM, van Schijndel GMW, van Lier RW, Miedema F. Regulatory role of CD19 molecules in B-cell activation and differentiation. Cellular Immunology 118(2), 368-381 (1989).
6. Tedder TF, Boyd AW, Freedman AS, Nadler LM, Schlossman SF. The B cell surface molecule B1 is functionally linked with B cell activation and differentiation. J Immunol 135(2), 973-979 (1985).
7. Murphy K, Weaver C. Antigenerkennung durch B-Zell- und T-Zell-Rezeptoren. In: Murphy K, Weaver C. Janeway Immunologie. 9. Edition, Springer Spektrum, Berlin, Heidelberg (2018).
8. Barber EK, Dasgupta JD, Schlossman SF, Trevillyan JM, Rudd CE. The CD4 and CD8 antigens are coupled to a protein-tyrosine kinase (p56lck) that phosphorylates the CD3 complex. Proc Natl Acad Sci U S A 86(9), 3277-3281 (1989).
9. Kambayashi T, Laufer TM. Atypical MHC class II-expressing antigen-presenting cells: can anything replace a dendritic cell? Nature Reviews Immunology 14(11), 719-730 (2014).
10. Zhu J, Paul WE. Peripheral CD4+ T-cell differentiation regulated by networks of cytokines and transcription factors. Immunol Rev 238(1), 247-262 (2010).
11. Mosmann TR, Cherwinski H, Bond MW, Giedlin MA, Coffman RL. Two types of murine helper T cell clone. I. Definition according to profiles of lymphokine activities and secreted proteins. J Immunol 136(7), 2348-2357 (1986).
12. Hsieh CS, Macatonia SE, Tripp CS, Wolf SF, O'Garra A, Murphy KM. Development of TH1 CD4+ T cells through IL-12 produced by Listeria-induced macrophages. Science 260(5107), 547-549 (1993).

13. Thierfelder WE, van Deursen JM, Yamamoto K, Tripp RA, Sarawar SR, Carson RT, Sangster MY, Vignali DA, Doherty PC, Grosveld GC, et al. Requirement for Stat4 in interleukin-12-mediated responses of natural killer and T cells. Nature 382(6587), 171-174 (1996).
14. Szabo SJ, Kim ST, Costa GL, Zhang X, Fathman CG, Glimcher LH. A novel transcription factor, T-bet, directs Th1 lineage commitment. Cell 100(6), 655-669 (2000).
15. Lighvani AA, Frucht DM, Jankovic D, Yamane H, Aliberti J, Hissong BD, Nguyen BV, Gadina M, Sher A, Paul WE, et al. T-bet is rapidly induced by interferon-gamma in lymphoid and myeloid cells. Proc Natl Acad Sci U S A 98(26), 15137-15142 (2001).
16. Dardalhon V, Korn T, Kuchroo VK, Anderson AC. Role of Th1 and Th17 cells in organ-specific autoimmunity. Journal of Autoimmunity 31(3), 252-256 (2008).
17. Zekzer D, Wong FS, Ayalon O, Millet I, Altieri M, Shintani S, Solimena M, Sherwin RS. GAD-reactive CD4+ Th1 cells induce diabetes in NOD/SCID mice. The Journal of Clinical Investigation 101(1), 68-73 (1998).
18. Kaplan MH, Schindler U, Smiley ST, Grusby MJ. Stat6 is required for mediating responses to IL-4 and for development of Th2 cells. Immunity 4(3), 313-319 (1996).
19. Zheng W, Flavell RA. The transcription factor GATA-3 is necessary and sufficient for Th2 cytokine gene expression in CD4 T cells. Cell 89(4), 587-596 (1997).
20. Swain SL, Weinberg AD, English M, Huston G. IL-4 directs the development of Th2-like helper effectors. J Immunol 145(11), 3796-3806 (1990).
21. Steinke JW, Borish L. Th2 cytokines and asthma. Interleukin-4: its role in the pathogenesis of asthma, and targeting it for asthma treatment with interleukin-4 receptor antagonists. Respir Res 2(2), 66-70 (2001).
22. Harrington LE, Hatton RD, Mangan PR, Turner H, Murphy TL, Murphy KM, Weaver CT. Interleukin 17–producing CD4+ effector T cells develop via a lineage distinct from the T helper type 1 and 2 lineages. Nature Immunology 6(11), 1123-1132 (2005).
23. Langrish CL, Chen Y, Blumenschein WM, Mattson J, Basham B, Sedgwick JD, McClanahan T, Kastelein RA, Cua DJ. IL-23 drives a pathogenic T cell population that induces autoimmune inflammation. Journal of Experimental Medicine 201(2), 233-240 (2005).
24. Park H, Li Z, Yang XO, Chang SH, Nurieva R, Wang Y-H, Wang Y, Hood L, Zhu Z, Tian Q, et al. A distinct lineage of CD4 T cells regulates tissue inflammation by producing interleukin 17. Nature Immunology 6(11), 1133-1141 (2005).

25. van Beelen AJ, Teunissen MBM, Kapsenberg ML, de Jong EC. Interleukin-17 in inflammatory skin disorders. Current Opinion in Allergy and Clinical Immunology 7(5), (2007).
26. Kebir H, Kreymborg K, Ifergan I, Dodelet-Devillers A, Cayrol R, Bernard M, Giuliani F, Arbour N, Becher B, Prat A. Human TH17 lymphocytes promote blood-brain barrier disruption and central nervous system inflammation. Nat Med 13(10), 1173-1175 (2007).
27. Ivanov I, McKenzie BS, Zhou L, Tadokoro CE, Lepelley A, Lafaille JJ, Cua DJ, Littman DR. The orphan nuclear receptor RORgammat directs the differentiation program of proinflammatory IL-17+ T helper cells. Cell 126(6), 1121-1133 (2006).
28. Veldhoen M, Hocking RJ, Atkins CJ, Locksley RM, Stockinger B. TGFbeta in the context of an inflammatory cytokine milieu supports de novo differentiation of IL-17-producing T cells. Immunity 24(2), 179-189 (2006).
29. Bettelli E, Carrier Y, Gao W, Korn T, Strom TB, Oukka M, Weiner HL, Kuchroo VK. Reciprocal developmental pathways for the generation of pathogenic effector TH17 and regulatory T cells. Nature 441(7090), 235-238 (2006).
30. Yang L, Anderson DE, Baecher-Allan C, Hastings WD, Bettelli E, Oukka M, Kuchroo VK, Hafler DA. IL-21 and TGF-β are required for differentiation of human TH17 cells. Nature 454(7202), 350-352 (2008).
31. Korn T, Bettelli E, Gao W, Awasthi A, Jager A, Strom TB, Oukka M, Kuchroo VK. IL-21 initiates an alternative pathway to induce proinflammatory T(H)17 cells. Nature 448(7152), 484-487 (2007).
32. Gutcher I, Donkor MK, Ma Q, Rudensky AY, Flavell RA, Li MO. Autocrine transforming growth factor-β1 promotes in vivo Th17 cell differentiation. Immunity 34(3), 396-408 (2011).
33. Chen W, Jin W, Hardegen N, Lei KJ, Li L, Marinos N, McGrady G, Wahl SM. Conversion of peripheral CD4+CD25- naive T cells to CD4+CD25+ regulatory T cells by TGF-beta induction of transcription factor Foxp3. J Exp Med 198(12), 1875-1886 (2003).
34. Mahmud SA, Manlove LS, Farrar MA. Interleukin-2 and STAT5 in regulatory T cell development and function. JAK-STAT 2(1), e23154-e23154 (2013).

35. Andersson J, Tran DQ, Pesu M, Davidson TS, Ramsey H, O'Shea JJ, Shevach EM. CD4+ FoxP3+ regulatory T cells confer infectious tolerance in a TGF-beta-dependent manner. J Exp Med 205(9), 1975-1981 (2008).
36. Sakaguchi S, Sakaguchi N, Asano M, Itoh M, Toda M. Immunologic self-tolerance maintained by activated T cells expressing IL-2 receptor alpha-chains (CD25). Breakdown of a single mechanism of self-tolerance causes various autoimmune diseases. J Immunol 155(3), 1151-1164 (1995).
37. Ghoreschi K, Laurence A, Yang XP, Tato CM, McGeachy MJ, Konkel JE, Ramos HL, Wei L, Davidson TS, Bouladoux N, et al. Generation of pathogenic T(H)17 cells in the absence of TGF-beta signalling. Nature 467(7318), 967-971 (2010).
38. Hirota K, Duarte JH, Veldhoen M, Hornsby E, Li Y, Cua DJ, Ahlfors H, Wilhelm C, Tolaini M, Menzel U, et al. Fate mapping of IL-17-producing T cells in inflammatory responses. Nat Immunol 12(3), 255-263 (2011).
39. Kebir H, Ifergan I, Alvarez JI, Bernard M, Poirier J, Arbour N, Duquette P, Prat A. Preferential recruitment of interferon-gamma-expressing TH17 cells in multiple sclerosis. Ann Neurol 66(3), 390-402 (2009).
40. van Langelaar J, van der Vuurst de Vries RM, Janssen M, Wierenga-Wolf AF, Spilt IM, Siepman TA, Dankers W, Verjans G, de Vries HE, Lubberts E, et al. T helper 17.1 cells associate with multiple sclerosis disease activity: perspectives for early intervention. Brain 141(5), 1334-1349 (2018).
41. Acosta-Rodriguez EV, Rivino L, Geginat J, Jarrossay D, Gattorno M, Lanzavecchia A, Sallusto F, Napolitani G. Surface phenotype and antigenic specificity of human interleukin 17-producing T helper memory cells. Nat Immunol 8(6), 639-646 (2007).
42. Duhen T, Campbell DJ. IL-1beta promotes the differentiation of polyfunctional human CCR6+CXCR3+ Th1/17 cells that are specific for pathogenic and commensal microbes. J Immunol 193(1), 120-129 (2014).
43. Ma CS, Deenick EK, Batten M, Tangye SG. The origins, function, and regulation of T follicular helper cells. J Exp Med 209(7), 1241-1253 (2012).
44. Rao DA, Gurish MF, Marshall JL, Slowikowski K, Fonseka CY, Liu Y, Donlin LT, Henderson LA, Wei K, Mizoguchi F, et al. Pathologically expanded peripheral T helper cell subset drives B cells in rheumatoid arthritis. Nature 542(7639), 110-114 (2017).

45. Craft JE. Follicular helper T cells in immunity and systemic autoimmunity. Nat Rev Rheumatol 8(6), 337-347 (2012).
46. Crotty S. T follicular helper cell differentiation, function, and roles in disease. Immunity 41(4), 529-542 (2014).
47. Song W, Craft J. T follicular helper cell heterogeneity: Time, space, and function. Immunol Rev 288(1), 85-96 (2019).
48. O'Shea JJ, Holland SM, Staudt LM. JAKs and STATs in Immunity, Immunodeficiency, and Cancer. New England Journal of Medicine 368(2), 161-170 (2013).
49. O'Shea JJ, Schwartz DM, Villarino AV, Gadina M, McInnes IB, Laurence A. The JAK-STAT pathway: impact on human disease and therapeutic intervention. Annual review of medicine 66, 311-328 (2015).
50. Rochman Y, Spolski R, Leonard WJ. New insights into the regulation of T cells by gamma(c) family cytokines. Nature reviews. Immunology 9(7), 480-490 (2009).
51. Rane SG, Reddy EP. JAK3: a novel JAK kinase associated with terminal differentiation of hematopoietic cells. Oncogene 9(8), 2415-2423 (1994).
52. Ghoreschi K, Laurence A, O'Shea JJ. Janus kinases in immune cell signaling. Immunological Reviews 228(1), 273-287 (2009).
53. Pesu M, Candotti F, Husa M, Hofmann SR, Notarangelo LD, O'Shea JJ. Jak3, severe combined immunodeficiency, and a new class of immunosuppressive drugs. Immunological Reviews 203(1), 127-142 (2005).
54. Macchi P, Villa A, Giliani S, Sacco MG, Frattini A, Porta F, Ugazio AG, Johnston JA, Candotti F, O'Shea JJ, et al. Mutations of Jak-3 gene in patients with autosomal severe combined immune deficiency (SCID). Nature 377(6544), 65-68 (1995).
55. Flanagan ME, Blumenkopf TA, Brissette WH, Brown MF, Casavant JM, Shang-Poa C, Doty JL, Elliott EA, Fisher MB, Hines M, et al. Discovery of CP-690,550: a potent and selective Janus kinase (JAK) inhibitor for the treatment of autoimmune diseases and organ transplant rejection. J Med Chem 53(24), 8468-8484 (2010).
56. Ghoreschi K, Jesson MI, Li X, Lee JL, Ghosh S, Alsup JW, Warner JD, Tanaka M, Steward-Tharp SM, Gadina M, et al. Modulation of Innate and Adaptive Immune Responses by Tofacitinib (CP-690,550). The Journal of Immunology 186(7), 4234-4243 (2011).

57. Fleischmann R, Kremer J, Cush J, Schulze-Koops H, Connell CA, Bradley JD, Gruben D, Wallenstein GV, Zwillich SH, Kanik KS. Placebo-Controlled Trial of Tofacitinib Monotherapy in Rheumatoid Arthritis. New England Journal of Medicine 367(6), 495-507 (2012).
58. Schwartz DM, Kanno Y, Villarino A, Ward M, Gadina M, O'Shea JJ. JAK inhibition as a therapeutic strategy for immune and inflammatory diseases. Nat Rev Drug Discov 17(1), 78 (2017).
59. Grisouard J, Hao-Shen H, Dirnhofer S, Wagner KU, Skoda RC. Selective deletion of Jak2 in adult mouse hematopoietic cells leads to lethal anemia and thrombocytopenia. Haematologica 99(4), e52-54 (2014).
60. Hamm H. Grundlagen. In: Goebeler M, Hamm H. Basiswissen Dermatologie. 1. Edition, Springer-Lehrbuch, Berlin, Heidelberg (2017).
61. Röcken M, Schaller M, Sattler E, Burgdorf W. Grundlagen. In: Röcken M, Schaller M, Sattler E, Burgdorf W. Taschenatlas Dermatologie: Grundlagen, Diagnostik, Klinik. 1. Edition, Thieme, Stuttgart (2010).
62. Farquhar MG, Palade GE. Junctional complexes in various epithelia. J Cell Biol 17, 375-412 (1963).
63. Bizzozero G. Delle cellule cigliate del reticolo malpighiano dell'epidermide delle mucose e dei cancroidi. Annali Universali di Medicina 54, 111-118 (1864).
64. Fawcett DW, Selby CC. Observations on the fine structure of the turtle atrium. J Biophys Biochem Cytol 4(1), 63-72 (1958).
65. Odland GF. The fine structure of the interrelationship of cells in the human epidermis. J Biophys Biochem Cytol 4(5), 529-538 (1958).
66. Kelly DE. Fine structure of desmosomes. , hemidesmosomes, and an adepidermal globular layer in developing newt epidermis. J Cell Biol 28(1), 51-72 (1966).
67. Green KJ, Simpson CL. Desmosomes: new perspectives on a classic. J Invest Dermatol 127(11), 2499-2515 (2007).
68. Hatzfeld M. Plakophilins: Multifunctional proteins or just regulators of desmosomal adhesion? Biochim Biophys Acta 1773(1), 69-77 (2007).
69. Yin T, Green KJ. Regulation of desmosome assembly and adhesion. Semin Cell Dev Biol 15(6), 665-677 (2004).

70. Delva E, Tucker DK, Kowalczyk AP. The desmosome. Cold Spring Harb Perspect Biol 1(2), a002543 (2009).
71. Pokutta S, Weis WI. Structure and mechanism of cadherins and catenins in cell-cell contacts. Annu Rev Cell Dev Biol 23, 237-261 (2007).
72. Harrison OJ, Brasch J, Lasso G, Katsamba PS, Ahlsen G, Honig B, Shapiro L. Structural basis of adhesive binding by desmocollins and desmogleins. Proc Natl Acad Sci U S A 113(26), 7160-7165 (2016).
73. Kljuic A, Bazzi H, Sundberg JP, Martinez-Mir A, O'Shaughnessy R, Mahoney MG, Levy M, Montagutelli X, Ahmad W, Aita VM, et al. Desmoglein 4 in hair follicle differentiation and epidermal adhesion: evidence from inherited hypotrichosis and acquired pemphigus vulgaris. Cell 113(2), 249-260 (2003).
74. Nuber UA, Schafer S, Schmidt A, Koch PJ, Franke WW. The widespread human desmocollin Dsc2 and tissue-specific patterns of synthesis of various desmocollin subtypes. Eur J Cell Biol 66(1), 69-74 (1995).
75. Schafer S, Koch PJ, Franke WW. Identification of the ubiquitous human desmoglein, Dsg2, and the expression catalogue of the desmoglein subfamily of desmosomal cadherins. Exp Cell Res 211(2), 391-399 (1994).
76. Johnson JL, Najor NA, Green KJ. Desmosomes: regulators of cellular signaling and adhesion in epidermal health and disease. Cold Spring Harb Perspect Med 4(11), a015297 (2014).
77. Rosenblum MD, Remedios KA, Abbas AK. Mechanisms of human autoimmunity. J Clin Invest 125(6), 2228-2233 (2015).
78. Schmidt E, Zillikens D. Pemphigoid diseases. Lancet 381(9863), 320-332 (2013).
79. Schmidt E, Kasperkiewicz M, Joly P. Pemphigus. Lancet 394(10201), 882-894 (2019).
80. Alpsoy E, Akman-Karakas A, Uzun S. Geographic variations in epidemiology of two autoimmune bullous diseases: pemphigus and bullous pemphigoid. Arch Dermatol Res 307(4), 291-298 (2015).
81. Aoki V, Rivitti EA, Diaz LA, Cooperative Group on Fogo Selvagem R. Update on fogo selvagem, an endemic form of pemphigus foliaceus. J Dermatol 42(1), 18-26 (2015).
82. Morini JP, Jomaa B, Gorgi Y, Saguem MH, Nouira R, Roujeau JC, Revuz J. Pemphigus foliaceus in young women. An endemic focus in the Sousse area of Tunisia. Arch Dermatol 129(1), 69-73 (1993).

83. Tallab T, Joharji H, Bahamdan K, Karkashan E, Mourad M, Ibrahim K. The incidence of pemphigus in the southern region of Saudi Arabia. Int J Dermatol 40(9), 570-572 (2001).
84. Nanda A, Dvorak R, Al-Saeed K, Al-Sabah H, Alsaleh QA. Spectrum of autoimmune bullous diseases in Kuwait. Int J Dermatol 43(12), 876-881 (2004).
85. Bertram F, Brocker EB, Zillikens D, Schmidt E. Prospective analysis of the incidence of autoimmune bullous disorders in Lower Franconia, Germany. J Dtsch Dermatol Ges 7(5), 434-440 (2009).
86. Michailidou EZ, Belazi MA, Markopoulos AK, Tsatsos MI, Mourellou ON, Antoniades DZ. Epidemiologic survey of pemphigus vulgaris with oral manifestations in northern Greece: retrospective study of 129 patients. Int J Dermatol 46(4), 356-361 (2007).
87. Kridin K, Zelber-Sagi S, Khamaisi M, Cohen AD, Bergman R. Remarkable differences in the epidemiology of pemphigus among two ethnic populations in the same geographic region. J Am Acad Dermatol 75(5), 925-930 (2016).
88. Simon DG, Krutchkoff D, Kaslow RA, Zarbo R. Pemphigus in Hartford County, Connecticut, from 1972 to 1977. Arch Dermatol 116(9), 1035-1037 (1980).
89. Yan L, Wang J-M, Zeng K. Association between HLA-DRB1 polymorphisms and pemphigus vulgaris: a meta-analysis. British Journal of Dermatology 167(4), 768-777 (2012).
90. Gazit E, Loewenthal R. The immunogenetics of pemphigus vulgaris. Autoimmun Rev 4(1), 16-20 (2005).
91. Zhang SY, Zhou XY, Zhou XL, Zhang Y, Deng Y, Liao F, Yang M, Xia XY, Zhou YH, Yin DD, et al. Subtype-specific inherited predisposition to pemphigus in the Chinese population. British Journal of Dermatology 180(4), 828-835 (2019).
92. Kasperkiewicz M, Ellebrecht CT, Takahashi H, Yamagami J, Zillikens D, Payne AS, Amagai M. Pemphigus. Nat Rev Dis Primers 3, 17026 (2017).
93. Mahoney MG, Wang Z, Rothenberger K, Koch PJ, Amagai M, Stanley JR. Explanations for the clinical and microscopic localization of lesions in pemphigus foliaceus and vulgaris. J Clin Invest 103(4), 461-468 (1999).
94. Amagai M. Autoimmunity against desmosomal cadherins in pemphigus. J Dermatol Sci 20(2), 92-102 (1999).

95. Amagai M, Tsunoda K, Suzuki H, Nishifuji K, Koyasu S, Nishikawa T. Use of autoantigen-knockout mice in developing an active autoimmune disease model for pemphigus. J Clin Invest 105(5), 625-631 (2000).
96. Tsunoda K, Ota T, Aoki M, Yamada T, Nagai T, Nakagawa T, Koyasu S, Nishikawa T, Amagai M. Induction of pemphigus phenotype by a mouse monoclonal antibody against the amino-terminal adhesive interface of desmoglein 3. J Immunol 170(4), 2170-2178 (2003).
97. Heupel W-M, Zillikens D, Drenckhahn D, Waschke J. Pemphigus Vulgaris IgG Directly Inhibit Desmoglein 3-Mediated Transinteraction. The Journal of Immunology 181(3), 1825-1834 (2008).
98. Di Zenzo G, Di Lullo G, Corti D, Calabresi V, Sinistro A, Vanzetta F, Didona B, Cianchini G, Hertl M, Eming R, et al. Pemphigus autoantibodies generated through somatic mutations target the desmoglein-3 cis-interface. The Journal of Clinical Investigation 122(10), 3781-3790 (2012).
99. Sato M, Aoyama Y, Kitajima Y. Assembly Pathway of Desmoglein 3 to Desmosomes and Its Perturbation by Pemphigus Vulgaris-IgG in Cultured Keratinocytes, as Revealed by Time-Lapsed Labeling Immunoelectron Microscopy. Laboratory Investigation 80(10), 1583-1592 (2000).
100. Mao X, Choi EJ, Payne AS. Disruption of Desmosome Assembly by Monovalent Human Pemphigus Vulgaris Monoclonal Antibodies. Journal of Investigative Dermatology 129(4), 908-918 (2009).
101. Oktarina DAM, van der Wier G, Diercks GFH, Jonkman MF, Pas HH. IgG-induced clustering of desmogleins 1 and 3 in skin of patients with pemphigus fits with the desmoglein nonassembly depletion hypothesis. British Journal of Dermatology 165(3), 552-562 (2011).
102. Berkowitz P, Hu P, Liu Z, Diaz LA, Enghild JJ, Chua MP, Rubenstein DS. Desmosome Signaling: INHIBITION OF p38MAPK PREVENTS PEMPHIGUS VULGARIS IgG-INDUCED CYTOSKELETON REORGANIZATION. Journal of Biological Chemistry 280(25), 23778-23784 (2005).
103. Osada K, Seishima M, Kitajima Y. Pemphigus IgG Activates and Translocates Protein Kinase C from the Cytosol to the Particulate/Cytoskeleton Fractions in Human Keratinocytes. Journal of Investigative Dermatology 108(4), 482-487 (1997).

104. Esaki C, Seishima M, Yamada T, Osada K, Kitajima Y. Pharmacologic Evidence for Involvement of Phospholiphase C in Pemphigus IgG-Induced Inositol 1,4,5-Trisphosphate Generation, Intracellular Calcium Increase, and Plasminogen Activator Secretion in DJM-1 Cells, a Squamous Cell Carcinoma Line. Journal of Investigative Dermatology 105(3), 329-333 (1995).
105. Bektas M, Jolly PS, Berkowitz P, Amagai M, Rubenstein DS. A Pathophysiologic Role for Epidermal Growth Factor Receptor in Pemphigus Acantholysis. Journal of Biological Chemistry 288(13), 9447-9456 (2013).
106. Saito M, Stahley SN, Caughman CY, Mao X, Tucker DK, Payne AS, Amagai M, Kowalczyk AP. Signaling Dependent and Independent Mechanisms in Pemphigus Vulgaris Blister Formation. PLoS One 7(12), e50696 (2012).
107. Berkowitz P, Hu P, Warren S, Liu Z, Diaz LA, Rubenstein DS. p38MAPK inhibition prevents disease in pemphigus vulgaris mice. Proc Natl Acad Sci U S A 103(34), 12855-12860 (2006).
108. Kawasaki H, Tsunoda K, Hata T, Ishii K, Yamada T, Amagai M. Synergistic Pathogenic Effects of Combined Mouse Monoclonal Anti-Desmoglein 3 IgG Antibodies on Pemphigus Vulgaris Blister Formation. Journal of Investigative Dermatology 126(12), 2621-2630 (2006).
109. Takahashi H, Kuwana M, Amagai M. A Single Helper T Cell Clone Is Sufficient to Commit Polyclonal Naive B Cells to Produce Pathogenic IgG in Experimental Pemphigus Vulgaris. The Journal of Immunology 182(3), 1740-1745 (2009).
110. Zhu H, Chen Y, Zhou Y, Wang Y, Zheng J, Pan M. Cognate Th2-B cell interaction is essential for the autoantibody production in pemphigus vulgaris. J Clin Immunol 32(1), 114-123 (2012).
111. Rizzo C, Fotino M, Zhang Y, Chow S, Spizuoco A, Sinha AA. Direct characterization of human T cells in pemphigus vulgaris reveals elevated autoantigen-specific Th2 activity in association with active disease. Clin Exp Dermatol 30(5), 535-540 (2005).
112. Lin MS, Swartz SJ, Lopez A, Ding X, Fernandez-Vina MA, Stastny P, Fairley JA, Diaz LA. Development and characterization of desmoglein-3 specific T cells from patients with pemphigus vulgaris. J Clin Invest 99(1), 31-40 (1997).

113. Veldman C, Stauber A, Wassmuth R, Uter W, Schuler G, Hertl M. Dichotomy of autoreactive Th1 and Th2 cell responses to desmoglein 3 in patients with pemphigus vulgaris (PV) and healthy carriers of PV-associated HLA class II alleles. J Immunol 170(1), 635-642 (2003).
114. Satyam A, Khandpur S, Sharma VK, Sharma A. Involvement of TH1/TH2 Cytokines in the Pathogenesis of Autoimmune Skin Disease—Pemphigus Vulgaris. Immunological Investigations 38(6), 498-509 (2009).
115. D'Auria L, Bonifati C, Mussi A, D'Agosto G, De Simone C, Giacalone B, Ferraro C, Ameglio F. Cytokines in the sera of patients with pemphigus vulgaris: interleukin-6 and tumour necrosis factor-alpha levels are significantly increased as compared to healthy subjects and correlate with disease activity. Eur Cytokine Netw 8(4), 383-387 (1997).
116. Hennerici T, Pollmann R, Schmidt T, Seipelt M, Tackenberg B, Mobs C, Ghoreschi K, Hertl M, Eming R. Increased Frequency of T Follicular Helper Cells and Elevated Interleukin-27 Plasma Levels in Patients with Pemphigus. PLoS One 11(2), e0148919 (2016).
117. Timoteo RP, da Silva MV, Miguel CB, Silva DA, Catarino JD, Rodrigues Junior V, Sales-Campos H, Freire Oliveira CJ. Th1/Th17-Related Cytokines and Chemokines and Their Implications in the Pathogenesis of Pemphigus Vulgaris. Mediators Inflamm 2017, 7151285 (2017).
118. Rico MJ, Benning C, Weingart ES, Streilein RD, Hall RP, 3rd. Characterization of skin cytokines in bullous pemphigoid and pemphigus vulgaris. Br J Dermatol 140(6), 1079-1086 (1999).
119. Żebrowska A, Woźniacka A, Juczyńska K, Ociepa K, Waszczykowska E, Szymczak I, Pawliczak R. Correlation between IL-36α and IL-17 and Activity of the Disease in Selected Autoimmune Blistering Diseases. Mediators of Inflammation 2017, 8980534 (2017).
120. Xue J, Su W, Chen Z, Ke Y, Du X, Zhou Q. Overexpression of Interleukin-23 and Interleukin-17 in the Lesion of Pemphigus Vulgaris: A Preliminary Study. Mediators of Inflammation 2014, 463928 (2014).
121. Yuan H, Zhou S, Liu Z, Cong W, Fei X, Zeng W, Zhu H, Xu R, Wang Y, Zheng J, et al. Pivotal Role of Lesional and Perilesional T/B Lymphocytes in Pemphigus Pathogenesis. J Invest Dermatol 137(11), 2362-2370 (2017).

122. Asothai R, Anand V, Das D, Antil PS, Khandpur S, Sharma VK, Sharma A. Distinctive Treg associated CCR4-CCL22 expression profile with altered frequency of Th17/Treg cell in the immunopathogenesis of Pemphigus Vulgaris. Immunobiology 220(10), 1129-1135 (2015).
123. Xu RC, Zhu HQ, Li WP, Zhao XQ, Yuan HJ, Zheng J, Pan M. The imbalance of Th17 and regulatory T cells in pemphigus patients. Eur J Dermatol 23(6), 795-802 (2013).
124. Kneisel A, Hertl M. Autoimmune bullous skin diseases. Part 1: Clinical manifestations. JDDG: Journal der Deutschen Dermatologischen Gesellschaft 9(10), 844-857 (2011).
125. Hofmann SC, Juratli HA, Eming R. Bullous autoimmune dermatoses. JDDG: Journal der Deutschen Dermatologischen Gesellschaft 16(11), 1339-1358 (2018).
126. Schlesinger N, Katz M, Ingber A. Nail involvement in pemphigus vulgaris. Br J Dermatol 146(5), 836-839 (2002).
127. De D, Kumar S, Handa S, Mahajan R. Fingernail involvement in pemphigus and its correlation with disease severity and other clinicodemographic parameters. British Journal of Dermatology 180(3), 662-663 (2019).
128. Solimani F, Meier K, Zimmer CL, Hashimoto T. Immune serological diagnosis of pemphigus. G Ital Dermatol Venereol, (2020).
129. Kneisel A, Hertl M. Autoimmune bullous skin diseases. Part 2: diagnosis and therapy. JDDG: Journal der Deutschen Dermatologischen Gesellschaft 9(11), 927-947 (2011).
130. Amagai M, Komai A, Hashimoto T, Shirakata Y, Hashimoto K, Yamada T, Kitajima Y, Ohya K, Iwanami H, Nishikawa T. Usefulness of enzyme-linked immunosorbent assay using recombinant desmogleins 1 and 3 for serodiagnosis of pemphigus. Br J Dermatol 140(2), 351-357 (1999).
131. Harman KE, Seed PT, Gratian MJ, Bhogal BS, Challacombe SJ, Black MM. The severity of cutaneous and oral pemphigus is related to desmoglein 1 and 3 antibody levels. British Journal of Dermatology 144(4), 775-780 (2001).
132. Belloni-Fortina A, Faggion D, Pigozzi B, Peserico A, Bordignon M, Baldo V, Alaibac M. Detection of autoantibodies against recombinant desmoglein 1 and 3 molecules in patients with pemphigus vulgaris: correlation with disease extent at the time of diagnosis and during follow-up. Clin Dev Immunol 2009, 187864 (2009).

133. Murrell DF, Peña S, Joly P, Marinovic B, Hashimoto T, Diaz LA, Sinha AA, Payne AS, Daneshpazhooh M, Eming R, et al. Diagnosis and management of pemphigus: Recommendations of an international panel of experts. Journal of the American Academy of Dermatology 82(3), 575-585.e571 (2020).
134. Kridin K. Emerging treatment options for the management of pemphigus vulgaris. Ther Clin Risk Manag 14, 757-778 (2018).
135. Almugairen N, Hospital V, Bedane C, Duvert-Lehembre S, Picard D, Tronquoy A-F, Houivet E, D'Incan M, Joly P. Assessment of the rate of long-term complete remission off therapy in patients with pemphigus treated with different regimens including medium- and high-dose corticosteroids. Journal of the American Academy of Dermatology 69(4), 583-588 (2013).
136. Joly P, Maho-Vaillant M, Prost-Squarcioni C, Hebert V, Houivet E, Calbo S, Caillot F, Golinski ML, Labeille B, Picard-Dahan C, et al. First-line rituximab combined with short-term prednisone versus prednisone alone for the treatment of pemphigus (Ritux 3): a prospective, multicentre, parallel-group, open-label randomised trial. The Lancet 389(10083), 2031-2040 (2017).
137. Wang HH, Liu CW, Li YC, Huang YC. Efficacy of rituximab for pemphigus: a systematic review and meta-analysis of different regimens. Acta Derm Venereol 95(8), 928-932 (2015).
138. Ahmed AR, Shetty S. A comprehensive analysis of treatment outcomes in patients with pemphigus vulgaris treated with rituximab. Autoimmun Rev 14(4), 323-331 (2015).
139. Feldman RJ. Paradoxical worsening of pemphigus vulgaris following rituximab therapy. British Journal of Dermatology 173(3), 858-859 (2015).
140. Sharma V, Bhari N, Gupta S, Sahni K, Khanna N, Ramam M, Sethuraman G. Clinical efficacy of rituximab in the treatment of pemphigus: A retrospective study. Indian Journal of Dermatology, Venereology, and Leprology 82(4), 389-394 (2016).
141. Kasperkiewicz M, Eming R, Behzad M, Hunzelmann N, Meurer M, Schulze-Koops H, Wussow Pv, Hertl M, Zillikens D, Freivogel K, et al. Efficacy and safety of rituximab in pemphigus: experience of the German Registry of Autoimmune Diseases. JDDG: Journal der Deutschen Dermatologischen Gesellschaft 10, (2012).

142. Shimanovich I, Baumann T, Schmidt E, Zillikens D, Hammers CM. Long-term outcomes of rituximab therapy in pemphigus. J Eur Acad Dermatol Venereol 34(12), 2884-2889 (2020).
143. Pollmann R, Walter E, Schmidt T, Waschke J, Hertl M, Mobs C, Eming R. Identification of Autoreactive B Cell Subpopulations in Peripheral Blood of Autoimmune Patients With Pemphigus Vulgaris. Front Immunol 10, 1375 (2019).
144. Sabat R, Wolk K, Loyal L, Docke WD, Ghoreschi K. T cell pathology in skin inflammation. Semin Immunopathol 41(3), 359-377 (2019).
145. Pfutze M, Niedermeier A, Hertl M, Eming R. Introducing a novel Autoimmune Bullous Skin Disorder Intensity Score (ABSIS) in pemphigus. Eur J Dermatol 17(1), 4-11 (2007).
146. PeqGOLD Total RNA Kit Instruction Manual (V0815). Available online at: https://de.vwr.com/assetsvc/asset/de_DE/id/17035099/contents (Accessed: 14 October 2020).
147. PeqGOLD Micro RNA Kit Instruction Manual (V0815). Available online at: https://de.vwr.com/assetsvc/asset/de_DE/id/17035102/contents (Accessed: 14 October 2020).
148. TURBO DNA-free™ Kit User Guide (2018). Available online at: https://www.thermofisher.com/order/catalog/product/AM1907#/AM1907 (Accessed: 11 May 2020).
149. Andrews S. FastQC: A quality control tool for high throughput sequence data (2010). Available online at: https://www.bioinformatics.babraham.ac.uk/projects/fastqc/ (Accessed: 01 August 2019).
150. Ewels P, Magnusson M, Lundin S, Kaller M. MultiQC: summarize analysis results for multiple tools and samples in a single report. Bioinformatics 32(19), 3047-3048 (2016).
151. Patro R, Duggal G, Love MI, Irizarry RA, Kingsford C. Salmon provides fast and bias-aware quantification of transcript expression. Nat Methods 14(4), 417-419 (2017).
152. Frankish A, Diekhans M, Ferreira AM, Johnson R, Jungreis I, Loveland J, Mudge JM, Sisu C, Wright J, Armstrong J, et al. GENCODE reference annotation for the human and mouse genomes. Nucleic Acids Res 47(D1), D766-D773 (2019).
153. Soneson C, Love MI, Robinson MD. Differential analyses for RNA-seq: transcript-level estimates improve gene-level inferences. F1000Res 4, 1521 (2015).

154. Zerbino DR, Achuthan P, Akanni W, Amode MR, Barrell D, Bhai J, Billis K, Cummins C, Gall A, Giron CG, et al. Ensembl 2018. Nucleic Acids Res 46(D1), D754-D761 (2018).
155. Durinck S, Moreau Y, Kasprzyk A, Davis S, De Moor B, Brazma A, Huber W. BioMart and Bioconductor: a powerful link between biological databases and microarray data analysis. Bioinformatics 21(16), 3439-3440 (2005).
156. Durinck S, Spellman PT, Birney E, Huber W. Mapping identifiers for the integration of genomic datasets with the R/Bioconductor package biomaRt. Nat Protoc 4(8), 1184-1191 (2009).
157. Love MI, Huber W, Anders S. Moderated estimation of fold change and dispersion for RNA-seq data with DESeq2. Genome Biol 15(12), 550 (2014).
158. Ignatiadis N, Klaus B, Zaugg JB, Huber W. Data-driven hypothesis weighting increases detection power in genome-scale multiple testing. Nat Methods 13(7), 577-580 (2016).
159. Young MD, Wakefield MJ, Smyth GK, Oshlack A. Gene ontology analysis for RNA-seq: accounting for selection bias. Genome Biol 11(2), R14 (2010).
160. The Gene Ontology Consortium. The Gene Ontology Resource: 20 years and still GOing strong. Nucleic Acids Res 47(D1), D330-D338 (2019).
161. Kanehisa M, Sato Y, Furumichi M, Morishima K, Tanabe M. New approach for understanding genome variations in KEGG. Nucleic Acids Res 47(D1), D590-D595 (2019).
162. Kanehisa M, Goto S. KEGG: kyoto encyclopedia of genes and genomes. Nucleic Acids Res 28(1), 27-30 (2000).
163. Wilke CO. cowplot: Streamlined Plot Theme and Plot Annotations for 'ggplot2' (2019). Available online at: https://wilkelab.org/cowplot/ (Accessed: 01 August 2019).
164. Wickham H. ggplot2: Elegant Graphics for Data Analysis. 2. Edition, Springer International Publishing (2016).
165. Kassambara A. ggpubr: 'ggplot2' Based Publication Ready Plots (2019). Available online at: https://cran.r-project.org/web/packages/ggpubr/index.html (Accessed: 01 August 2019).
166. Walter W, Sanchez-Cabo F, Ricote M. GOplot: an R package for visually combining expression data with functional analysis. Bioinformatics 31(17), 2912-2914 (2015).
167. Luo W, Brouwer C. Pathview: an R/Bioconductor package for pathway-based data integration and visualization. Bioinformatics 29(14), 1830-1831 (2013).

168. Kolde, R. pheatmap: Pretty Heatmaps (2019). Available online at: https://cran.r-project.org/web/packages/pheatmap/index.html (Accessed: 01 August 2019).
169. Zhu A, Ibrahim JG, Love MI. Heavy-tailed prior distributions for sequence count data: removing the noise and preserving large differences. Bioinformatics 35(12), 2084-2092 (2019).
170. Livak KJ, Schmittgen TD. Analysis of relative gene expression data using real-time quantitative PCR and the 2(-Delta Delta C(T)) Method. Methods 25(4), 402-408 (2001).
171. Morita R, Schmitt N, Bentebibel SE, Ranganathan R, Bourdery L, Zurawski G, Foucat E, Dullaers M, Oh S, Sabzghabaei N, et al. Human blood CXCR5(+)CD4(+) T cells are counterparts of T follicular cells and contain specific subsets that differentially support antibody secretion. Immunity 34(1), 108-121 (2011).
172. CD4 MicroBeads, human Datasheet. Available online at: https://www.miltenyibiotec.com/DE-en/products/cd4-microbeads-human.html#gref (Accessed: 02 November 2020).
173. Beckert B, Panico F, Pollmann R, Eming R, Banning A, Tikkanen R. Immortalized Human hTert/KER-CT Keratinocytes a Model System for Research on Desmosomal Adhesion and Pathogenesis of Pemphigus Vulgaris. Int J Mol Sci 20(13), (2019).
174. Laemmli UK. Cleavage of structural proteins during the assembly of the head of bacteriophage T4. Nature 227(5259), 680-685 (1970).
175. Crowe AR, Yue W. Semi-quantitative Determination of Protein Expression using Immunohistochemistry Staining and Analysis: An Integrated Protocol. Bio Protoc 9(24), (2019).
176. Holstein J, Solimani F, Baum C, Meier K, Pollmann R, Didona D, Tekath T, Dugas M, Casadei N, Hudemann C, et al. Immunophenotyping in pemphigus reveals a Th17/Tfh17-dominated immune response promoting desmoglein1/3-specific autoantibody production. J Allergy Clin Immunol 147(6), 2358-2369 (2021).
177. Forster M, Chaikuad A, Bauer SM, Holstein J, Robers MB, Corona CR, Gehringer M, Pfaffenrot E, Ghoreschi K, Knapp S, et al. Selective JAK3 Inhibitors with a Covalent Reversible Binding Mode Targeting a New Induced Fit Binding Pocket. Cell Chem Biol 23(11), 1335-1340 (2016).

178. Forster M, Chaikuad A, Dimitrov T, Doring E, Holstein J, Berger BT, Gehringer M, Ghoreschi K, Muller S, Knapp S, et al. Development, Optimization, and Structure-Activity Relationships of Covalent-Reversible JAK3 Inhibitors Based on a Tricyclic Imidazo[5,4-d]pyrrolo[2,3- b]pyridine Scaffold. J Med Chem 61(12), 5350-5366 (2018).
179. Kumari S, Bonnet MC, Ulvmar MH, Wolk K, Karagianni N, Witte E, Uthoff-Hachenberg C, Renauld JC, Kollias G, Toftgard R, et al. Tumor necrosis factor receptor signaling in keratinocytes triggers interleukin-24-dependent psoriasis-like skin inflammation in mice. Immunity 39(5), 899-911 (2013).
180. Panzer M, Sitte S, Wirth S, Drexler I, Sparwasser T, Voehringer D. Rapid In Vivo Conversion of Effector T Cells into Th2 Cells during Helminth Infection. The Journal of Immunology 188(2), 615-623 (2012).
181. Wang Y-H, Voo KS, Liu B, Chen C-Y, Uygungil B, Spoede W, Bernstein JA, Huston DP, Liu Y-J. A novel subset of CD4(+) T(H)2 memory/effector cells that produce inflammatory IL-17 cytokine and promote the exacerbation of chronic allergic asthma. The Journal of experimental medicine 207(11), 2479-2491 (2010).
182. Walter E, Vielmuth F, Rotkopf L, Sardy M, Horvath ON, Goebeler M, Schmidt E, Eming R, Hertl M, Spindler V, et al. Different signaling patterns contribute to loss of keratinocyte cohesion dependent on autoantibody profile in pemphigus. Sci Rep 7(1), 3579 (2017).
183. Spindler V, Rötzer V, Dehner C, Kempf B, Gliem M, Radeva M, Hartlieb E, Harms GS, Schmidt E, Waschke J. Peptide-mediated desmoglein 3 crosslinking prevents pemphigus vulgaris autoantibody-induced skin blistering. The Journal of Clinical Investigation 123(2), 800-811 (2013).
184. Koeberle SC, Romir J, Fischer S, Koeberle A, Schattel V, Albrecht W, Grutter C, Werz O, Rauh D, Stehle T, et al. Skepinone-L is a selective p38 mitogen-activated protein kinase inhibitor. Nat Chem Biol 8(2), 141-143 (2011).
185. Hald A, Andrés RM, Salskov-Iversen ML, Kjellerup RB, Iversen L, Johansen C. STAT1 expression and activation is increased in lesional psoriatic skin. Br J Dermatol 168(2), 302-310 (2013).
186. Alves de Medeiros AK, Speeckaert R, Desmet E, Van Gele M, De Schepper S, Lambert J. JAK3 as an Emerging Target for Topical Treatment of Inflammatory Skin Diseases. PLoS One 11(10), e0164080 (2016).

187. Takahashi H, Amagai M, Nishikawa T, Fujii Y, Kawakami Y, Kuwana M. Novel system evaluating in vivo pathogenicity of desmoglein 3-reactive T cell clones using murine pemphigus vulgaris. J Immunol 181(2), 1526-1535 (2008).
188. Amber KT, Maglie R, Solimani F, Eming R, Hertl M. Targeted Therapies for Autoimmune Bullous Diseases: Current Status. Drugs 78(15), 1527-1548 (2018).
189. Aoki-Ota M, Tsunoda K, Ota T, Iwasaki T, Koyasu S, Amagai M, Nishikawa T. A mouse model of pemphigus vulgaris by adoptive transfer of naive splenocytes from desmoglein 3 knockout mice. British Journal of Dermatology 151(2), 346-354 (2004).
190. Wei L, Laurence A, Elias KM, O'Shea JJ. IL-21 is produced by Th17 cells and drives IL-17 production in a STAT3-dependent manner. J Biol Chem 282(48), 34605-34610 (2007).
191. Ettinger R, Kuchen S, Lipsky PE. The role of IL-21 in regulating B-cell function in health and disease. Immunol Rev 223, 60-86 (2008).
192. Singh PK, Jia HP, Wiles K, Hesselberth J, Liu L, Conway BA, Greenberg EP, Valore EV, Welsh MJ, Ganz T, et al. Production of beta-defensins by human airway epithelia. Proceedings of the National Academy of Sciences of the United States of America 95(25), 14961-14966 (1998).
193. Kolls JK, McCray PB, Jr., Chan YR. Cytokine-mediated regulation of antimicrobial proteins. Nature reviews. Immunology 8(11), 829-835 (2008).
194. Cho KA, Suh JW, Lee KH, Kang JL, Woo SY. IL-17 and IL-22 enhance skin inflammation by stimulating the secretion of IL-1β by keratinocytes via the ROS-NLRP3-caspase-1 pathway. Int Immunol 24(3), 147-158 (2012).
195. Witte E, Kokolakis G, Witte K, Philipp S, Doecke W-D, Babel N, Wittig BM, Warszawska K, Kurek A, Erdmann-Keding M, et al. IL-19 Is a Component of the Pathogenetic IL-23/IL-17 Cascade in Psoriasis. Journal of Investigative Dermatology 134(11), 2757-2767 (2014).
196. Kunz S, Wolk K, Witte E, Witte K, Doecke W-D, Volk H-D, Sterry W, Asadullah K, Sabat R. Interleukin (IL)-19, IL-20 and IL-24 are produced by and act on keratinocytes and are distinct from classical ILs. Experimental Dermatology 15(12), 991-1004 (2006).
197. Gallagher G, Dickensheets H, Eskdale J, Izotova LS, Mirochnitchenko OV, Peat JD, Vazquez N, Pestka S, Donnelly RP, Kotenko SV. Cloning, expression and initial characterisation of interleukin-19 (IL-19), a novel homologue of human interleukin-10 (IL-10). Genes & Immunity 1(7), 442-450 (2000).

198. Wolk K, Kunz S, Asadullah K, Sabat R. Cutting Edge: Immune Cells as Sources and Targets of the IL-10 Family Members? The Journal of Immunology 168(11), 5397-5402 (2002).
199. Rutz S, Wang X, Ouyang W. The IL-20 subfamily of cytokines — from host defence to tissue homeostasis. Nature Reviews Immunology 14(12), 783-795 (2014).
200. Jin SH, Choi D, Chun Y-J, Noh M. Keratinocyte-derived IL-24 plays a role in the positive feedback regulation of epidermal inflammation in response to environmental and endogenous toxic stressors. Toxicology and Applied Pharmacology 280(2), 199-206 (2014).
201. Zheng Y, Danilenko DM, Valdez P, Kasman I, Eastham-Anderson J, Wu J, Ouyang W. Interleukin-22, a TH17 cytokine, mediates IL-23-induced dermal inflammation and acanthosis. Nature 445(7128), 648-651 (2007).
202. Mortazavi H, Esmaili N, Khezri S, Khamesipour A, Vasheghani Farahani I, Daneshpazhooh M, Rezaei N. The effect of conventional immunosuppressive therapy on cytokine serum levels in pemphigus vulgaris patients. Iran J Allergy Asthma Immunol 13(3), 174-183 (2014).
203. Ghoreschi K, Thomas P, Breit S, Dugas M, Mailhammer R, van Eden W, van der Zee R, Biedermann T, Prinz J, Mack M, et al. Interleukin-4 therapy of psoriasis induces Th2 responses and improves human autoimmune disease. Nat Med 9(1), 40-46 (2003).
204. Kohlmann J, Simon JC, Kunz M, Treudler R. [Possible effect of interleukin-17 blockade in pemphigus foliaceus and neutrophilic diseases]. Hautarzt 70(8), 641-644 (2019).
205. Zhu C, Ma J, Liu Y, Tong J, Tian J, Chen J, Tang X, Xu H, Lu L, Wang S. Increased Frequency of Follicular Helper T Cells in Patients with Autoimmune Thyroid Disease. The Journal of Clinical Endocrinology & Metabolism 97(3), 943-950 (2012).
206. Linterman MA, Rigby RJ, Wong RK, Yu D, Brink R, Cannons JL, Schwartzberg PL, Cook MC, Walters GD, Vinuesa CG. Follicular helper T cells are required for systemic autoimmunity. J Exp Med 206(3), 561-576 (2009).
207. Cosmi L, Cimaz R, Maggi L, Santarlasci V, Capone M, Borriello F, Frosali F, Querci V, Simonini G, Barra G, et al. Evidence of the transient nature of the Th17 phenotype of CD4+CD161+ T cells in the synovial fluid of patients with juvenile idiopathic arthritis. Arthritis Rheum 63(8), 2504-2515 (2011).

208. Nanke Y, Kobashigawa T, Yago T, Kawamoto M, Yamanaka H, Kotake S. Detection of IFN-γ+IL-17+ cells in salivary glands of patients with Sjögren's syndrome and Mikulicz's disease: Potential role of Th17•Th1 in the pathogenesis of autoimmune diseases. Nihon Rinsho Meneki Gakkai Kaishi 39(5), 473-477 (2016).
209. Codarri L, Gyülvészi G, Tosevski V, Hesske L, Fontana A, Magnenat L, Suter T, Becher B. RORγt drives production of the cytokine GM-CSF in helper T cells, which is essential for the effector phase of autoimmune neuroinflammation. Nature Immunology 12(6), 560-567 (2011).
210. Nishifuji K, Amagai M, Kuwana M, Iwasaki T, Nishikawa T. Detection of Antigen-Specific B Cells in Patients with Pemphigus Vulgaris by Enzyme-Linked Immunospot Assay: Requirement of T Cell Collaboration for Autoantibody Production. Journal of Investigative Dermatology 114(1), 88-94 (2000).
211. Prüßmann W, Prüßmann J, Koga H, Recke A, Iwata H, Juhl D, Görg S, Henschler R, Hashimoto T, Schmidt E, et al. Prevalence of pemphigus and pemphigoid autoantibodies in the general population. Orphanet J Rare Dis 10, 63 (2015).
212. Lobo PI. Role of Natural Autoantibodies and Natural IgM Anti-Leucocyte Autoantibodies in Health and Disease. Front Immunol 7, 198 (2016).
213. Takahashi H, Amagai M, Tanikawa A, Suzuki S, Ikeda Y, Nishikawa T, Kawakami Y, Kuwana M. T Helper Type 2-Biased Natural Killer Cell Phenotype in Patients with Pemphigus Vulgaris. Journal of Investigative Dermatology 127(2), 324-330 (2007).
214. Martín-Fontecha A, Thomsen LL, Brett S, Gerard C, Lipp M, Lanzavecchia A, Sallusto F. Induced recruitment of NK cells to lymph nodes provides IFN-γ for TH1 priming. Nature Immunology 5(12), 1260-1265 (2004).
215. Ferlazzo G, Pack M, Thomas D, Paludan C, Schmid D, Strowig T, Bougras G, Muller WA, Moretta L, Münz C. Distinct roles of IL-12 and IL-15 in human natural killer cell activation by dendritic cells from secondary lymphoid organs. Proceedings of the National Academy of Sciences of the United States of America 101(47), 16606-16611 (2004).
216. Hirota K, Turner JE, Villa M, Duarte JH, Demengeot J, Steinmetz OM, Stockinger B. Plasticity of Th17 cells in Peyer's patches is responsible for the induction of T cell-dependent IgA responses. Nat Immunol 14(4), 372-379 (2013).

217. Pfeifle R, Rothe T, Ipseiz N, Scherer HU, Culemann S, Harre U, Ackermann JA, Seefried M, Kleyer A, Uderhardt S, et al. Regulation of autoantibody activity by the IL-23-T(H)17 axis determines the onset of autoimmune disease. Nature Immunology 18(1), 104-113 (2017).
218. Stockinger B, Omenetti S. The dichotomous nature of T helper 17 cells. Nature reviews. Immunology 17(9), 535-544 (2017).
219. Jin S, Park CO, Shin JU, Noh JY, Lee YS, Lee NR, Kim HR, Noh S, Lee Y, Lee JH, et al. DAMP molecules S100A9 and S100A8 activated by IL-17A and house-dust mites are increased in atopic dermatitis. Exp Dermatol 23(12), 938-941 (2014).
220. Millar NL, Akbar M, Campbell AL, Reilly JH, Kerr SC, McLean M, Frleta-Gilchrist M, Fazzi UG, Leach WJ, Rooney BP, et al. IL-17A mediates inflammatory and tissue remodelling events in early human tendinopathy. Scientific reports 6, 27149-27149 (2016).
221. Ahmed AR, Moy R. Death in pemphigus. J Am Acad Dermatol 7(2), 221-228 (1982).
222. Shen F-F, Zhang F, Yang H-J, Li J-K, Su J-F, Yu P-T, Zhou F-Y, Che G-W. ADAMTS9-AS2 and CADM2 expression and association with the prognosis in esophageal squamous cell carcinoma. Biomarkers in Medicine 14(15), 1415-1426 (2020).
223. Lo PH, Lung HL, Cheung AK, Apte SS, Chan KW, Kwong FM, Ko JM, Cheng Y, Law S, Srivastava G, et al. Extracellular protease ADAMTS9 suppresses esophageal and nasopharyngeal carcinoma tumor formation by inhibiting angiogenesis. Cancer Res 70(13), 5567-5576 (2010).
224. Li X, Chen D, Li M, Gao X, Shi G, Zhao H. The CADM2/Akt pathway is involved in the inhibitory effect of miR-21-5p downregulation on proliferation and apoptosis in esophageal squamous cell carcinoma cells. Chem Biol Interact 288, 76-82 (2018).
225. Kridin K, Zelber-Sagi S, Comaneshter D, Cohen AD. Coexistent Solid Malignancies in Pemphigus: A Population-Based Study. JAMA Dermatology 154(4), 435-440 (2018).
226. Welsch K, Holstein J, Laurence A, Ghoreschi K. Targeting JAK/STAT signalling in inflammatory skin diseases with small molecule inhibitors. Eur J Immunol 47(7), 1096-1107 (2017).
227. Thoma G, Nuninger F, Falchetto R, Hermes E, Tavares GA, Vangrevelinghe E, Zerwes HG. Identification of a potent Janus kinase 3 inhibitor with high selectivity within the Janus kinase family. J Med Chem 54(1), 284-288 (2011).

228. Haan C, Rolvering C, Raulf F, Kapp M, Drückes P, Thoma G, Behrmann I, Zerwes HG. Jak1 has a dominant role over Jak3 in signal transduction through γc-containing cytokine receptors. Chem Biol 18(3), 314-323 (2011).
229. Thorarensen A, Banker ME, Fensome A, Telliez JB, Juba B, Vincent F, Czerwinski RM, Casimiro-Garcia A. ATP-mediated kinome selectivity: the missing link in understanding the contribution of individual JAK Kinase isoforms to cellular signaling. ACS Chem Biol 9(7), 1552-1558 (2014).
230. Onda M, Ghoreschi K, Steward-Tharp S, Thomas C, O'Shea JJ, Pastan IH, FitzGerald DJ. Tofacitinib suppresses antibody responses to protein therapeutics in murine hosts. J Immunol 193(1), 48-55 (2014).
231. Ma CS, Avery DT, Chan A, Batten M, Bustamante J, Boisson-Dupuis S, Arkwright PD, Kreins AY, Averbuch D, Engelhard D, et al. Functional STAT3 deficiency compromises the generation of human T follicular helper cells. Blood 119(17), 3997-4008 (2012).
232. Choi YS, Eto D, Yang JA, Lao C, Crotty S. Cutting edge: STAT1 is required for IL-6-mediated Bcl6 induction for early follicular helper cell differentiation. J Immunol 190(7), 3049-3053 (2013).
233. Rauch I, Müller M, Decker T. The regulation of inflammation by interferons and their STATs. JAK-STAT 2(1), e23820-e23820 (2013).
234. Boehm U, Klamp T, Groot M, Howard JC. CELLULAR RESPONSES TO INTERFERON-γ. Annual Review of Immunology 15(1), 749-795 (1997).
235. Radeva MY, Walter E, Stach RA, Yazdi AS, Schlegel N, Sarig O, Sprecher E, Waschke J. ST18 Enhances PV-IgG-Induced Loss of Keratinocyte Cohesion in Parallel to Increased ERK Activation. Frontiers in Immunology 10, 770 (2019).
236. Wolk K, Haugen HS, Xu W, Witte E, Waggie K, Anderson M, vom Baur E, Witte K, Warszawska K, Philipp S, et al. IL-22 and IL-20 are key mediators of the epidermal alterations in psoriasis while IL-17 and IFN-γ are not. Journal of Molecular Medicine 87(5), 523-536 (2009).
237. Leonard WJ, O'Shea JJ. JAKS AND STATS: Biological Implications. Annual Review of Immunology 16(1), 293-322 (1998).

238. Takeuchi T, Tanaka Y, Iwasaki M, Ishikura H, Saeki S, Kaneko Y. Efficacy and safety of the oral Janus kinase inhibitor peficitinib (ASP015K) monotherapy in patients with moderate to severe rheumatoid arthritis in Japan: a 12-week, randomised, double-blind, placebo-controlled phase IIb study. Annals of the Rheumatic Diseases 75(6), 1057 (2016).
239. Farmer LJ, Ledeboer MW, Hoock T, Arnost MJ, Bethiel RS, Bennani YL, Black JJ, Brummel CL, Chakilam A, Dorsch WA, et al. Discovery of VX-509 (Decernotinib): A Potent and Selective Janus Kinase 3 Inhibitor for the Treatment of Autoimmune Diseases. J Med Chem 58(18), 7195-7216 (2015).
240. Juczynska K, Wozniacka A, Waszczykowska E, Danilewicz M, Wagrowska-Danilewicz M, Wieczfinska J, Pawliczak R, Zebrowska A. Expression of the JAK/STAT Signaling Pathway in Bullous Pemphigoid and Dermatitis Herpetiformis. Mediators Inflamm 2017, 6716419 (2017).
241. Juczynska K, Wozniacka A, Waszczykowska E, Danilewicz M, Wągrowska-Danilewicz M, Zebrowska A. Expression of JAK3, STAT2, STAT4, and STAT6 in pemphigus vulgaris. Immunologic Research 68(2), 97-103 (2020).
242. Wolk K, Witte E, Wallace E, Döcke WD, Kunz S, Asadullah K, Volk HD, Sterry W, Sabat R. IL-22 regulates the expression of genes responsible for antimicrobial defense, cellular differentiation, and mobility in keratinocytes: a potential role in psoriasis. Eur J Immunol 36(5), 1309-1323 (2006).
243. Yao Z, Fanslow WC, Seldin MF, Rousseau A-M, Painter SL, Comeau MR, Cohen JI, Spriggs MK. Herpesvirus Saimiri encodes a new cytokine, IL-17, which binds to a novel cytokine receptor. Immunity 3(6), 811-821 (1995).
244. Subramaniam SV, Cooper RS, Adunyah SE. Evidence for the Involvement of JAK/STAT Pathway in the Signaling Mechanism of Interleukin-17. Biochemical and Biophysical Research Communications 262(1), 14-19 (1999).
245. Rahman MS, Yamasaki A, Yang J, Shan L, Halayko AJ, Gounni AS. IL-17A Induces Eotaxin-1/CC Chemokine Ligand 11 Expression in Human Airway Smooth Muscle Cells: Role of MAPK (Erk1/2, JNK, and p38) Pathways. The Journal of Immunology 177(6), 4064 (2006).
246. Shi X, Jin L, Dang E, Chang T, Feng Z, Liu Y, Wang G. IL-17A upregulates keratin 17 expression in keratinocytes through STAT1- and STAT3-dependent mechanisms. J Invest Dermatol 131(12), 2401-2408 (2011).

247. Kao C-Y, Chen Y, Thai P, Wachi S, Huang F, Kim C, Harper RW, Wu R. IL-17 Markedly Up-Regulates β-Defensin-2 Expression in Human Airway Epithelium via JAK and NF-κB Signaling Pathways. The Journal of Immunology 173(5), 3482-3491 (2004).
248. Mao X, Cho MJT, Ellebrecht CT, Mukherjee EM, Payne AS. Stat3 regulates desmoglein 3 transcription in epithelial keratinocytes. JCI Insight 2(9), (2017).
249. Srivastava A, Ståhle M, Pivarcsi A, Sonkoly E. Tofacitinib Represses the Janus Kinase-Signal Transducer and Activators of Transcription Signalling Pathway in Keratinocytes. Acta Derm Venereol 98(8), 772-775 (2018).
250. Nishio H, Matsui K, Tsuji H, Tamura A, Suzuki K. Immunolocalisation of the janus kinases (JAK)--signal transducers and activators of transcription (STAT) pathway in human epidermis. J Anat 198(Pt 5), 581-589 (2001).
251. Samadi A, Ahmad Nasrollahi S, Hashemi A, Nassiri Kashani M, Firooz A. Janus kinase (JAK) inhibitors for the treatment of skin and hair disorders: a review of literature. J Dermatolog Treat 28(6), 476-483 (2017).
252. Abraham A, Roga G. Topical steroid-damaged skin. Indian J Dermatol 59(5), 456-459 (2014).

7. APPENDIX

7.1. Additional information on bioinformatics

R sessionInfo()

```
R version 3.5.1 (2018-07-02)
Platform: x86_64-pc-linux-gnu (64-bit)
Running under: Debian GNU/Linux 9 (stretch)

Matrix products: default
BLAS: /usr/lib/openblas-base/libblas.so.3
LAPACK: /usr/lib/libopenblasp-r0.2.19.so

locale:
 [1] LC_CTYPE=en_US.UTF-8       LC_NUMERIC=C
LC_TIME=en_US.UTF-8        LC_COLLATE=en_US.UTF-8
 [5] LC_MONETARY=en_US.UTF-8    LC_MESSAGES=C
LC_PAPER=en_US.UTF-8       LC_NAME=C
 [9] LC_ADDRESS=C               LC_TELEPHONE=C
LC_MEASUREMENT=en_US.UTF-8 LC_IDENTIFICATION=C

attached base packages:
[1] stats4    parallel  stats     graphics  grDevices utils     datasets
methods   base

other attached packages:
 [1] ggpubr_0.2.1               magrittr_1.5               cowplot_1.0.0
GOplot_1.0.2
 [5] RColorBrewer_1.1-2         gridExtra_2.3              ggdendro_0.1-
20             ggplot2_3.1.0
 [9] pheatmap_1.0.12            pathview_1.22.3
org.Hs.eg.db_3.7.0          openxlsx_4.1.0.1
[13] goseq_1.34.1               geneLenDataBase_1.18.0     BiasedUrn_1.07
IHW_1.10.1
[17] DESeq2_1.22.2              SummarizedExperiment_1.12.0
DelayedArray_0.8.0          BiocParallel_1.16.5
[21] matrixStats_0.54.0         biomaRt_2.38.0
GenomicFeatures_1.34.3      AnnotationDbi_1.44.0
[25] Biobase_2.42.0             GenomicRanges_1.34.0
GenomeInfoDb_1.18.1         IRanges_2.16.0
[29] S4Vectors_0.20.1           BiocGenerics_0.28.0

loaded via a namespace (and not attached):
 [1] nlme_3.1-137            bitops_1.0-6            bit64_0.9-7
progress_1.2.0          httr_1.4.0
 [6] Rgraphviz_2.26.0        tools_3.5.1             backports_1.1.3
R6_2.3.0                rpart_4.1-13
[11] Hmisc_4.2-0             DBI_1.0.0               lazyeval_0.2.1
mgcv_1.8-24             colorspace_1.4-0
[16] nnet_7.3-12             withr_2.1.2             tidyselect_0.2.5
prettyunits_1.0.2       bit_1.1-14
```

```
[21] compiler_3.5.1           fdrtool_1.2.15          graph_1.60.0
htmlTable_1.13.1          rtracklayer_1.42.1
[26] slam_0.1-45              KEGGgraph_1.42.0        scales_1.0.0
checkmate_1.9.1           genefilter_1.64.0
[31] stringr_1.3.1            digest_0.6.18           Rsamtools_1.34.0
foreign_0.8-70            XVector_0.22.0
[36] base64enc_0.1-3          pkgconfig_2.0.2         htmltools_0.3.6
lpsymphony_1.10.0         htmlwidgets_1.3
[41] rlang_0.4.0              rstudioapi_0.9.0        RSQLite_2.1.1
zip_2.0.3                 acepack_1.4.1
[46] dplyr_0.8.3              RCurl_1.95-4.11         GO.db_3.7.0
GenomeInfoDbData_1.2.0    Formula_1.2-3
[51] Matrix_1.2-14            Rcpp_1.0.2              munsell_0.5.0
stringi_1.2.4             yaml_2.2.0
[56] MASS_7.3-50              zlibbioc_1.28.0         plyr_1.8.4
grid_3.5.1                blob_1.1.1
[61] crayon_1.3.4             lattice_0.20-35         Biostrings_2.50.2
splines_3.5.1             annotate_1.60.0
[66] KEGGREST_1.22.0          hms_0.4.2               locfit_1.5-9.1
knitr_1.21                pillar_1.3.1
[71] ggsignif_0.5.0           geneplotter_1.60.0      XML_3.98-1.16
glue_1.3.0                latticeExtra_0.6-28
[76] data.table_1.12.0        png_0.1-7               gtable_0.2.0
purrr_0.3.2               assertthat_0.2.0
[81] xfun_0.4                 xtable_1.8-3            survival_2.42-3
tibble_2.0.1              GenomicAlignments_1.18.1
[86] memoise_1.1.0            cluster_2.0.7-1
```

7.2. Characteristics on patients included in the study

Table A1: Clinical characteristics of patients recruited for mRNA expression analysis

Patient	Sex	Age	Pemphigus type	Conc. [U/ml] Dsg1	Dsg3	Disease stage	Lesional skin biopsy location
1[a]	M	71	PV	>200	135	Acute	Neck
2	M	75	PF	>200	5	Acute	Back
3[a]	M	36	PV	>200	>200	Acute	Back
4	F	43	PF	>200	4	Acute	Back
5	F	66	PF	>200	<2	Acute	Back
6	M	76	PF	>200	32	Acute	Chest
7	M	56	PV	121	86	Acute	Abdomen
8[b]	F	49	PV	>200	177	Acute	Back
9[a]	F	52	PV	116	>200	Chronic	Hand
10[a]	M	56	PV	33	22	Chronic	Chest
11	M	75	PF	>200	<2	Chronic	Back
12	M	88	PF	57	<2	Chronic	Abdomen
13[a]	M	49	PV	176	>200	Chronic	Back
14	F	44	PF	>200	4	Chronic	Back
15	M	53	PF	85	28	Chronic	Head
16	M	50	PV	>200	4	Chronic	Back
17[b]	M	78	PV	>200	28	Chronic	Chest
18[b]	M	39	PF	>200	<2	Chronic	Chest
19[b]	M	61	PF	>200	<2	Chronic	Back
20[b]	F	54	PV	>200	>200	Chronic	Back
21	F	45	PV	33	17	Chronic	Abdomen
22	M	53	PV	28	>200	Chronic	Scalp
23	M	58	PV	5	173	Chronic	Back
24[a]	F	59	PV	60	>200	Remission	Back
25	F	31	PV	10	>200	Remission	Head
26	M	41	PV	6	3	Remission	Chest
27[b]	F	59	PV	197	<2	Remission	Back
28	M	65	PV	15	130	Remission	Neck
29	M	51	PF	<2	8	Remission	Back

[a] Sample also used for RNA-seq analyses

[b] Lesional and perilesional skin biopsies

Table A2: Summary of patients involved in flow cytometric analysis of T cell subsets in peripheral blood mononuclear cells

Patient	Sex	Age	Pemphigus type	Conc. [U/ml] Dsg1	Dsg3	Disease stage
1	M	71	PV	>200	135	Acute
2	F	41	PV	10	>200	Acute
3	F	62	PV	<2	8	Acute
4[a]	F	35	PV	3	4	Acute
5[b]	F	33	PV	11	>200	Acute
6[a, b]	F	50	PV	2	>200	Acute
7[b]	F	43	PV	13	189	Acute
8	M	75	PF	>200	5	Acute
9	F	67	PF	>200	<2	Acute
10	F	53	PV	5	130	Chronic
11[b]	M	53	PV	46	31	Chronic
12	M	58	PV	42	70	Chronic
13[b]	M	50	PV	>200	>200	Chronic
14	M	68	PV	9	182	Chronic
15	F	44	PV	151	>200	Chronic
16[b]	F	55	PV	5	90	Chronic
17[a, b]	F	55	PV	26	>200	Chronic
18[b]	F	52	PV	117	>200	Chronic
19[b]	M	52	PV	26	2	Chronic
20[b]	F	64	PV	<2	6	Chronic
21[a]	F	48	PV	45	>200	Chronic
22[b]	F	57	PV	43	>200	Chronic
23[b]	M	81	PV	27	40	Chronic
24[b]	F	53	PV	3	22	Chronic
25[b]	M	50	PV	6.1	72	Chronic
26[a]	F	52	PV	<2	>200	Chronic
27[b]	F	54	PV	>200	>200	Chronic
28	F	53	PV	<2	51	Chronic
29	F	51	PV	5	>200	Chronic

[a] Cell sorting and qPCR of T cell subsets

[b] Analyses of autoreactive $Dsg3^+$ B cells

Table A2 (continued)

Patient	Sex	Age	Pemphigus type	Conc. [U/ml]		Disease stage
				Dsg1	Dsg3	
30	M	53	PV	5	173	Chronic
31	F	60	PV	<2	155	Chronic
32[b]	F	64	PV	9	160	Chronic
33[b]	M	53	PV	109	>200	Chronic
34[b]	F	33	PV	<2	>200	Chronic
35	F	68	PV	15	113	Chronic
36[b]	F	41	PV	13	45	Chronic
37	F	44	PF	>200	4	Chronic
38	M	53	PF	86	29	Chronic
39	M	69	PF	<2	<2	Chronic
40	F	83	PF	>200	<2	Chronic
41	M	46	PF	>200	4	Chronic
42	F	89	PV	3	<2	Remission
43	M	70	PV	<2	>200	Remission
44[b]	F	78	PV	<2	<2	Remission
45[b]	F	79	PV	<2	>200	Remission
46	M	74	PV	2	117	Remission
47[b]	F	76	PV	18	4	Remission
48[b]	M	64	PV	<2	32	Remission
49[b]	F	24	PV	3	<2	Remission
50	M	78	PV	4	149	Remission
51[a, b]	F	68	PV	9	10	Remission
52	F	66	PV	<2	136	Remission
53[b]	M	78	PV	197	14	Remission
54[b]	F	46	PV	17	>200	Remission
55	M	50	PV	<2	6	Remission
56	M	55	PV	62	33	Remission
57[b]	F	58	PV	<2	197	Remission
58[b]	M	62	PV	10	17	Remission
59[b]	F	63	PV	7	<2	Remission

[a] Cell sorting and qPCR of T cell subsets

[b] Analyses of autoreactive Dsg3$^+$ B cells

Table A2 (continued)

Patient	Sex	Age	Pemphigus type	Conc. [U/ml] Dsg1	Dsg3	Disease stage
60[b]	M	27	PV	<2	100	Remission
61[b]	M	63	PV	3	>200	Remission
62[b]	M	40	PV	<2	<2	Remission
63[b]	M	70	PV	7	153	Remission
64[b]	M	56	PV	5	16	Remission
65	F	80	PV	3	5	Remission
66	F	62	PV	3	2	Remission
67	F	56	PV	<2	4	Remission
68	M	80	PV	3	>200	Remission
69	M	55	PV	10	157	Remission
70[b]	M	45	PV	5	2	Remission
71[b]	M	66	PV	46	178	Remission
72[b]	F	59	PV	10	>200	Remission
73	M	54	PV	6	72	Remission
74	F	62	PV	<2	65	Remission
75[b]	F	57	PV	5	>200	Remission
76	M	70	PF	<2	<2	Remission
77	M	38	PF	>200	<2	Remission
78	m	75	PF	73	35	Remission
79	F	59	PF	<2	<2	Remission

[a] Cell sorting and qPCR of T cell subsets

[b] Analyses of autoreactive Dsg3$^+$ B cells

Table A3: Patients for intracellular flow cytometric analysis of cytokine-producing T cell subsets in peripheral blood mononuclear cells

Patient	Sex	Age	Pemphigus type	Conc. [U/ml] Dsg1	Dsg3	Disease Stage
1	F	37	PV	<2	22	Acute
2	F	54	PV	<2	80	Acute
3	M	78	PF	97	<2	Chronic
4	F	56	PV	12	>200	Chronic
5	F	44	PV	3	12	Remission
6	F	35	PV	11	>200	Remission
7	M	82	PV	<2	165	Remission
8	M	49	PV	9	>200	Remission
9	M	57	PV	154	6	Remission

Table A4: Pemphigus patients for immunohistochemical staining

Patient	Sex	Age	Pemphigus type	Conc. [U/ml] Dsg1	Dsg3	Disease Stage
1[a]	F	43	PF	>200	4	Acute
2	M	72	PV	>200	135	Acute
3	M	75	PF	>200	5	Acute
4[a]	M	50	PV	>200	180	Chronic
5	M	87	PF	>200	<2	Chronic
6[b]	M	66	PF	>200	4	Chronic
7[b]	F	60	PV	60	>200	Chronic
8[c]	F	51	PV	116	>200	Chronic
9[c]	F	66	PF	>200	<2	Chronic
10	M	50	PV	>200	>200	Chronic

[a] Representative images showing high expression of pSTAT1 and pSTAT3

[b] Representative image showing low expression of pSTAT3

[c] Representative image showing low expression of pSTAT1

7.3. Supplementary figures

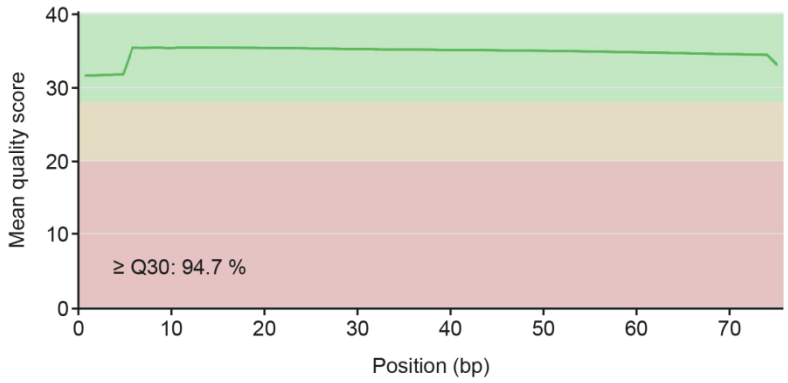

Figure A1: All 12 samples analyzed by RNA-seq display a high read quality. Quality control of raw sequence data was performed using FastQC. The sequence quality histogram shows high mean quality scores across each base position in the reads. 94.7 % of the reads demonstrated quality values higher than Q30. No adapter sequences or contaminations were detected.

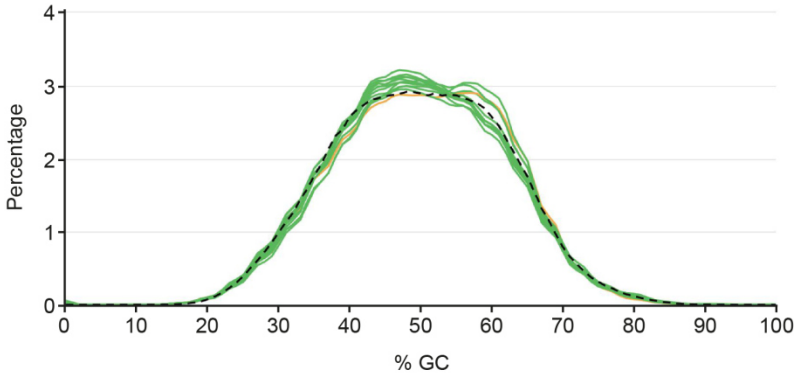

Figure A2: Guanine-cytosine distribution of all samples fits well with the reference transcriptome. Per sequence guanine-cytosine (GC)-content was determined by FastQC in the process of quality control of raw sequence data. The GC-content of all reads formed a normal distribution in all samples and fitted with the GC-content of the human reference transcriptome v29 (black dashed line). Individual samples are represented as green lines, except for one sample in orange (S02_Pemphigus), which showed a slightly elevated GC-content, but remained within an acceptable tolerance.

Sample Name	% Aligned	M Aligned
S01_Pemphigus	90.5 %	23.2
S02_Pemphigus	89.0 %	26.7
S03_Pemphigus	87.8 %	23.6
S04_Pemphigus	92.3 %	23.9
S05_Pemphigus	93.6 %	22.3
S06_Pemphigus	88.7 %	20.4
S07_Control	87.2 %	21.8
S08_Control	86.8 %	18.6
S09_Control	88.6 %	23.3
S10_Control	88.2 %	23.7
S11_Control	89.4 %	22.9
S12_Control	88.3 %	21.5

Figure A3: All samples demonstrate high mapping rates to the reference transcriptome. Reads were aligned to the human reference transcriptome v29 using Salmon. Proportion of uniquely mapped reads (% Aligned) and total uniquely mapped reads (millions, M Aligned) are listed for each sample analyzed by RNA-seq. The mean mapping rate (SD) was 89.21 % (1.98 %), indicating trouble free quantification.

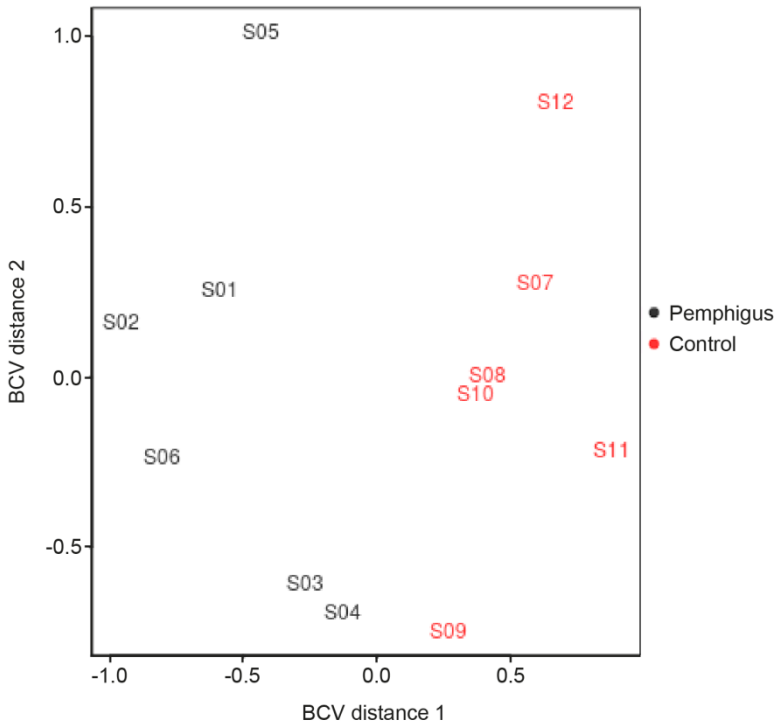

Figure A4: Multidimensional scaling analysis shows separation between pemphigus and control group. Spatial distances between the individual samples correspond to differences in sample properties and approximate the typical expression differences (log_2 fold change) between samples. BCV: biological coefficient of variation.

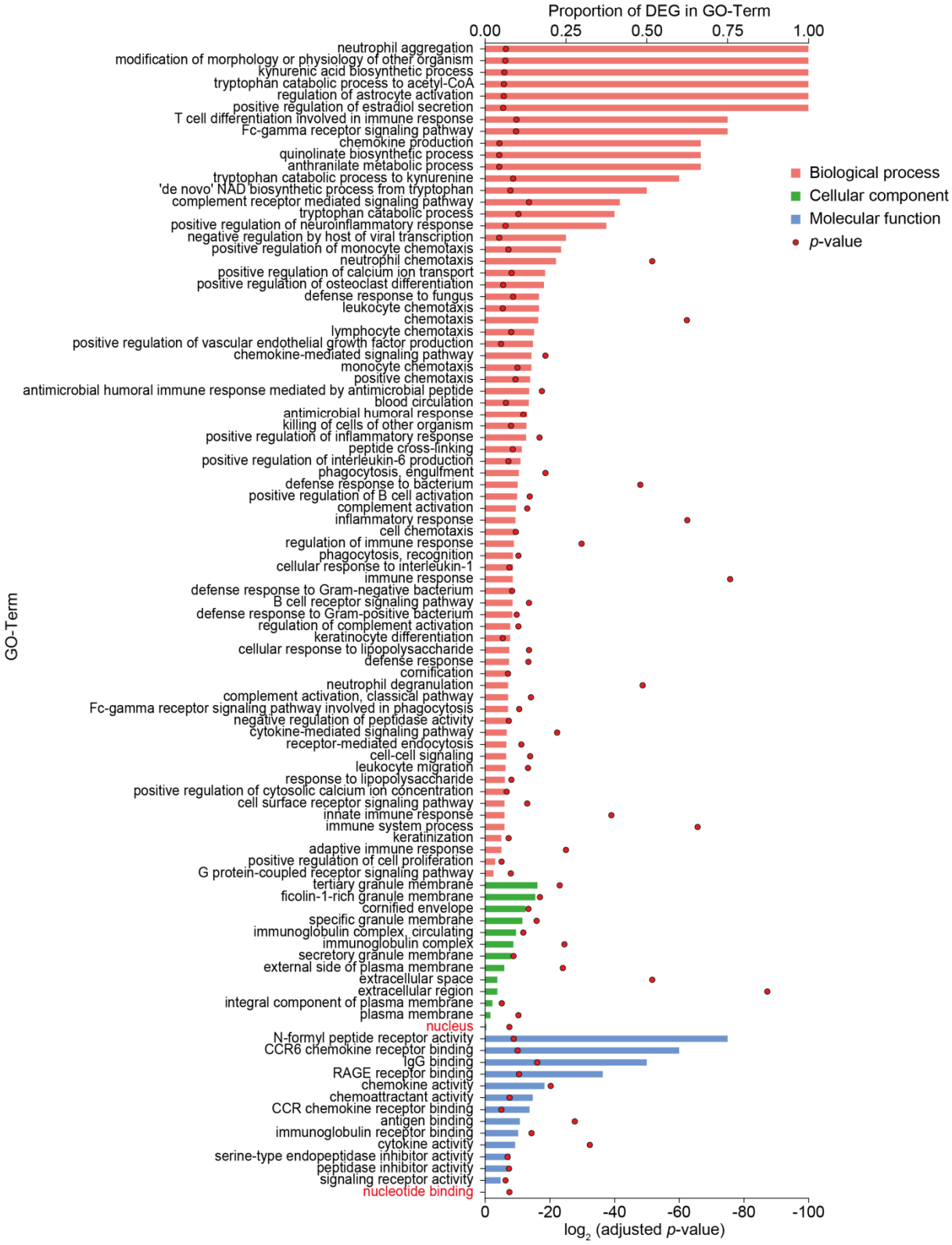

Figure A5: Most upregulated genes involved in biological process. Gene Ontology (GO) enrichment analysis of differentially expressed genes (DEGs) was performed and GO-terms were classified into biological process, cellular component and molecular function. Under-represented GO-terms are marked in red. RNA-seq analysis of lesional skin biopsies from pemphigus patients (n=6) was compared to healthy skin biopsies (n=6). Part of the data was published in [176].

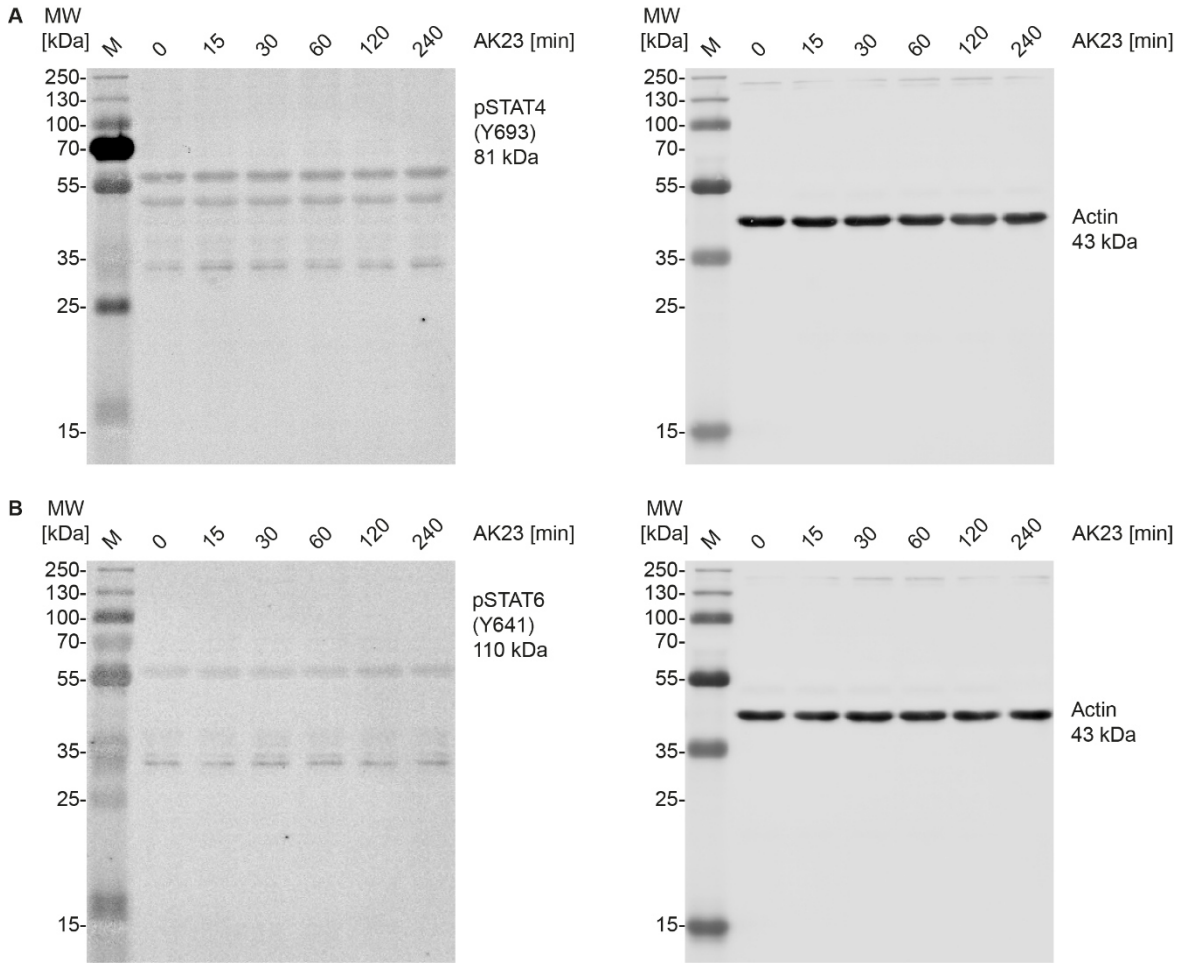

Figure A6: No activation of STAT4 and STAT6 by AK23 in human keratinocytes. Normal human epidermal keratinocytes were incubated with 20 µg/ml AK23 for 0 to 240 min (as indicated) and activation of STAT proteins was analyzed by immunoblotting (n=2). **(A)** Representative blot from one donor is shown for pSTAT4. **(B)** Detection of pSTAT6 in AK23 treated NHEK from one donor. MW: Molecular weight, M: Marker.

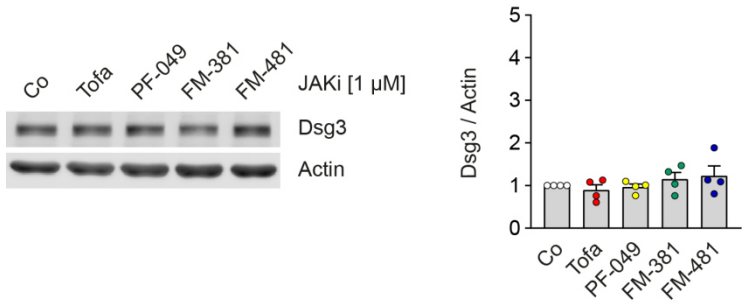

Figure A7: Desmoglein 3 is not altered by JAK inhibitors in human keratinocytes. Normal human epidermal keratinocytes were treated with 1 µM of the indicated JAKi or DMSO only (Co) for 5 h and protein levels of Dsg3 were determined by immunoblotting (n=4). Representative images of one experiment and semi-quantitative analysis (single donors and mean with SEM) of the specific Dsg3 signals relative to Actin are presented.

7.4. Supplementary tables

Table A5: Correlation analysis between Dsg3-specific B cells and distinct T cell subsets. Spearman's correlation coefficient *r* and *p*-values are indicated (ns not significant, ** $p<0.01$).

	Th17	Th17.1	Th2	Th1	Treg	Tfh17	Tfh17.1	Tfh2	Tfh1	Tfr
Dsg3-specific B cells										
Active										
r	0.0971	0.3363	-0.2748	-0.3512	0.0822	0.6523	0.3775	-0.1624	-0.4118	0.4172
p	0.6926	0.1592	0.2549	0.1404	0.7527	0.0025	0.111	0.5065	0.0798	0.0966
	ns	ns	ns	ns	ns	**	ns	ns	ns	ns
Remittent										
r	-0.1940	0.0436	0.1128	-0.1744	0.2445	0.0196	0.1534	-0.0888	-0.0421	0.3190
p	0.4125	0.8551	0.6359	0.4620	0.2989	0.9348	0.5185	0.7098	0.8600	0.1704
	ns	ns	ns	ns	ns	ns	ns	ns	ns	ns
Control										
r	0.1908	0.2580	-0.2111	-0.2145	-0.1504	0.0262	0.0017	0.0391	-0.1201	-0.1768
p	0.3833	0.2347	0.3337	0.3257	0.5514	0.9056	0.9937	0.8594	0.5851	0.4827
	ns	ns	ns	ns	ns	ns	ns	ns	ns	ns

ACKNOWLEDGEMENTS

First of all, I would like to express my gratitude to my supervisor Prof. Dr. Kamran Ghoreschi for giving me the opportunity to work on several interesting projects in his lab, including my PhD thesis. He always made time for discussions and offered helpful advice.

Sincere thanks to Prof. Dr. Franziska Ghoreschi, who employed me in the first place, arranged for me to join the group of Kamran Ghoreschi and always supported me.

I further wish to acknowledge Prof. Dr. Robert Feil for being the second supervisor and reviewer of this thesis within the Faculty of Science.

Next, I want to thank all current and former lab members of the Ghoreschi group. I very much appreciate the assistance provided by Dr. Jürgen Brück. Thank you, Kirsten Deinert, Dr. Katharina Welsch, Maximilian Rentschler and Dr. Melanie Carevic-Neri for the pleasant working atmosphere and a lot of fun in the lab but also outside the lab.

Many thanks to all collaboration partners, all co-authors and the whole PEGASUS consortium, especially to Dr. Farzan Solimani for his support with the preparation of our manuscript. Also, a big thank you to Iris Schäfer for her help with the FACS measurements and Tobias Tekath for his support analyzing the RNA-seq data. Furthermore, many thanks to the clinical team, particularly Dr. Katharina Meier, for their efforts in recruiting patients and taking blood as well as tissue samples.

Finally, very special thanks to my family and friends and my husband for their continuous support and understanding.

LIST OF PUBLICATIONS

Neri D, Carevic-Neri M, Brück J, Holstein J, Schäfer I, Solimani F, Handgretinger R, Hartl D, Ghoreschi K. Arginase 1^+ IL-10^+ polymorphonuclear myeloid-derived suppressor cells are elevated in patients with active pemphigus and correlate with an increased Th2/Th1 response. Experimental Dermatology 30(6), 782-791 (2021).

Brück J, Calaminus C, Hoffmann SHL, Schwenck J, Holstein J, Yazdi AS, Pichler B, Kneilling M, Ghoreschi K. Non invasive *in vivo* monitoring of dimethyl fumarate treatment in EAE by assessing the glucose metabolism in secondary lymphoid organs. European Journal of Immunology 51(4), 1006-1009 (2021).

Holstein J, Solimani F, Baum C, Meier K, Pollmann R, Didona D, Tekath T, Dugas M, Casadei N, Hudemann C, Polakova A, Matthes J, Schäfer I, Yazdi AS, Eming R, Hertl M, Pfützner W, Ghoreschi K, Möbs C. Immunophenotyping in pemphigus reveals a Th17/Tfh17-dominated immune response promoting desmoglein1/3-specific autoantibody production. Journal of Allergy and Clinical Immunology 147(6), 2358-2369 (2021).

Pietschke K, Holstein J, Meier K, Schäfer I, Müller-Hermelink E, Gonzalez-Menendez I, Quintanilla-Martinez L, Ghoreschi FC, Solimani F, Ghoreschi K. The inflammation in cutaneous lichen planus is dominated by IFN-ϒ and IL-21 - a basis for therapeutic JAK1 inhibition. Experimental Dermatology 30(2), 262-270 (2021).

Meier K, Holstein J, Solimani F, Waschke J, Ghoreschi K. Case Report: Apremilast for therapy-resistant pemphigus vulgaris. Frontiers in Immunology 11:588315 (2020).

Schwenck J, Maurer A, Fehrenbacher B, Mehling R, Knopf P, Mucha N, Haupt D, Fuchs K, Griessinger CM, Bukala D, Holstein J, Schaller M, Menendez IG, Ghoreschi K, Quintanilla-Martinez L, Gütschow M, Laufer S, Reinheckel T, Röcken M, Kalbacher H, Pichler BJ, Kneilling M. Cysteine-type cathepsins promote the effector phase of acute cutaneous delayed-type hypersensitivity reactions. Theranostics 9(13), 3903-3917 (2019).

Forster M, Chaikuad A, Dimitrov T, Döring E, Holstein J, Berger BT, Gehringer M, Ghoreschi K, Müller S, Knapp S, Laufer SA. Development, Optimization, and Structure-Activity Relationships of Covalent-Reversible JAK3 Inhibitors Based on a Tricyclic Imidazo[5,4- d]pyrrolo[2,3-b]pyridine Scaffold. Journal of Medicinal Chemistry 61(12), 5350-5366 (2018).

Holstein J, Fehrenbacher B, Brück J, Müller-Hermelink E, Schäfer I, Carevic M, Schittek B, Schaller M, Ghoreschi K, Eberle FC. Anthralin modulates the expression pattern of cytokeratins and antimicrobial peptides by psoriatic keratinocytes. Journal of Dermatological Science 87(3), 236-245 (2017).

Welsch K, Holstein J, Laurence A, Ghoreschi K. Targeting JAK/STAT signalling in inflammatory skin diseases with small molecule inhibitors. European Journal of Immunology 47(7), 1096-1107 (2017).

Brück J, Holstein J, Glocova I, Seidel U, Geisel J, Kanno T, Kumagai J, Mato N, Sudowe S, Widmaier K, Sinnberg T, Yazdi AS, Eberle FC, Hirahara K, Nakayama T, Röcken M, Ghoreschi K. Nutritional control of IL-23/Th17-mediated autoimmune disease through HO-1/STAT3 activation. Scientific Reports 7, 44482 (2017).

Eberle FC, Holstein J, Scheu A, Fend F, Yazdi AS. Intralesional anti-CD20 antibody for low-grade primary cutaneous B-cell lymphoma: Adverse reactions correlate with favorable clinical outcome. Journal der Deutschen Dermatologischen Gesellschaft 15(3), 319-323 (2017).

Forster M, Chaikuad A, Bauer SM, Holstein J, Robers MB, Corona CR, Gehringer M, Pfaffenrot E, Ghoreschi K, Knapp S, Laufer SA. Selective JAK3 Inhibitors with a Covalent Reversible Binding Mode Targeting a New Induced Fit Binding Pocket. Cell Chemical Biology 23(11), 1335-1340 (2016).

Eberle FC, Brück J, Holstein J, Hirahara K, Ghoreschi K. Recent advances in understanding psoriasis [version 1; peer review: 2 approved]. F1000Research 5(F1000 Faculty Rev), 770 (2016).